Knee Valgus vs. Knee Abduction Angle:
Comparative Analysis of Valgus Alignment Measurement Methods in Female Athletes

by

Taylor Oldfather

A dissertation submitted to the Graduate Faculty of
Auburn University
in partial fulfillment of the
requirements for the Degree of
Doctor of Philosophy

Auburn, Alabama
August 8, 2020

Keywords: Knee Valgus, Motion Capture,
Biomechanics, ACL, Injury

Approved by

Michael Zabala, Chair, Assistant Professor of Mechanical Engineering
Nels Madsen, Professor Emeritus of Mechanical Engineering
Dan Marghitu, Professor of Mechanical Engineering
Jaimie Roper, Assistant Professor of Kinesiology

Abstract

Precise mathematical methods have been developed to quantify lower limb kinematics in anatomically meaningful ways to aid clinicians and researchers in a range of ways from injury prevention to rehabilitation practices. The improvement of technology in recent years, namely motion capture and non-invasive imaging, has resulted in an increase in research utilizing angles associated with human anatomy. Now, measuring lower extremity joint angles is a standard practice in many labs and clinics. Knee valgus angle (KVA), the angle created when the shank is rotated away from the midline of the body, has shown to correlate with subsequent anterior cruciate ligament (ACL) ruptures when measured during drop-jump tasks. As a result, this angle has garnered much attention in the field of biomechanics. KVA can be calculated in multiple ways by modifying the defined frontal plane and reference axis. The extensive research with KVA and the varying methods used to calculate the angle has led to ambiguity on how these different KVAs relate to one another and on the importance of individual joint angles that comprise KVAs. Additionally, changes in processing methods, namely the modification of the lower extremity joint constraints, and changing the movement task in which KVA is measured can influence the value of KVA. To study this angle, the kinematics of 23 female athletes, D1 soccer, D1 basketball, and club soccer (height $= 171.2 \pm 88.9cm$, weight $= 66.3 \pm 8.6$kg, age $= 19.8 \pm 1.9$yrs), was analyzed using a motion capture system during tasks related to their sport and daily living. This work aims to determine the relationship between KVA calculated with different mathematical methods, kinematic processing models, and different movement tasks as well as to determine how the combination of lower extremity joint angles contribute to multiple types of KVA so that researchers and clinicians can properly evaluate KVA.

Acknowledgments

First and foremost, I would like to express my heartfelt gratitude to my adviser, Dr. Michael Zabala, for his continuous encouragement and support. If every adviser was like Dr. Zabala, there would be no horror stories about graduate school and everyone would be getting graduate degrees. I would also like to thank my committee members Dr. Nels Madsen, Dr. Dan Marghitu, and Dr. Jaimie Roper for supporting my endeavors.

I would like to thank the coauthors on my papers, Dr. Michael Goodlet, MD, head physician for Auburn Athletics, Megan Young the strength and conditioning coach for the Auburn woman's soccer team, and Dr. William (Hank) Murrah in the Educational Foundations, Leadership, and Technology Department. I would like to thank the Auburn Athletic Department for their assistance in this project and Edward Via College of Osteopathic Medicine (VCOM) Research Eureka Accelerator Program (REAP) for their financial support of this project.

I would like to thank Dr. Wendi Weimar for introducing me to the world of biomechanics and facilitating a learning environment that always encouraged me to ask questions and think critically. I would also like to thank Dr. Hamid Ghaednia for helping me transition into graduate student life at Auburn University and keeping me from failing before I even started, as well as Dr. George Flowers not only for teaching me all about Euler angles, but for his support and great leadership as the Dean of Graduate School. I would like to thank Dr. Richard Williams, Dr. Zabala, and Dr. Madsen for showing and advising me how to be a good instructor and student mentor. I also wish to thank Reed Rodich, Scott Kennedy, Jacob Larson, Taylor Troutman, and Kasey Cooper for helping with the logistics of the study; Chris Weathers for helping me process data; Lexey Blakely for helping me categorize countless articles on knee valgus; and Claire Oldfather and Bailey Garrett for editing my writing.

I would not have been able to come near to finishing this work without the support of my husband, David Oldfather, with his never ending encouraging words: "Taylor, you've got this, just sit down and write." He believed in me and supported my dreams when it would have been easy to abandon the struggle and admit defeat. Many, many thanks to my parents, Ed and Julia Wright, for homeschooling me and teaching me how to learn. If it was not for the lifestyle of curiosity and critical thinking they instilled in me, I would not have considered graduate school

in the first place. Also, I thank my siblings and siblings-in-law for being there when I needed their help and ribbing me when I did not. I am extremely grateful to Dr. Skylar Moore, DNP, CRNP, for treating my medical well-being for the past eight years and keeping me in a place where I could work despite the illnesses I have faced. Many thanks to my lovable furballs, Watson, Potato, Sabastian, and Finch (RIP), for filling the shadows with their presence and their many kitty cuddles. Finally, I want to thank my God, who has always been a source of strength to me.

Table of Contents

List of Tables

List of Figures

Nomenclature

α	Flexion angle[57]
β	Abduction angle[57]
β_1	An abduction angle measuring $0°$
β_2	An abduction angle measuring $90°$
β_{Left}	The abduction angle (β) for the right leg
β_{Right}	The abduction angle (β) for the right leg
γ	Internal rotation angle[57]
θ	Angle between the lateral global axis and the lateral pelvis axis
e_1	Lateral axis of the proximal segment
e_1^r	Anterior axis of the proximal segment
e_2	Floating axis derived from e_1 and e_3
e_3	Vertical axis of the distal segment
e_3^r	Anterior axis of the distal segment
$e_{3,III}$	e_3 in Quadrant III
$e_{3,II}$	e_3 in Quadrant II
$e_{3,IV}$	e_3 in Quadrant IV
$e_{3,I}$	e_3 in Quadrant I
G_X	Lateral global axis on the floor plane
G_Y	Anterior global axis on the floor plane
G_Z	Vertical global axis perpendicular to the floor plane
P'_X	The projection of P_X onto the $G_X - G_Y$ plane
P_X	Lateral pelvic axis projected onto the floor plane
P_Y	Anterior pelvic axis projected onto the floor plane
$Thigh_Z$	Vertical axis of the thigh segment
322	A lower extremity kinematic model with 3 degrees of freedom (flexion, abduction, and internal rotation) in the hip; and 2 degrees of freedom (flexion and abduction) in the ankle and knee

332 A lower extremity kinematic model with 3 degrees of freedom (flexion, abduction, and internal rotation) in the knee, and hip; and 2 degrees of freedom (flexion and abduction) in the ankle

333 A lower extremity kinematic model with 3 degrees of freedom (flexion, abduction, and internal rotation) in the ankle, knee, and hip

666 A lower extremity kinematic model with 6 degrees of freedom in the ankle, knee, and hip

ACL Anterior cruciate ligament

AMA Anatomical-mechanical angle

CT Computed topography

D1 Division 1

DOF Degree of freedom

DS Down stairs

FMA Femoral mechanical anatomic angle

IRB Internal Review Board

ISB International Society of Biomechanics

JCS Joint coordinate system

KV Knee valgus

KVA Knee valgus angle

KVA 2G Knee valgus angle calculated using the global coordinate system in two dimensions

KVA 2P Knee valgus angle calculated using the pelvic coordinate system in two dimensions

KVA 3G Knee valgus angle calculated using the global coordinate system in three dimensions

KVA 3GA Knee valgus angle calculated using the global coordinate system in three dimensions with the anatomical coordinate system sign convention

KVA 3GC Knee valgus angle calculated using the global coordinate system in three dimensions with the Cartesian coordinate system sign convention

LESS Landing Error Scoring System

LR Lateral leg reach

MPCS Modified pelvis coordinate system

MRI Magnetic Resonance Imaging

OA Osteoarthritis

P Significance

PVC polyvinyl chloride

r Pearson correlation coefficient

SD Standard deviation

SPSS Statistical Package for the Social Sciences

STA Soft tissue artifact

TRUFI True fast imaging

vGRF Vertical ground reaction force

1 Introduction

1.1 Knee Valgus Angle

Precise mathematical methods have been developed to quantify lower limb kinematics in anatomically meaningful ways to aid clinicians and researchers in a range of ways from injury prevention to rehabilitation practices. The improvement of technology in recent years, namely motion capture and non-invasive imaging, such as magnetic resonance imaging (MRI), has resulted in an increase in research utilizing angles associated with human anatomy. Now, measuring biomechanical angles is a standard practice in many research labs and clinics.

Research and clinical fields concerned with ACL rupture often consider lower extremity joint angles when determining risk factors, injury prevention programs, and rehabilitation programs[10,23,56,83,189,197]. Lower extremity joint angles are also used in the analysis of conditions associated with ACL injuries, such as knee osteoarthritis[5,65,66]. One angle that has been evaluated many times to measure ACL injury risk is the knee valgus angle (KVA)[10,50,65,86,142,151,192] [23,29,67,78,83,189,197]. This angle is found when the shank rotates outwards from the body. This angle is especially popular in research on ACL injuries because in tests where it is measured during a drop-jump (jumping off of a box and rebounding vertically), it has been shown to correlate to ACL injuries[10,29,50,65,78,86,151,192].

The angle describing an anatomical segment moving outward from the midline of the body has been around for centuries and has slowly developed into a variety of unique mathematical calculations[57,65,201]. Many of the calculations used to describe the KVA appear similar, but are in fact biomechanically distinct[29,57,65]. However, because the variety of methods used to calculate KVA do describe the general medial alignment to which the term valgus refers, the many calculation methods are often treated as producing the same angle[29,52,71,81,97,140,147,150,151,192].

1.2 Varying Methods of Measuring KVA

One difference in the methods of calculating KVA is that not all KVA methods use the same reference frame. Some KVA calculation methods use a global reference frame while others use a body fixed reference frame[10,16,36,37,44,63,65,95,116,119,133,191,198,202]. Detailed descriptions would help prevent such confusions, but such descriptions are not always present in the literature[14,17,29,67,81,84,86,90,142,151,192]. Misinterpretation across research papers and groups of researchers makes building off of one another's work challenging.

1.3 Lower Extremity Joint Angles and KVA

The orientation of the lower extremities is influenced by the ankle, knee, and hip, each with six degrees of freedom (DOF)[57,65]. Therefore, a single joint angle does not solely contribute to the lower extremity aliment. However, a number of studies focus on individual joint angles associated with KVA in order to reduce KVA and therefore reduce ACL ruptures or improve rehabilitation programs[30,49,76,78,87,112,148,158]. The amount of influence the ankle, knee, and hip orientation have on KVA compared with one another and during different tasks is unknown. Identifying how the ankle, knee, and hip are associated with KVA during multiple tasks will greatly contribute to the development of injury prevention and rehabilitation programs.

1.4 Soft Tissue Artifacts and Joint Angles

The instrumentation used to capture human movement has improved through the years, from the manual marking of camera film to the digital reconstruction of movement using multi-camera systems. However, there are still limitations in how movement data is collected which prevent accurate measurement of human movement[40,185]. Motion capture systems that use surface markers encounter soft tissue artifacts (STAs), which occur when the surface of the skin moves in relation to the underlying bone[40,185]. Due to the relative movement, the captured po-

sition of body segments does not accurately represent the position and orientation of the bones in space. As a result, steps have been taken to reduce the STA effect on the resulting data, such as restricting the degrees-of-freedom (DOF) of joints in the model, filtering the data, choosing different markers sets, or weighing and scaling markers[9,13,15,16,20,22,25,40,47,48,105,108,122,173].

There are a number of studies restricting the DOFs of the ankle, knee, and hip; some by restricting translations and others by restricting translations and rotations. The kinematic model resolves the segment's orientation in space with the given constraints. Previous studies have observed how modifying DOFs might change knee angles in walking, but have not measured the differences between high and low impact tasks, such as running and jumping[20,48,196]. Motion capture of high impact tasks are frequently examined when considering KVA and ACL ruptures and rehabilitation and therefore should be considered in this context when determining DOF of joints during data processing.

1.5 Motivation and Purpose of this Work

The purpose of this work is to determine 1) whether or not angles associated with KVA are correlated with one another, 2) what combination of lower extremity joint angles make up the different calculation methods of KVA, and 3) how constraining joint rotations and translations during data processing effects the value of the multiple methods of calculating KVAs.

- **Study 1 Hypothesis:** Measures of KVA are equivalent despite changes in measurement calculations methods and movement task.
- **Study 2 Hypothesis: A)** Lower extremity joint angles can predict the KVA and knee abduction angle given different joint constraints and movement tasks, and **B)** An angle or combination of angles can be found that contribute the most to KVA.
- **Study 3 Hypothesis:** Calculating KVA using different lower extremity joint constraints

will result in KVAs that are not correlated with one another.

2 Background

2.1 Terminology

2.1.1 The Origin and Definition of 'Valgus'

The exact origin of the terms 'valgus' and its opposite 'varus', are unknown; however, the etymology of the word can be traced back at least two thousand years[201]. Plautus (254—184 BCE), a Roman playwright wrote of valgus and varus in his play *Miles Gloriousus*, "Aut varum aut valgum aut compernem (3.1.128)"[201]. *Valgum* and *varum* are the Latin form of valgus and varus, and, in Plautus' script, were used in reference to the lateral rotation of an anatomical segment away from the midline[201]. The first modern publication of the terms 'valgus' and 'varus' was in "The Account of Diseases in Liverpool Dispensary in 1801"[201]. This is cited by many dictionaries and encyclopedias as the first known use of the words[1,2]. However, in the 1801 text, Watt explains that the terms 'valgus' and 'varus' were already widely used, remarking that "they [valgus and varus] have been used not only by medical writers, but even by classical authors, and in common language, for at least two thousand years"[201]. These terms have been continually used since the ancient times and are not likely to become obsolete in the near future. As such, the terms are ingrained in modern language and resolving the confusion between angle definitions by discarding the terms 'valgus' and 'varus' is unfeasible.

The general definitions for valgus and varus are vague and have been defined "of, relating to, or being a deformity in which an anatomical part is turned outward away from the midline of the body to an abnormal degree" and, "of, relating to, or being a deformity in which an anatomical part is turned inward toward the midline of the body to an abnormal degree", respectively (Figure 1),[1,2]. Varus (turning inwards) should not be confused with the inward positioning of the knee, which typically results in a valgus angle of the knee (tibia away from the femur or midline of the body), shown in Figure 2. The term 'valgus' has become even more vague as

studies began to use the term ‘knee valgus’ to describe distances (not angles) associated with the knee-in and shank out alignment that is shown in Figure 2[10].

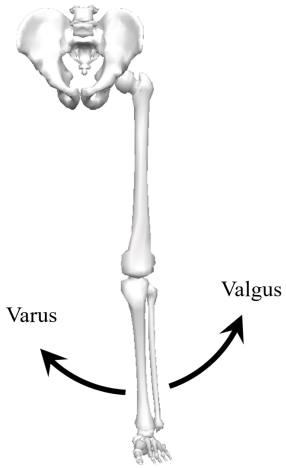

Figure 1: Knee valgus and varus rotations.

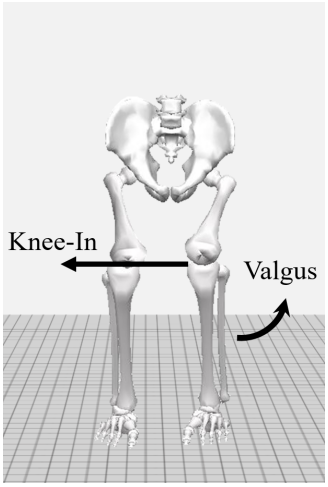

Figure 2: Lower body alignment: Knee-in and valgus rotation.

2.1.2 Angle Discontinuity

A significant number of the calculations used to describe the KVA appear similar, but are in fact biomechanically distinct due to the differing methods used to calculate them[29,57,65]. Because of the similar anatomical meaning, they are often treated as the same angle, leading to much confusion in the research literature on KVA[29,52,71,81,97,140,147,150,151 192].

One source of confusion between the different methods of calculation is that not all KVA

measures use the same reference frame. Some angles use a global reference frame while others use a body-fixed reference frame. Another factor is that some angles are measured in three dimensions while others are measured in two dimensions. Detailed descriptions help prevent such confusions, but such descriptions are not always available[14,17,29,67,86,142,151,192].

2.1.3 Additional Terms

In the literature associated with KVA, additional terms have been introduced in an attempt to clarify the mathematical calculations and distinguish the various methods used to calculate KVA. Because of this it would be helpful to have a systematic review performed where a term or multiple terms are used. In standard systematic reviews, a method is utilized in which a term or terms are searched to identify manuscripts of interest. However, in this case the standard systematic review method cannot be used to identify manuscripts of interest because numerous names are used to identify this type of angle and multiple different kinds of calculations are used to measure the angle. For example, if the term 'knee valgus angle' was used, the search query would omit papers referencing 'abduction'. Likewise, if the term 'abduction' was used, the search query would omit 'Q-angle'. Therefore, in order to capture the body of manuscripts which discuss the concept, a variety of search methods must be used. The analyzed publications were gathered using a number of retrieval methods and are not intended to make any statistical analyses of the literature but rather to introduce the reader to the multiple definitions used in the research.

A total of 143 publications were analzyed, and Table 1 lists each of the reviewed publication and associated terms identified to be closely related to the Webster definition of knee valgus. In the review, the term 'valgus' and 'valgus angle' were distinguished from one another, because the term 'valgus' has been used to reference angles, distances, or moments. Many times the differences between the three types of valgus was identified; however, in some instances the

type of valgus was inferred through the context. Therefore, in order to show the discrepancy across publications, the distinction between ‘valgus’ and ‘valgus angle’ was included.

If a term in the reviewed papers was used fewer than three times, then it was marked in the column ‘other’. The following terms met this criteria: ‘valgus orientation’, ‘knee valgus motion’, ‘knee valgus angular displacement’, ‘frontal plane knee angle’, ‘mechanical axis angle’, ‘mechanical axis alignment’, ‘valgus alignment’, ‘femoral shaft-tibial shaft’, ‘valgus angle, functional knee valgus, 3D KV’, ‘2D KV’, ‘active valgus’, ‘tibial valgus’, ‘valgus deformity’, ‘coronal plane KV’, ‘coronal plane KVA’, ‘total frontal plane knee excursion’, ‘valgus malalignment’, ‘total frontal plane valgus movement’, ‘valgus lower extremity position’, ‘valgus rotation’, ‘valgus angulation’, ‘valgus position’, ‘valgus knee position’, ‘apparent valgus’, ‘mechanical femorotibial angle’, ‘knock knee’, ‘valgus displacement’, ‘valgus collapse position’, ‘KV excursion’, ‘functional valgus collapse’, ‘inward knee movement’, ‘medial knee displacement’, ‘mechanical lateral distal femoral angle’, ‘mechanical medial proximal tibial angle’, ‘anatomical lateral distal femoral angle’, ‘anatomical medial proximal femoral angle’, ‘mechanical lateral distal tibial angle’, ‘femur-tibia’, ‘hip-knee-ankle angle’, and ‘hip-knee-ankle mechanical angle’.

It should be noted again that this collection of papers is not a proper statistical sample and therefore the terms listed in Table 1 might be represented more in the full body of literature. Instead this list is meant to show the variety of terms present in the literature.

Table 1: The terms used in a collection of reviewed papers associated with KVA. Terms that are used fewer than three times are counted as 'other'.

	Angle Name									
Paper	Knee Valgus Valgus Knee	Knee Valgus Angle	Knee Abduction Knee Adduction	Dynamic Knee Valgus	Dynamic Lower Extremity Valgus	Lower Extremity Valgus	Valgus Collapse	Q-Angle	Tibiofemoral Angle	Other
Akins et al., 2013 [4]	✓	✓	✓	✓			✓			
Alentorn-Geli et al., 2009 [5]	✓	✓	✓	✓			✓			
Almeida et al., 2016 [6]		✓	✓	✓				✓		✓
Ambegaonkar et al., 2008 [7]	✓		✓							✓
Arai et al., 2013 [10]	✓									
Bates et al., 2017 [12]	✓			✓						
Battaglia et al., 2009 [14]	✓									
Benoit et al., 2006 [16]			✓							
Boling et al., 2009 [17]	✓									
Brent et al., 2013 [18]	✓	✓	✓	✓	✓					
Butler et al., 2011 [19]	✓		✓							
Cesar et al., 2016 [23]	✓			✓						
Charlton et al., 2004 [24]		✓	✓							✓
Clement et al., 2015 [25]		✓	✓							✓
Cooke et al., 2007 [26]	✓									✓
Cortes et al., 2011 [27]			✓							
Cowley et al., 2006 [28]	✓	✓	✓	✓						✓
Creaby et al., 2017 [29]	✓	✓								✓
Cronin et al., 2016 [30]	✓	✓								
Cruz et al., 2013 [31]	✓		✓							
Danino et al., 2019 [32]										✓
DeFrate et al., 2006 [36]			✓							✓
Dempsey et al., 2012 [37]	✓		✓							
Donnelly et al., 2012 [39]			✓							✓
Eberbach et al., 2017 [41]	✓									✓
Ema et al., 2017 [42]								✓		✓

Continued on next page

Table 1 – continued from previous page

	Angle Name									
Paper	Knee Valgus Valgus Knee	Knee Valgus Angle Knee Angle	Abduction	Dynamic Knee Valgus	Dynamic Lower Extremity Valgus	Lower Extremity Valgus	Valgus Collapse	Q-Angle	Tibiofemoral Angle	Other
Erhart-Hledik et al., 2018 [11]			✓							
Erhart-Hledik et al., 2019 [45]		✓	✓							
Ettinger et al., 2016 [46]		✓								
Ford et al., 2003 [50]	✓									
Ford et al., 2005 [51]	✓	✓				✓				
Ford et al., 2011 [52]	✓									
Ford et al., 2015 [49]				✓	✓					
Gardner et al., 2015 [53]			✓							
Gerber et al. 2019 [54]	✓									
Ghosh et al., 2016 [55]		✓	✓							
Graci et al., 2012 [56]									✓	✓
Grood and Suntay, 1983 [57]			✓							
Guo et al., 2019 [58]	✓									
Hall et al., 2018 [59]			✓							✓
Hanni et al., 2006 [28]	✓					✓				✓
Hardgrib et al., 2018 [60]		✓								
Hewett et al., 2005 [65]					✓					
Hewett et al., 2006 [64]	✓		✓			✓				
Hewett et al., 2008 [68]				✓	✓					
Hewett et al., 2009 [69]			✓			✓	✓			
Hewett et al., 2010 [63]			✓	✓	✓					✓
Hewett et al., 2012 [132]		✓	✓	✓	✓					
Hewett et al., 2014 [70]						✓				✓
Hewett et al., 2015 [67]			✓							
Hewett et al., 2014 [70]		✓				✓			✓	✓
Hewett et al., 2002 [71]	✓									✓
Ho et al., 2012 [73]										1

Continued on next page

Table 1 – continued from previous page

	Angle Name									
Paper	Knee Valgus Valgus Knee	Knee Valgus Angle Knee Angle	Abduction	Dynamic Knee Valgus	Dynamic Lower Extremity Valgus	Lower Extremity Valgus	Valgus Collapse	Q-Angle	Tibiofemoral Angle	Other
Hoch et al., 2017 [74]			✓							
Holden et al., 2017 [75]	✓		✓					✓		✓
Hopper et al., 2017 [77]	✓				✓					
Howard et al., 2011 [78]	✓									
Hollman et al., 2009 [76]	✓									
Hull et al., 1996 [79]		✓								
Imwalle et al., 2009 [81]	✓		✓			✓				
Ishida et al., 2011 [82]			✓	✓						
Ishida et al., 2014 [83]	✓			✓						
Issa et al., 2007 [84]	✓								✓	
Jones et al., 2014 [86]			✓	✓						
Kagaya et al., 2018 [87]	✓	✓	✓	✓						
Kellis et al., 2019 [89]										✓
Kezunović et al., 2013 [90]	✓									
Khasawneh et al., 2019 [91]								✓		✓
Kim et al., 2015 [93]	✓									
Kim et al., 2017 [92]	✓									
Kim et al., 2018 [94]	✓									
Kobayashi et al., 2010 [95]	✓		✓							✓
Kocabiyik et al., 2017 [96]	✓									
Krosshaug et al., 2007 [97]	✓									
Kunugi et al., 2018 [99]	✓									✓
Kushner et al., 2015 [101]	✓			✓						✓
Kusiak et al., 2018 [102]								✓		✓
Lam et al., 2003 [103]		✓								
Lee et al., 2018 [106]		✓								

Continued on next page

Table 1 – continued from previous page

	Angle Name									
Paper	Knee Valgus Valgus Knee	Knee Valgus Angle Knee Angle	Abduction	Dynamic Knee Valgus	Dynamic Lower Extremity Valgus	Lower Extremity Valgus	Valgus Collapse	Q-Angle	Tibiofemoral Angle	Other
Lu et al., 2019 [114]		✓								✓
Masouros et al., 2010 [116]	✓		✓							
McLean et al., 2005 [118]	✓			✓		✓				
McLean et al., 2010 [119]			✓							
Mendiguchia et al., 2011 [121]	✓					✓	✓			✓
Mendiguchia et al., 2015 [121]										✓
Mizuno et al., 2001 [124]								✓		✓
McLean et al., 2010 [119]			✓							
Myer et al., 2004 [129]	✓	✓		✓						
Myer et al., 2005 [131]	✓			✓						✓
Myer et al., 2006 [127]	✓	✓				✓				✓
Myer et al., 2008 [130]	✓		✓	✓		✓				✓
Myer et al., 2011 [126]	✓		✓	✓						
Myer et al., 2012 [132]	✓			✓						✓
Myer et al., 2014 [128]			✓							
Nagano et al., 2008 [134]	✓		✓	✓						
Naili et al., 2017 [135]	✓		✓							
Nguyen et al., 2007 [139]	✓							✓		✓
Nguyen et al., 2011 [141]		✓								
Nguyen et al., 2015 [140]	✓	✓								✓
Nilstad et al., 2015 [142]	✓			✓						
Numata et al., 2018 [144]	✓			✓			✓			
O'Kane et al., 2017 [145]										✓
Olesen et al., 2019 [146]										
Orishimo et al., 2014 [149]	✓	✓	✓							
Padua et al., 2009 [151]	✓	✓								
Palad et al., 2018 [152]		✓								

Continued on next page

Table 1 – continued from previous page

	Angle Name									
Paper	Knee Valgus Valgus Knee	Knee Valgus Angle Knee Angle	Abduction	Dynamic Knee Valgus	Dynamic Lower Extremity Valgus	Lower Extremity Valgus	Valgus Collapse	Q-Angle	Tibiofemoral Angle	Other
Palanisami et al., 2019 [153]	✓									
Palmer et al., 2019 [153]	✓			✓						✓
Palmieri-Smith et al., 2007 [155]	✓	✓	✓							✓
Patel et al., 2004 [156]	✓									
Patrek et al., 2011 [158]	✓		✓							
Paterno et al., 2010 [157]	✓									
Petersen et al., 2017 [159]	✓		✓	✓	✓				✓	✓
Pitcairn et al., 2018 [162]		✓								
Pollard et al., 2009 [163]	✓	✓								
Popkov et al., 2017 [164]	✓									✓
Rajasekar et al., 2017 [165]	✓	✓	✓	✓						
Resende et al., 2016 [166]			✓							
Ribeiro et al., 2013 [167]	✓									
Saç et al., 2018 [168]								✓		✓
Sakurai et al., 2019 [170]	✓		✓	✓						
Salsich et al., 2013 [171]									✓	
Sanfridsson et al., 2001 [172]								✓		✓
Schmidt et al., 2017 [174]		✓	✓	✓						
Sener et al., 2019 [43]								✓		✓
Sheehy et al., 2011 [178]										
Sheehy et al., 2015 [177]	✓									✓
Shin et al., 2009 [179]	✓	✓								✓
Stickler et al., 2015 [188]										
Tamura et al., 2017 [189]				✓						
Teng et al., 2014 [191]			✓						✓	✓
Teng et al., 2017 [192]	✓	✓								
Tokuhara et al., 2003 [193]										✓

Continued on next page

Table 1 – continued from previous page

	Angle Name									
Paper	Knee Valgus Valgus Knee	Knee Valgus Angle Knee Angle	Abduction	Dynamic Knee Valgus	Dynamic Lower Extremity Valgus	Lower Extremity Valgus	Valgus Collapse	Q-Angle	Tibiofemoral Angle	Other
Tran et al., 2016 [194]	✓			✓						
Turner et al., 2018 [197]	✓	✓								✓
Uttarkar et al., 2013 [197]							✓			✓
Vanrenterghem et al., 2012 [199]	✓									✓
Weinhandl et al., 2015 [202]			✓							✓
Xie et al., 2018 [206]										✓
Yang et al., 2010 [207]	✓									✓
Yoo et al., 2008 [208]		✓								✓
Zazulak et al., 2005 [209]					✓	✓	✓			✓

Table 2 lists the number of times each term was used in the 143 publications. In many cases, more than one knee valgus (KV) term was used in a single paper. As a result, the total number of uses listed in Table 2 does not equal the number of papers analyzed. In many of those instances, the different terms in the paper are actually describing multiple types mathematical calculations of the KVA. In other cases, the different terms in a paper are only referencing a single mathematical measurement of that KVA.

Table 2: The number of terms used in 143 publications. Note that the total number of uses and number of publications are not equal, because more than one term can be used in a single publication.

Term	**Number of uses**
Knee Valgus — Valgus Knee	79
Knee Valgus Angle — Knee Angle (refering to KVA)	37
Abduction — Adduction	52
Dynamic Knee Valgus	31
Dynamic Lower Extremity Valgus	9
Lower Extremity Valgus	14
Valgus Collapse	7
Q-Angle	10
Tibiofemoral	6
Other	57
Total Number of Terms:	302
Number of Publications:	143

2.2 Calculation Variations

2.2.1 Introducing Angle Measurements

KVA can be calculated in multiple ways and they can be broken down into four components: rotating axis, reference axis, frontal plane, and dimensions. The rotating axis is defined by the vertical axis of the shank; this definition is unchanging across publications. The reference axis is the 'zero axis'. The KVA is the measure between the rotating axis and the reference axis. Often times the rotating axis or the reference axis are projected onto a frontal plane that is a predetermined representation of the human anatomy. Lastly, the dimensions of the angle can be determined by whether the axes are projected onto a frontal plane (2D) or measured freely in space (3D). Each of these elements determine the type of KVA measured. One combination of the KVA elements is not necessarily better than another; the type of angle measured is dependent on the purpose for the measurement and available instrumentation. As a result, many measurement calculation methods have been developed. The reference axis and frontal plane is largely dependent on available coordinate systems and the dimensionality is dependent on the use of the frontal plane.

2.2.2 Coordinate Systems

There are a variety of coordinate systems used to evaluate the KVA. The most frequently used methods utilize local (coordinate systems fixed to the thigh and shank segments), global (fixed, non-accelerating coordinate system external to the individual), or a combination of the two coordinate systems.

Joint Coordinate System

The local coordinate system used to quantify knee orientation has been described by Grood and Suntay in what they called the 'joint coordinate system' (JCS)[57]. This is a non-orthogonal

coordinate system calculated from the axes on the proximal segment (lateral axis: e_1; anterior axis: e_1^r) and distal segment (vertical axis: e_3; anterior axis: e_3^r). The axes e_1 and e_3 are used to define e_2. Rotation about the e_1, e_2, and e_3 axes are flexion (α), abduction (β), and internal rotation (γ), respectively. These axes and angles can be seen in Figure 3. This method of measuring joint angles is commonly accepted amongst researchers and medical professionals as the coordinate system used to measure flexion, abduction, and internal rotation of the knee[16,36,51,57,78,119,151,198].

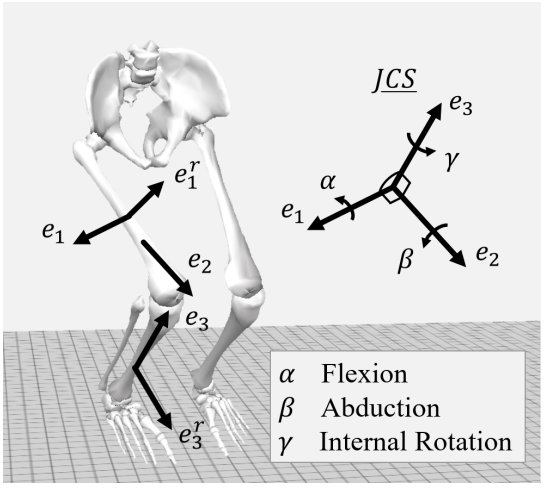

Figure 3: The JCS by Grood and Suntay using the local coordinates (e_1, e_1^r, e_3, and e_3^r) and floating vector (e_2) to calculate flexion (α), abduction (β), and internal rotation (γ)[57].

Global Coordinate System

Alternatively, the global coordinate system is not defined by the position of individual. The coordinate system is a non-accelerating, earth-fixed reference frame that is commonly placed with its origin in the motion capture lab[10,37,63,65,95,133,191]. It is standard practice in biomechanical studies to define the X and Y axes as the floor plane and the Z axis as the vertical axes (G_X, G_Y, and G_Z, respectively), shown in Figure 4. A coordinate system may use one or all of these axes from the JCS and the global coordinate system to define medial knee alignment.

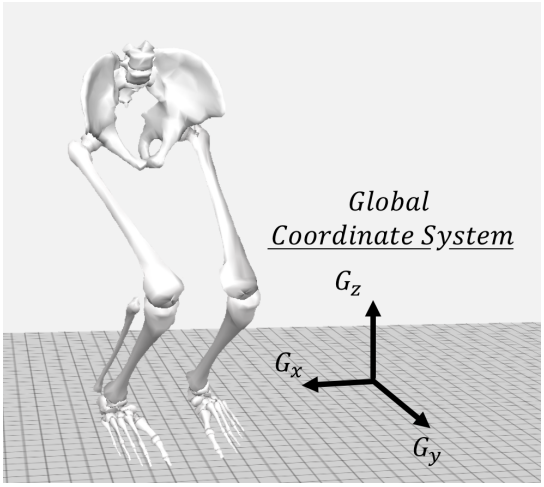

Figure 4: The global coordinate system where G_Z is orthogonal to the floor plane[65].

2.2.3 Reference Axis

The reference axis is the 'zero axis' at which the vertical axis of the shank (e_3) is measured. The KVA is the angle between the reference axis and the e_3 axis. Most commonly, the reference axis is either the vertical thigh axis ($Thigh_Z$) or G_Z.

2.2.4 Frontal Plane

Defining the frontal plane (the plane in which KVA is measured) is essential when measuring KVA, even if only to distinguish between valgus and varus. The definition of the frontal plane determines the facing of the coordinate system in space and gives meaning to that orientation. In a local coordinate system, the frontal plane of the femur (e_1 and $Thigh_Z$) is used as the frontal plane for KVA. The global coordinate system is pre-defined by the configuration of the testing space, firstly by either designating a 2D camera facing or a 3D coordinate system defined in the space, and, secondly, by the subject moving through the capture volume.

There are less common methods of defining the frontal plane. An alternative method is to mix the local and global coordinate system, using the pelvis to define the lateral axis and

the global coordinate system to define the vertical axis. These two axes come together to define the frontal plane. This frontal plane rotates as the subject moves through the capture volume. Another is to define the frontal plane in gait analysis by the plane perpendicular to the line of action. If the subject moves from one side of the capture volume to the other, the perpendicular plane then becomes the frontal plane. These last two methods are used in biomechanics research, but are uncommon in the measurement of KVA associated with ACL ruptures.

2.2.5 Dimensions

KVA can be measured in both two- or three-dimensions (2D and 3D, respectively). If measured in 2D, the value of the KVA is measured in the defined frontal plane. If measured in 3D, the plane of the angle becomes a pseudo-frontal plane, since it is not certain to have anatomical meaning. For example, if the frontal plane was defined by e_3 and G_Z, the plane would rotate about the G_Z axis depending on the orientation of the shank. If defined in this way, the 'frontal plane' could have any orientation all of which would not necessarily be in any anatomical frontal plane orientation.

2.2.6 Angle Calculation Examples

For clarity, examples of different configurations of KVA utilizing the elements previously described are shown below. Additionally, possible reasons behind the use of that particular method of calculation are given to show the reasoning behind the use of a wide variety of measures for KVA. Popular uses of the examples given will be discussed in Sections 2.3 and 2.4. Each example angle has three components: 1) vertical axis, 2) frontal plane, and 3) dimensions used. The fourth component, rotating axis, is assumed to be e_3 in each of the following examples.

These components can be seen listed in Table 3 and include specific elements for each of the components. The thigh vertical axis is the vertical axis of the thigh defined by Wu et al.[204]. The vertical axis of the global plane (G_Z) and the global frontal plane (G_X-G_Z) can be seen in Figure 4. The pelvis frontal plane is defined by the lateral axis of the pelvis (P_X) and the global vertical axis (G_Z); details of this plane will be discussed later in this section.

Table 3: The three components that define KVA: 1) reference axis, 2) frontal plane, and 3) dimensions. The rotating axis is assumed to be e_3.

Reference Axis	**Frontal Plane**	**Dimensions**
Thigh ($Thigh_Z$)	Thigh (e_1-e_3)	2D
Global (G_Z)	Global (G_X-G_Z)	3D
	Pelvis (P_X-G_Z)	

Example Angles 1-3

For Example Angles 1-3, the angles are measured using the frontal plane of the global system (G_X-G_Z) (Table 4 and Figure 5; Table 5 and Figure 6; and Table 6 and Figure 7). For Example Angle 1 (Table 4 and Figure 5), the angle is measured between the thigh and the shank in the global frontal plane. For Example Angle 2 (Table 5 and Figure 6), the angle is measured between the shank and the vertical global axis in the global frontal plane. For Example Angle 3 (Table 6 and Figure 7), the angle is measured between the shank and the global vertical axis with no defined frontal plane. Angles 1 and 2 do not require 3D instrumentation because the shank and thigh axis are projected onto a frontal plane. However, 3D instrumentation can be used to calculate these angles. These 2D measurements restrict the task movement because of the predefined frontal plane in the global system. Angle 3 does require 3D instrumentation because the shank axis is not necessarily oriented with the global axes.

Table 4: The elements for Angle 1 are 1) reference axis = $Thigh_Z$, 2) frontal plane = G_X-G_Z, and 3) dimensions = 2D. Emboldened text represent the elements used for this angle.

Reference Axis	**Frontal Plane**	**Dimensions**
Thigh ($Thigh_Z$)	Thigh (e_1-e_3)	**2D**
Global (G_Z)	**Global (G_X-G_Z)**	3D
	Pelvis (P_X-G_Z)	

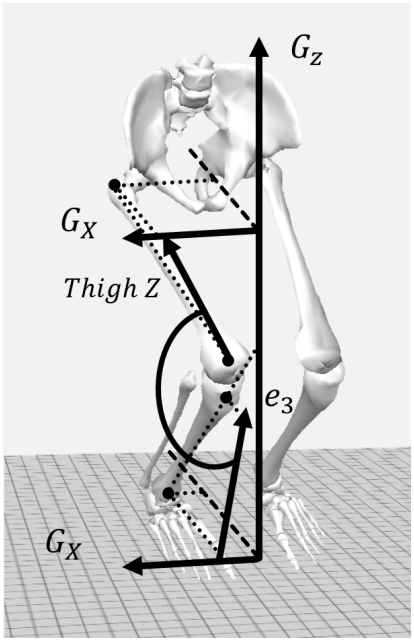

Figure 5: Angle 1: 1) vertical axis = $Thigh_Z$, 2) frontal plane = G_X-G_Z, and 3) dimensions = 2D. See Table 4.

Table 5: The elements for Angle 2 are 1) reference axis = G_Z, 2) frontal plane = G_X-G_Z, and 3) dimensions = 2D. Emboldened text represent the elements used for this angle.

Reference Axis	**Frontal Plane**	**Dimensions**
Thigh ($Thigh_Z$)	Thigh (e_1-e_3)	**2D**
Global (G_Z)	**Global (G_X-G_Z)**	3D
	Pelvis (P_X-G_Z)	

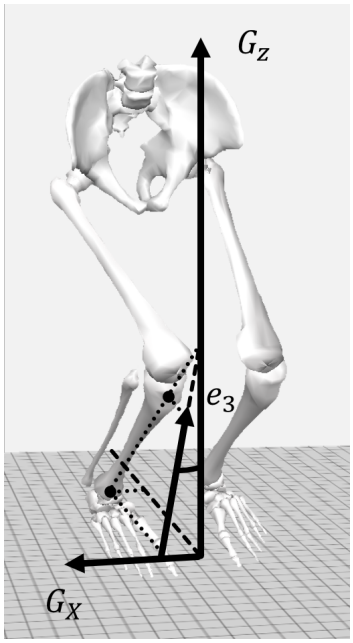

Figure 6: Angle 2: 1) vertical axis = G_Z, 2) frontal plane = G_X-G_Z, and 3) dimensions = 2D. See Table 5.

Table 6: The elements for Angle 3 are 1) reference axis = G_Z, 2) frontal plane = G_X-G_Z, and 3) dimensions = 3D. Emboldened text represent the elements used for this angle.

Reference Axis	**Frontal Plane**	**Dimensions**
Thigh ($Thigh_Z$)	Thigh (e_1-e_3)	2D
Global (G_Z)	**Global (G_X-G_Z)**	**3D**
	Pelvis (P_X-G_Z)	

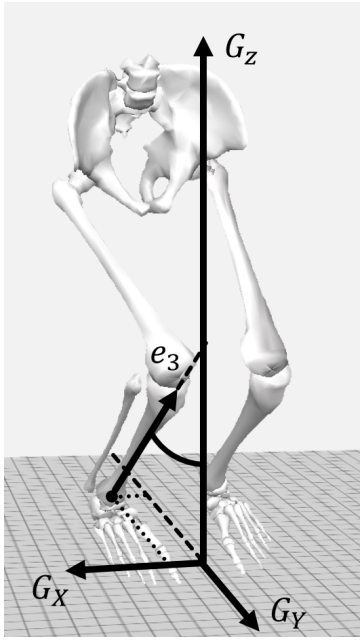

Figure 7: Angle 3: 1) vertical axis = G_Z, 2) frontal plane = G_X-G_Z, and 3) dimensions = 3D. See Table 6.

Example Angle 4

Example Angle 4 is measured between the shank and the global vertical axis in the pelvis frontal plane (Table 7 and Figure 7). The frontal plane fixed to the subject allows for freedom of movement based on its dynamically changing reference frame.

Table 7: The elements for Angle 4 are 1) reference axis = G_Z, 2) frontal plane = P_X-G_Z, and 3) dimensions = 2D. Emboldened text represent the elements used for this angle.

Reference Axis	**Frontal Plane**	**Dimensions**
Thigh ($Thigh_Z$)	Thigh (e_1-e_3)	**2D**
Global (G_Z)	Global (G_X-G_Z)	3D
	Pelvis (P_X-G_Z)	

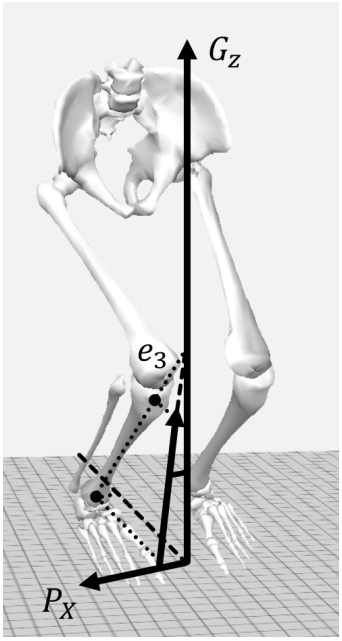

Figure 8: The elements for Angle 4 are 1) vertical axis = G_Z, 2) frontal plane = P_X-G_Z, and 3) dimensions = 2D. See Table 7.

Angle 5

Example Angle 5 is measured between the shank and the thigh in the thigh frontal plane (Table 8 and Figure 8). This is also defined as the perpendicular to e_1[57]. The frontal plane is fixed to the thigh and therefore dynamically changes with the subject. This allows the subject to move around the capture volume freely.

Table 8: The elements for Angle 5 are 1) reference axis = $Thigh_Z$ or $\perp$ e_1, 2) frontal plane = e_1-e_3, and 3) dimensions = 2D. Emboldened text represent the elements used for this angle[57].

Reference Axis	**Frontal Plane**	**Dimensions**
Thigh ($Thigh_Z$)	**Thigh** (e_1-e_3)	**2D**
Global (G_Z)	Global (G_X-G_Z)	3D
	Pelvis (P_X-G_Z)	

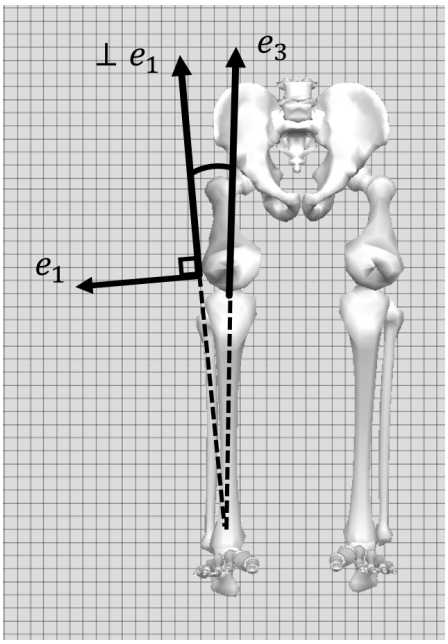

Figure 9: Angle 5: 1) vertical axis = $\perp e_1$, 2) frontal plane = e_1-e_3, and 3) dimensions = 2D[57]. See Table 8.

2.2.7 Angle Calculation References

The papers reviewed in Section 2.1.3 were published in a variety of journals from *Robotica* to *Journal of Strength Conditioning Research* and *Journal of Children's Orthopaedics* to *Cartilage*. The wide application of KVA in different fields of study means that some studying or making use of the KVA might not have extensive training in mathematics. Therefore, for some, the slight distinction between the angles described in Sections 2.2.6 becomes enigmatic. Table 9 lists the journals where the papers in Table 1 were published.

Table 9: The journals where the papers from Table 1 were published.

Journal Name	Number of Papers	Journal Name	Number of Papers
Acta Radiologica	1	*Journal of Science and Medicine in Sport*	2
American Journal of Sports Medicine	13	*Journal of Sport and Health Science*	2
Annals of Internal Medicine	1	*Journal of Sport Rehabilitation*	1
Archives of Orthopaedic and Trauma Surgery	1	*Journal of Sports Medicine*	1
Arthritis Care and Research	1	*Journal of Sports Sciences*	1
Asia-Pacific Journal of Sports Medicine, Arthroscopy,	1	*Journal of Strength Conditioning Research*	4
Rehabilitation and Technology	1	*The Knee*	8
Athletic Therapy Today	1	*Knee Surgery and Related Research*	1
British Journal of Sports Medicine	2	*Knee Surgery, Sports Traumatology, Arthroscopy*	3
Cartilage	1	*Medicine and Science in Sports and Exercise*	4
Clinical Biomechanics	5	*Montenegrin Journal of Sports Science and Medicine*	1
Clinical Orthopaedics and Related Research	2	*North American Journal of Sports Physical Therapy*	1
Danish Medical Journal	1	*Orthopaedic Journal of Sports Medicine*	2
Exercise and Sport Sciences Reviews	2	*Orthopaedics and Trauma*	1
Frontiers in Physiology	1	*Osteoarthritis and Cartilage*	3
Gait and Posture	4	*Physical Therapy*	1
International Orthopaedics	1	*Physical Therapy in Sport*	4
Isokinetics and Exercise Science	2	*Physiotherapy Quarterly*	1
Journal of Sport Rehabilitation	1	*PLoS ONE*	3
Journal of Arthroplasty	1	*Research in Sports Medicine*	1
Journal of Athletic Training	8	*Revista Brasileira de Ortopedia (English Edition)*	1
Journal of Biomechanical Engineering	1	*Robotica*	1
Journal of Biomechanics	7	*Scandinavian Journal of Medicine and Science in Sports*	2
Journal of Bodywork and Movement Therapies	1	*Sports*	1
Journal of Bone and Joint Surgery	2	*Sports Biomechanics*	2
Journal of Children's Orthopaedics	1	*Sports Medicine*	1
Journal of Education and Training Studies	1	*Stem Cell Research and Therapy*	1
Journal of Electromyography and Kinesiology	1	*Strategies in Trauma and Limb Reconstruction*	1
Journal of Experimental Orthopaedics	1	*Strength and Conditioning Journal*	2
Journal of Korean Medical Science	1	*The American Journal of Sports Medicine*	1
Journal of Orthopaedic and Sports Physical Therapy	3	*The Bone and Joint Journal*	1
Journal of Orthopaedic Research	5	*Turkish Journal of Physical Medicine and Rehabilitation*	1
Journal of Orthopaedics	1		

Table 10 lists the method of calculating the angle associated with KV for each study. A number of papers discussed KVA in the introduction or background and cited other studies discussing KVA, but those citations often referenced multiple publications with different types of

KVA or studies that also had undefined KVA. Therefore, in this review, the paper was considered to have an undefined KVA if the angle was not explicitly defined.

Table 10: The mathematical calculation of angles associated with KVA in a collection of papers.

Reference Axis:	$Thigh_Z$			G_Z		
Frontal Plane:	e_1-e_3	G_Z-e_3	None	G_X-G_Z	Undefined	Exceptions
Dimensions:	2D	2D	3D	2D		
Akins et al., 2013 [4]					Reference wu	
Almeida et al., 2016 [6]		✓				
Benoit et al., 2006 [16]	✓					
Boling et al., 2009 [17]	✓	✓			✓	
Butler et al., 2011 [19]					✓	
Cesar et al., 2016 [23]	✓					
Charlton et al., 2004 [24]	✓					
Clement et al., 2015 [25]					✓	
Cooke et al., 2007 [26]		✓				
Cowley et al., 2006 [28]					✓	
Creaby et al., 2017 [29]		✓				
DeFrate et al., 2006 [36]	✓					
Dempsey et al., 2012 [37]			✓			
Donnelly et al., 2012 [39]						
Eberbach et al., 2017 [41]					✓	
Ford et al., 2005 [51]	✓					
Gerber et al., 2019 [54]					✓	
Graci et al., 2012 [56]	✓					
Grood and Suntay, 1983 [57]	✓					
Hall et al., 2018 [59]					✓	
Hewett et al., 2005 [65]					✓	
Hewett et al., 2010 [63]	✓		✓			
Hopper et al., 2017 [77]					✓	
Howard et al., 2011 [78]	✓					
Hull et al., 1996 [79]					✓	
Imwalle et al., 2009 [81]					✓	
Issa et al., 2007 [84]					✓	
Kagaya et al., 2018 [87]					✓	
Kezunović et al., 2013 [90]					✓	
Kobayashi et al., 2010 [95]						Game footage
Kushner et al., 2015 [101]					✓	
Masouros et al., 2010 [116]	✓					
McLean et al., 2010 [119]	✓					
Nagano et al., 2008 [134]	✓					
Nguyen et al., 2007 [139]			✓			
Nguyen et al., 2015 [140]						
Nilstad et al., 2015 [142]					✓	
O'Kane et al., 2017 [145]						
Orishimo et al., 2014 [149]					✓	

Continued on next page

Table 10 – continued from previous page

Reference Axis:	$Thigh_Z$ - e_3		G_Z - e_3			
Frontal Plane:	e_1-e_3	G_Z-e_3	None	G_Z-e_3	Undefined	Exceptions
Dimensions:	2D	2D	3D	2D		
Padua et al., 2009 [151]	✓					
Palmer et al., 2018 [154]						Horizontal distance between the toe and knee
Palmieri-Smith et al., 2007 [155]					✓	
Patel et al., 2004 [156]	✓					
Paterno et al., 2010 [157]		✓				
Pollard et al., 2009 [163]					✓	
Rajasekar et al., 2017 [165]						Horizontal distance between the toe and knee
Ribeiro et al., 2013 [167]					✓	
Saç et al., 2018 [168]						
Sakurai et al., 2019 [170]	✓				✓	
Sanfridsson et al., 2001 [172]		✓				
Schmidt et al., 2017 [174]					✓	
Sheehy et al., 2015 [177]					✓	
Shin et al., 2009 [179]					✓	
Shultz 2012 [181]			✓			
Stickler et al., 2015 [188]		✓				
Teng et al., 2017 [192]	✓					
Turner et al., 2018 [197]			✓			
Uttarkar et al., 2013 [197]	✓					
Zazulak et al., 2005 [209]						

A number of papers listed in Table 10 used angles that were undefined. Even though many papers did not explicitly define KVA, they cited other publications in the introduction or background that did have definitions for KVA. However, even though the 2005 publication by Hewett et al. entitled "Biomechanical Measures of Neuromuscular Control and Valgus Loading of the Knee Predict Anterior Cruciate Ligament Injury Risk in Female Athletes: A Prospective Study" (valgus: reference axis = G_Z, frontal plane = G_X-G_Z, and dimensions = 3D) has been cited 2,870 times[65]. However, all of those 2,870 publications do not necessarily use the KVA 3G calculation method to calculate their KVA. Likewise, the 1983 publication by Grood and Suntay entitled "A Joint Coordinate System for the Clinical Description of Three-Dimensional Motions: Application to the Knee" (knee abduction angle: the angle between e_1 and e_3) has been cited by 3,493 publications[57]. This does not mean that all 3,493 publications

used the knee abduction angle to define KVA.

The mass use of angles associated valgus has led to the development of many terms and calculation methods meant to define the alignment. As a result, ambiguity exists in the literature on how the KVAs are labeled and calculated.

2.3 Joint Coordinate System (Grood and Suntay, 1983)[57]

To measure angles using the joint coordinate system, orthogonal, local coordinate systems are fixed to the proximal and distal segments (Femur (thigh) and Tibia (shank), respectively). Using the notation from Grood and Suntay's work, the proximal segment is defined by the lateral axis (e_1) and anterior axis (e_1^r) shown in Figure 10[57]. The distal segment is defined by the anterior axis (e_3^r) and superior axis (e_3), Figure 10[57]. The proximal superior axis and distal lateral axis were not defined by Grood and Suntay[57]; in this work they will be referred to as thigh Z and shank X, respectively. A new coordinate system, JCS, is created by crossing e_1 with e_3 which creates the third axis, e_2, shown in Equation 1 and Figure 10. The axes e_1 and e_3 are not orthogonal to one another and therefore this coordinate system is a non-orthogonal coordinate system. Additionally, e_1 and e_3 are located on two different segments that are not positionally connected with one another, so the axis created from them, e_2, has no defined position in space. As result, the e_2 axis and JCS are referred to as a floating axis and coordinate system[57]. The axes of the coordinate system align with anatomical rotations given to joints where the rotation about e_1 is flexion, e_2 is abduction, and e_3 is internal rotation, Figure 10 and 11.

$$e_2 = \frac{e_3 \times e_1}{\|e_3 \times e_1\|} \tag{1}$$

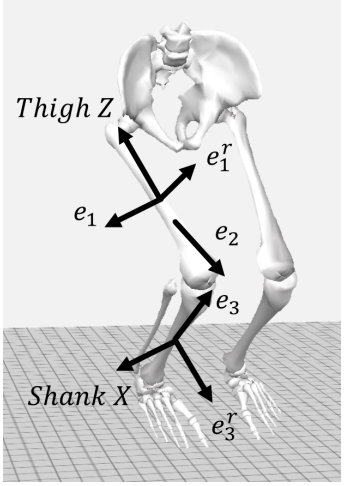

Figure 10: Proximal and distal coordinate system as well as the e_2 floating vector used to define the joint coordinate system (JCS) by Grood and Suntay[57].

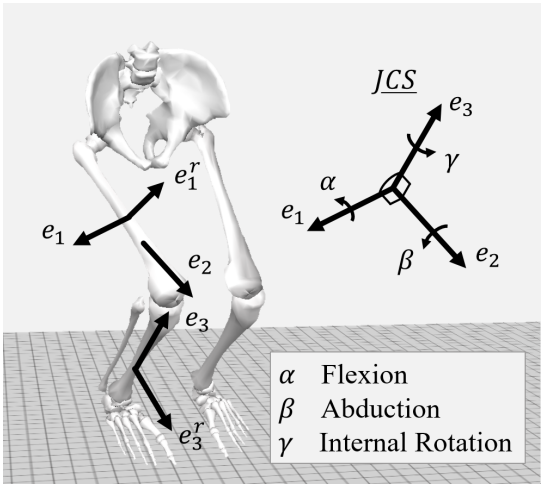

Figure 11: The non-orthogonal, sequence independent JCS by Grood and Suntay using the local coordinates (e_1, e_1^r, e_3, and e_3^r) to calculate flexion (α), abduction (β), and internal rotation (γ)[57].

2.3.1 Knee Flexion Calculation

The knee flexion angle is measured between the shank and the thigh in the thigh sagittal plane. The proximal (thigh) anterior axis (e_1^r) is used as a reference axis to the distal segment (thigh) to measure the degree of rotation about the e_1 axis. Initially, e_1^r and e_2 are perfectly aligned. When in flexion, e_2 is rotated about e_1 while e_1^r becomes the reference axis. Because both e_1^r (by definition) and e_2 (by calculation) are always orthogonal to e_1 the angle measured between

these two axes, using the dot product, is an angle measured in the e_1 plane (proximal sagittal plane; e_1^r-e_2 plane) about e_1 (proximal lateral axis). This angle can be calculated using the cross product in Equation 1 in combination with the dot product of e_1^r and e_2, shown in Equation 2 and Figure 12. This type of calculation is referred to as a scalar triple product.

$$\cos\alpha = e_1^r \cdot \frac{e_3 \times e_1}{\|e_3 \times e_1\|} = e_1^r \cdot e_2 \tag{2}$$

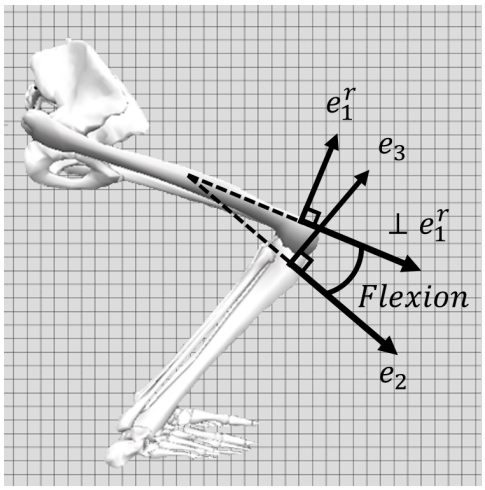

Figure 12: Flexion: Lateral view of the lower limb depicting the axes used to calculate flexion using the JCS by Grood and Suntay[57].

Conceptually, the flexion angle can be understood as the angle between the projection of e_3 onto e_1 and the proximal Z axis. Additionally, flexion can be calculated using the first rotation of an X-Y-Z Euler sequence. Details of the conversion between the JCS and X-Y-Z Euler rotations can be found in Appendix A.

2.3.2 Knee Flexion Angle Usage

The JCS is widely used by researchers and medical professionals to measure flexion in an anatomical joint[16,17,23,24,51,56,63,116,119,134,151,183,192,198]. Even before Grood and Suntay published the JCS that clarified and documented a specified way of calculating knee flexion, the first rotation of the Euler XYZ sequence was already being used to calculate this angle[57].

2.3.3 Knee Abduction Angle Calculation

The knee abduction angle (β) is measured as the angle between e_1 and e_3 (the JCS is not orthogonal). The axis, e_1, is the reference axis and the angle is a result of e_3 rotation about e_2 (floating axis). This angle can be calculated using the dot product of e_1 and e_3 to calculate β' (Equation 3). For the right leg 90-degrees are added to β so that the calculated angle is from the e_1 plane (proximal sagittal plane; e_1^r-e_2 plane) to the e_3 axis (distal vertical axis), shown in Equation 4 and Figure 13. The reverse is true for the left leg.

$$\cos \beta' = e_1 \cdot e_3 \tag{3}$$

$$\beta + \frac{\pi}{2} = \beta' \tag{4}$$

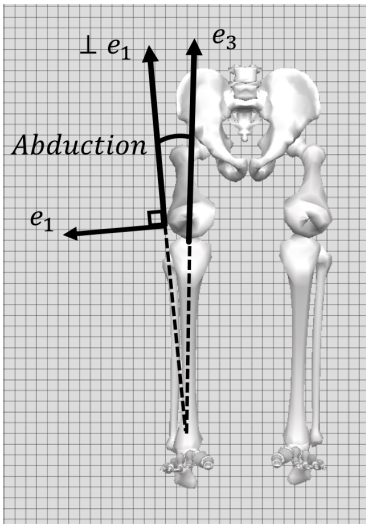

Figure 13: The knee abduction angle: Inferior view of the femur and frontal view of the shank depicting the axes used to calculate the knee abduction angle using the JCS by Grood and Suntay[57].

Conceptually, the knee abduction angle can be understood as an angle between the projection of e_3 onto the e_1 plane (proximal sagittal plane; e_1^r-e_2 plane) and e_3 (distal superior axis). Additionally, the knee abduction angle can be calculated using the second rotation of an Euler

XYZ sequence. Details of the conversion between the JCS and X-Y-Z Euler rotations can be found in Appendix A.

Even though the terms 'valgus' and 'varus' were not in Grood and Suntay's publication, the knee abduction angle has since been referred to as the valgus angle due to the definition of valgus[57]. In this work, the JCS abduction angle will be referred to as 'abduction angle' (not valgus angle).

2.3.4 Knee Abduction Usage

The abduction angle is also used to determine knee alignment as it relates to ACL injuries and health[16,36,44,116,119,198,202]. Because the calculation of the knee abduction angle only requires the shank and femur, it is often used in imaging, such as magnetic resonance imaging (MRI) and computed tomography (CT) scans, where the global axes is arbitrary it is often used to measure the valgus knee angle[10,44].

2.3.5 Knee Internal Rotation Angle Calculation

The internal rotation angle is calculated much like the flexion angle, with the triple cross product. The angle is measured between the shank and the thigh in the shank transverse plane. The distal (shank) anterior axis (e_3^r) was used in reference to the proximal segment to measure the degree of rotation about the e_3 axis. Initially, e_3^r and e_2 are perfectly aligned. When in a rotated position, e_3^r is rotated about e_3 and the e_2 axis becomes the reference axis. Because e_3^r (by definition) and e_2 (by calculation) are always orthogonal to e_3, the angle measured between these two axes, using the dot product, is an angle measured in the e_3 plane (distal transverse plane; e_3^r-$e2$ plane)about e_3 (distal vertical axis). This angle can be calculated using the cross product

in Equation 1 in combination with the dot product of e_3^r and e_2, shown in Equation 5.

$$\cos\gamma = \frac{e_3 \times e_1}{\|e_3 \times e_1\|} \cdot e_3^r = e_2 \cdot e_3^r \tag{5}$$

2.3.6 Unique, Independent Angles

The angles calculated from the JCS (flexion, abduction, and internal rotation) are unique angles that are independent from one another. JCS angles can also be calculated using an X-Y-Z Euler sequence, see Appendix A. The Euler rotation sequence is a commonly used mathematical calculation amongst engineers and mathematicians and is therefore a commonly used method used to calculate joint angles. However, though it is straightforward, the Euler calculation of the angles can be misleading because the calculation is sequence-dependent and the JCS angles are independent. Additionally, the fact that the JCS angles are independent can be difficult to conceptualize, given the movement of the segments in 3D space. Figures 14 and 15 are examples showing how flexion and internal rotation angles do not influence the magnitude of the abduction angle (Equation 3). Figure 14 has four configurations of the e_1 and e_3 axes. When the angle between e_1 and e_3 is 90°, β_1, there is no knee abduction angle. When the angle between e_1 and e_3 is $> 90°$, β_2, there is an abduction angle equal to $\beta_2 - \beta_1$. Any amount of rotation about the e_1 axis (which would be flexion), does not change the abduction angle (β_1 or β_2). When the angle between e_1 and e_3 is $> 90°$, β_2, there is a knee abduction angle equal to $\beta_2 - \beta_1$. Any amount of rotation about the e_3 axis (which would be an internal rotation angle), would not change the knee abduction angle (β_1 or β_2).

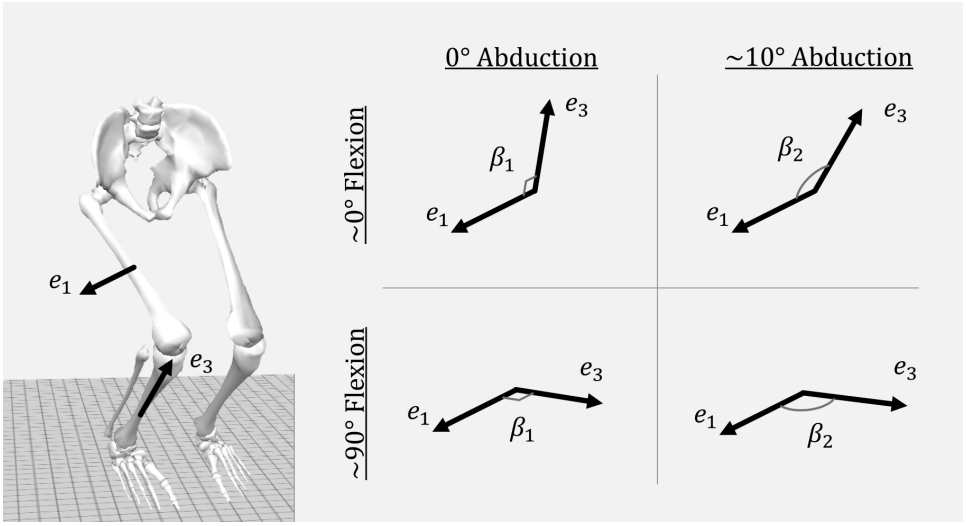

Figure 14: The unchanging knee abduction angle given a rotation about the e_1 axis (flexion angle).

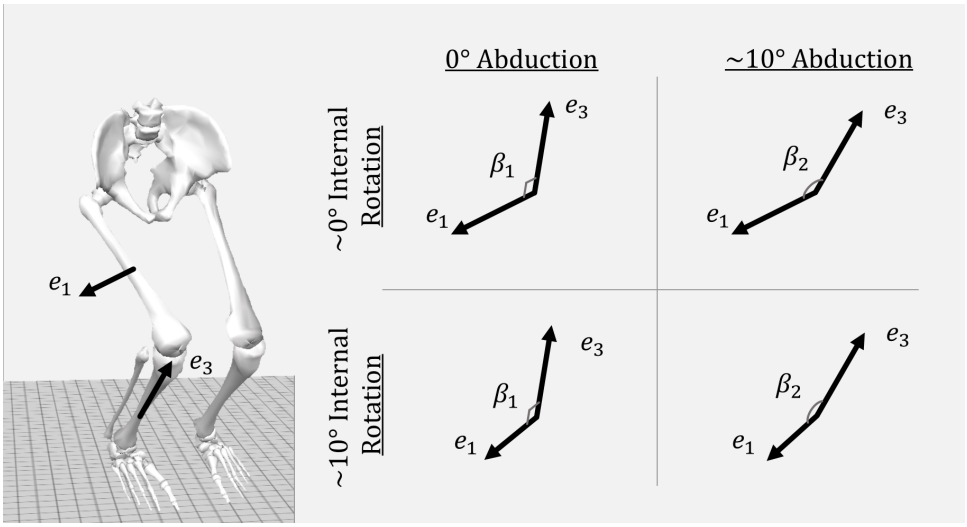

Figure 15: The unchanging knee abduction angle given rotation about the e_3 axis (internal rotation angle).

2.4 Dynamic Knee Valgus Angle (Hewett et al., 2005)[65]

In 2005, Hewett et al. defined an angle for knee valgus that could be calculated from an external perspective using the global reference frame that is fixed to the ground[65]. Illustrated in Figures 4 and 16, this coordinate system can be imagined as the external visual perspective of the patient, athlete, client etc. by the physical therapist, athletic trainers, strength and conditioning

coaches, personal trainers etc..

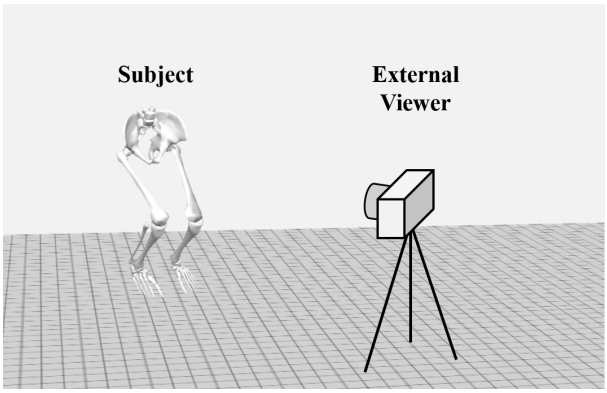

Figure 16: An external view of a subject.

Before the angle can be calculated, the global coordinate system is first fixed to the space. The floor plane is defined as G_Y-G_X, where G_Y is fixed as the anterior axes and G_X is fixed as the lateral axis. Consequently, G_Z is perpendicular to the G_X-G_Y plane and is fixed as the vertical axis. The direction of the G_X and G_Y axes are predetermined based on the orientation of the room (or force plates) and planned task of the subject. When force plates are present, the G_Y axis is typically aligned with force plates and the intended anterior axis of the subject. Similarly, G_X is aligned with the force plates and lateral axis of the subject. As a result, the G_X-G_Z plane is defined as the frontal plane. For example, if the subject plans to jog or walk, the G_Y axis faces the direction in which the subject intends to jog across the force plates, as in Figure 17. Likewise, if the subject plans to perform a drop-jump, the G_Y will rotate to match the new need of the force plates, Figure 18. In both Figure 17 and 18 the subject's anterior axis is G_Y, lateral axis is G_X, and G_Z is perpendicular to the force plates.

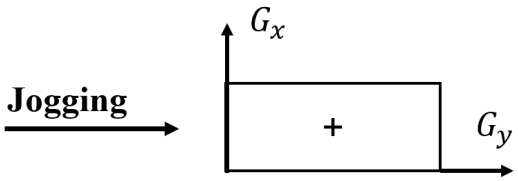

Figure 17: Example of jogging direction on force plates in reference to the global coordinate system (G_X and G_Y). The subject is jogging in the direction indicated by the emboldened arrow. The directions of the G_X and G_Y axes are determined by the position of the subject. G_X is defined as the lateral axis and G_Y is defined as the anterior axis.

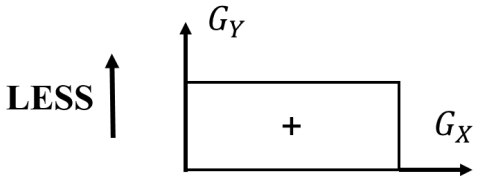

Figure 18: Example of LESS direction on force plates in reference to the global coordinate system (G_X and G_Y). The subject is performing a drop jump by jumping in the direction indicated by the emboldened arrow. The directions of the G_X and G_Y axes are determined by the position of the subject. G_X is defined as the lateral axis and G_Y is defined as the anterior axis.

2.4.1 Global Reference 2D

KVA 2G is a projection of the shank onto the global frontal plane (G_X-G_Z). The angle can then be calculated between the shank and the vertical axis, shown in Figure 19. Because this angle is projected onto the global frontal plane, it can be measured with a wide variety of instrumentation, from motion capture to simple 2D photography. This makes the angle easily accessible as it can be calculated with simple photography.

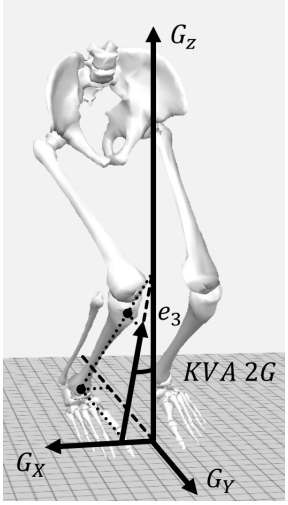

Figure 19: KVA measured in two dimensions (KVA 2G) between the shank (e_3) and the global vertical axis (G_Z).

2.4.2 KVA Global Reference 3D

For the calculation of KVA 3G, the distal shank (e_3) and the global coordinate system are the only axes needed. The dot product is used between e_3 and G_Z, shown in Equation 6 and Figure 20. The axis e_3 is not projected onto a frontal plane, and therefore the angle calculated then becomes the frontal plane. This calculation measures an angle with magnitude and no direction, as the shank can rotation around the G_Z while keeping the same value for KVA 3G. Hewett et al. found this angle correlated with future ACL injuries when measured during a drop-jump task, jumping off a box and rebounding vertically[65].

$$\cos(KVA\,3G) = G_z \cdot e_3 \tag{6}$$

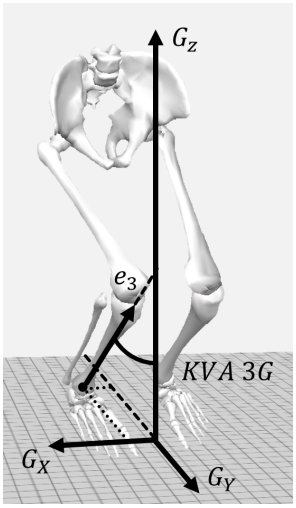

Figure 20: KVA measured in three dimensions (KVA 3G) between the shank (e_3) and the global vertical axis (G_Z) as calculated by Hewett et al.[65].

2.4.3 KVA Global Coordinate System Sign Convention

The KVA 3G angle is sometimes only measured in magnitude[65] rather than magnitude and direction. Because of the directionless calculation, the angle cannot be considered valgus or varus in general terms[1,2], but in literature has still been considered a valgus angle. However, the sign of e_3 can be calculated (positive or negative) to determine if KVA 3G should be considered valgus or varus.

If anatomical references were to be used to calculation the sign of e_3, such as a positive or negative angle in the frontal plane (G_X-G_Z, similar to KVA 2G), the KVA 3G angle can be given in terms of the general definition of valgus and varus[1,2], shown in Figures 21 and 22, respectively.

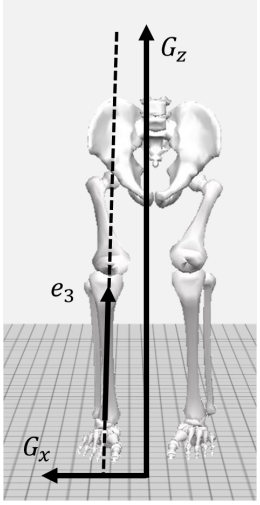

Figure 21: Valgus lower limb alignment.

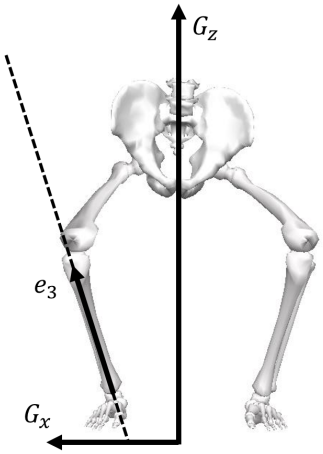

Figure 22: Varus lower limb alignment.

Alternatively, classic Cartesian coordinate vector sign definition can also be used. In this system, a vector whose projection is along the positive X and Y axes (G_X and G_Y) will be considered positive, shown in Figure 23, quadrant I. Similarly, a vector whose projection is along the negative X and Y axes ($-G_X$ and $-G_Y$) will be considered positive as well, shown in Figure 23, quadrant III. Alternatively, a vector whose projection is along the negative X and positive Y ($-G_X$ and G_Y) will result in a negative vector or positive X and negative Y (G_X and $-G_Y$), shown in Figure 23, quadrant II and IV, respectively. This type of system can be categorized into four quadrants where quadrant I and III are positive and quadrant II and

IV are negative. If X and Y are fixed to the G_X and G_Y axes, the quadrants can be labeled accordingly, see Figure 23. With this system, e_3 in quadrant I ($e_{3,I}$) and III ($e_{3,III}$) are positive signs, denoting valgus, and e_3 in quadrant II ($e_{3,II}$) and IV ($e_{3,IV}$) are negative, denoting varus). This system is meant to define the slope of a line and does not fit with the anatomical meaning given for varus and valgus[1,2]. However, this is a method used in some research to define the sign of vectors and a number of papers do not define their methodology of sign convention, so it cannot be ruled out.

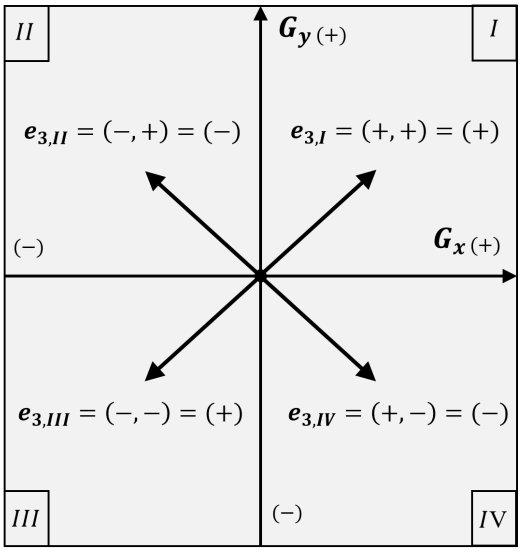

Figure 23: The four quadrants (I, II, III, and IV) of a Cartesian coordinate system used to define positive and negative vectors based on the slope of the line.

2.5 Pelvis Frontal Plane

Because of the reliance of the KVA used by Hewett et al. on a global coordinate system, this angle cannot be measured during rotating tasks, such as pivot turns, as shown in Figure 24; and does not account for rotation during linear tasks due to movement pattern variability, shown in Figure 25[65]. The pelvis, shoulder, and head are unilateral and rotate along with the body. Due to the mobility of the spine, the head and shoulders are not necessarily indicative of the position of the lower limbs. However, the pelvis is directly connected to the lower limbs and

can therefore give information on their location. If the frontal plane was connected to the pelvis instead of the global system, the orientation of that system would rotate along with the rotation of the subject during pivoting and other similar tasks.

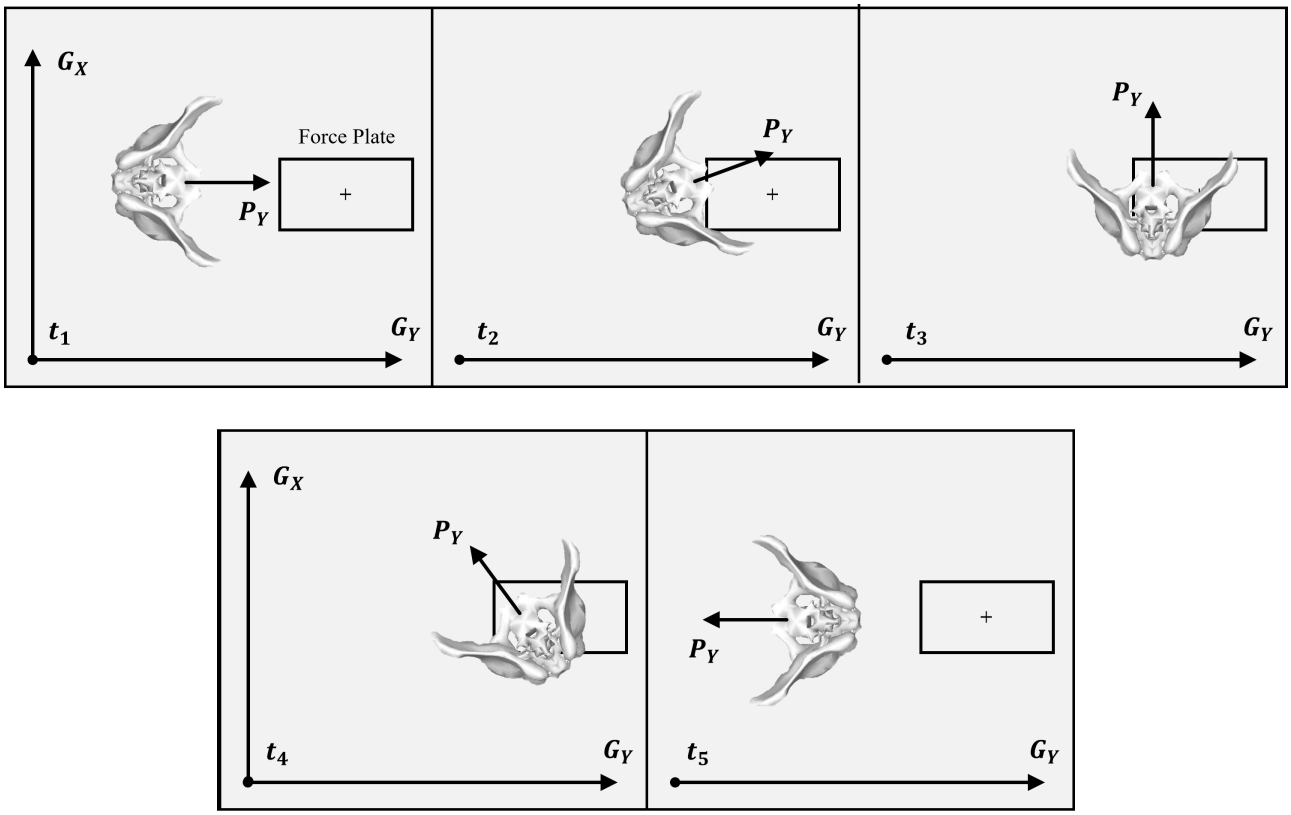

Figure 24: The rotation of P_Y (pelvis Y axis) of a pivoting task over time: t_1) approach the force plate, t_2) begin rotating, t_3) continued rotation, t_4) complete rotation, and t_5) return to starting point.

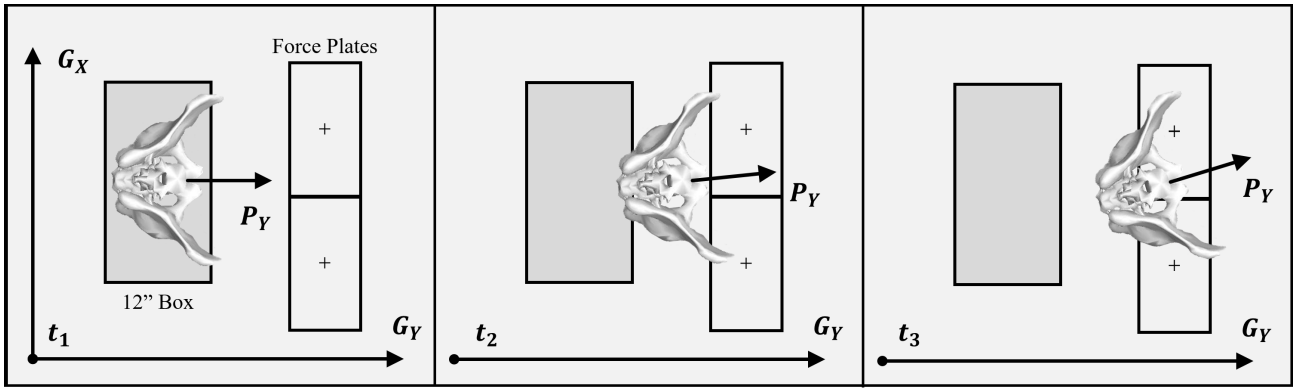

Figure 25: The rotation of P_Y (pelvis Y axis) of a linear jumping task over time: t_1) takeoff, t_2) flight phase, and t_3) landing.

The pelvis frontal plane is most commonly used in identifying the location for the acetabular cup implant in hip replacements[117]. In rare cases, it has been used to quantify gait mechanics, but only in the analysis of the lower spine rather than full lower limb mechanics[107]. Due to the value of the KVA 3G and KVA 2G in lower limb analysis, the adaptation of these angles using the pelvis to rotating tasks warrants consideration as it could be beneficial to the future study of ACL injuries. Using the P_x and G_z axes instead of the G_x and G_z axes to define the frontal plane could provide the means to account for a broader range of variability in movement and could, by extension, apply to a broader category of tasks.

2.6 Lower Limb Joint Orientation and KVA

The exclusive evaluation of KVA (calculated using a fixed global reference frame) and the associated joint angles at the knee without regard to other lower limb joints can misidentify the risk an individual might have of an ACL rupture. For example, if an individual has extremely internally rotated hips and a large KVA, it might be assumed that the knee is compromised and the ACL will inevitably rupture. However, the ankle of the shank with respect to the thigh can have multiple orientations and might affect whether an individual is actually at risk of injury. If, for instance, the knee had relatively no knee abduction and external rotation angles, as shown in Figure 26.a., then the alignment might not be as compromising to the ACL as was originally thought. Similarly, an individual could have a large amount of external rotation of the hips and a large varus angle, as shown in Figure 26.b.. If this individual also had little knee abduction and external rotation angles, then the individual would likely have a large toe-out angle. Even though the knee appears to have good support as it is tracking over the toe, the large toe-out angle would indicate a high risk of ACL rupture[95,192]. Therefore, even though the hip internal rotation angle changes from Figure 26.a. to Figure 26.b., resulting in a change from valgus to varus angle, the knee abduction and internal rotation angle could possibly remain the same.

Even though the KVA is large with internal rotation of the hips and the toes facing inwards (Figure 26.a.), neither of these two examples (Figures 26.a. and 26.b.) would be considered as compromising for the ACL as a configuration where the hip is internally rotated and the toes are facing forward, as shown in Figure 26.c..

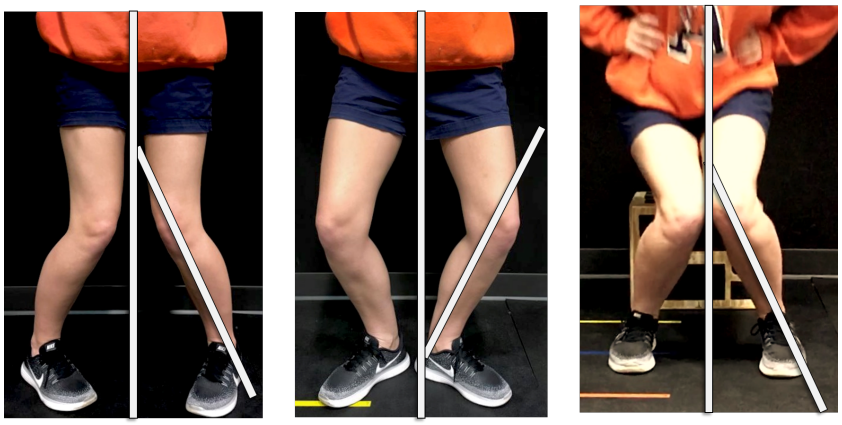

a b c

Figure 26: Examples of lower body alignment: a) internal rotation of the hips with little knee abduction and external rotation angles and a considerable KVA, b) external rotation of the hips with little knee abduction and external rotation angles and a considerable knee varus angle, and c) internal rotation of the hips with the toes facing forward and a considerable KVA.

This discrepancy between individual joint angles, KVA, and ACL ruptures is seen when observing individuals trained in different fields. Performing artists (specifically classical ballet dancers and modern dancers) and athletes who play sports at high risk of ACL ruptures (such as soccer and handball) have been observed and compared to determine if individual joint angles are to be considered as risk factor for ACL ruptures[110,111,136,149]. Dancers have a lower risk of ACL rupture than athletes, even though dancers perform activities (such as drop-jumps) with large angles that are identified as risk factors for ACL rupture[110,111,136,149]. Because dancers have large angles that are identified with ACL ruptures without a high record of ACL ruptures, it is likely that the individual angles alone are not responsible for ACL injuries[110,111,136,149].

2.7 Modeling

2.7.1 History of Skin Motion Artifacts

Instrumentation used to capture human movement has improved through the years from manually marking directly on film to multi-camera systems that digitally reconstruct movement. However, limitations still exist, which prevent the accurate measurement of human movement. Soft tissue artifacts (STA), where the retro-reflective markers connected to the skin move in relation to the bone they are representing, affect the accuracy of collected movements by misrepresenting where the body segments are in space. Even with these limitations, steps can be made to reduce STA's effect on the resulting data, such as restricting the degrees-of-freedom (DOF) of joints, filtering the data, choosing different markers sets, or weighting and scaling markers. Directly measuring movement using methods such as fluouroscopy and bone pins have their own limitations, such as small motion capture volumes and *in vivo* risks. Therefore, studies that compare the effect of STAs on human movement are also restricted. Even still, using the various methods which have been developed to reduce the effects of STAs allow for the study of human movement using markers placed atop the skin.

2.7.2 Retro-Reflective Marker Sets

A variety of marker placement sets are used to define limbs. These marker sets are optimized to accurately and precisely measure the movement of the limbs and to reduce artifacts caused by STAs[9,122,161]. Once the markers locate the body in space, segments, such as the foot, shank, and thigh, are defined from these markers. Typically, the International Society of Biomechanics' (ISB) recommendations of body segments given by Wu et al. are used to define these segments[204,205]. The standard for relating these segments together was published by Grood and Suntay in their JCS[57]. Even though the exact marker placement is not standard, the method of

collecting the marker data and modeling it to a human subject has been standardized.

2.7.3 History of Validation

The validity of the markers correctly representing the body segments despite STAs has been tested with methods such as bone pins and fluoroscopy[8,16,25,47,100,196]. These types of studies have limitations: bone pin studies are limited by ethical boundaries, pain, expense, and skin restriction; and fluoroscopy by small motion capture volumes, expense, and the limitation of captured frames per second. Because of these restrictions, there has not been extensive work on the effect STAs. However, the overall conclusion is that skin movement during testing can affect the ability of marker data accurately represent the position of the underlying bones[8,16,25,47,100,196].

2.7.4 Methods of Reducing STAs Effect on Data

Even though the collection of marker data is quasi-standardized, the existence of artifacts caused by STAs without a concrete method of reducing STAs has led to the development of multiple processing methods. Many studies have focused on STAs in particular and how they affect the quality of the data[8,16,21,21,25,47,100,196]. One of the most common methods of reducing erroneous data is to run a lowpass filter on the raw data. This is usually done at 15Hz, but it can vary. Another method of reducing STAs is to weigh and scale the markers influence on the segment position; this is typically combined with a point cluster marker placement technique[9]. Still another common method used to reduce the DOF of joints is to constrain the segment movements[8,24,25,47,120,122,173]. The translation of two segments at a joint is often extremely small and essentially unidentifiable by motion capture systems. As a result, some studies assume the translation of joints to be zero[8,24,25,120,173]. The restricted translation of the segments can reduce error caused by STA by preventing segments from having large distances between them.

However, misplaced joint centers can cause segments to morph in order to meet the zero translation requirement, and will therefore misrepresent the joint angles. The joint center must be calculated correctly in order for the rotations to occur about the right axes. Additionally, as the nature of human anatomy allows joints to glide and slide, many joints cannot be represented as a single point. For this reason, much effort has been put into calculating the optimal location for joint centers, and special attention is taken when choosing non-evasive methods of defining joint centers[61,72,113,122,143,160,161,175,182,186].

2.7.5 History of Models

In a joint, angles and translations that are significantly smaller relative to other joint angles and translations in that same joint (i.e. internal rotation of the knee compared with flexion) are assumed to be zero in some cases. The differing assumptions in the various studies has led to the development of multiple joint DOF models. Fiorentino et al. assume no translation in the ankle, knee, and hip[47]. Mentiplay et al. assume no translation in the ankle, knee, and hip, as well as zero abduction and internal rotation angles of the knee[122]. Such assumptions are meant to eliminate errors in the data collection and processing, errors which would cause an uncharacteristically large value in an angle or a translation component which should be small.

Some analysis has been done to compare these models to determine whether they differ greatly from each other. The conclusion was that there is not much difference between joint constraint models[8]. However, this examination of modeling difference was compared during a walking trial, which has much less impact and skin deformation than a jumping or jogging trial. A thorough analysis of how joint angles are affected by changes in joint constraint models, as well as how the changes in the amount of impact experienced during different tasks, could influence the use of such models.

2.8 Conclusion

The theoretical differences have been noted between angles based on differences on calculation methods and processing methods (joint constraint models). However, these differences are inconsequential if, in practical uses, the angles are correlated. The three studies in this research determine whether these differences are only theoretical in nature or if they are exhibited in practice. The specific hypotheses of each study can be found in Section 1.5.

3 Methods

3.1 Participants

This study collected whole body biomechanics during various exercises from 23 female division 1 (D1) soccer and basketball, and club soccer teams from Auburn University (height $= 171.2 \pm 8.9$ cm, weight $= 66.3 \pm 8.6$ kg age $= 19.8 \pm 1.9$ yr). Athletes were not excluded based on injury history; however, athletes were excluded if an injury prevented them from actively playing their sport at their designated level. Out of the 23 athletes, 9 had unilateral ACL reconstructions, 2 had bilateral ACL reconstructions, and 12 did not have previous ACL injuries. Each subject signed informed consent forms approved by the Auburn University Internal Review Board (IRB). The forms approved by the IRB are provided in Appendix B.

3.2 Instrumentation

The subjects were fitted with 79 retroreflective markers using the point cluster technique shown in Figure 27[9]. Kinematic and kinetic data was captured with a 10-camera motion capture system (Vicon, Vantage V5 Wide Optics cameras with 22 high-powered IR LED strobe at 85 nm) and two force plates embedded in the floor (AMTI BP400600, 2000 lb. capacity). The cameras were configured so that the motion capture volume (the volume at which three or more cameras can view a single marker) was directly above the force plates embedded in the floor. Data from the Vicon system and force plates was collected using Nexus software (Version 2.6.1; Vicon Motion Systems Ltd, Oxford Industrial Park, Oxford, UK).

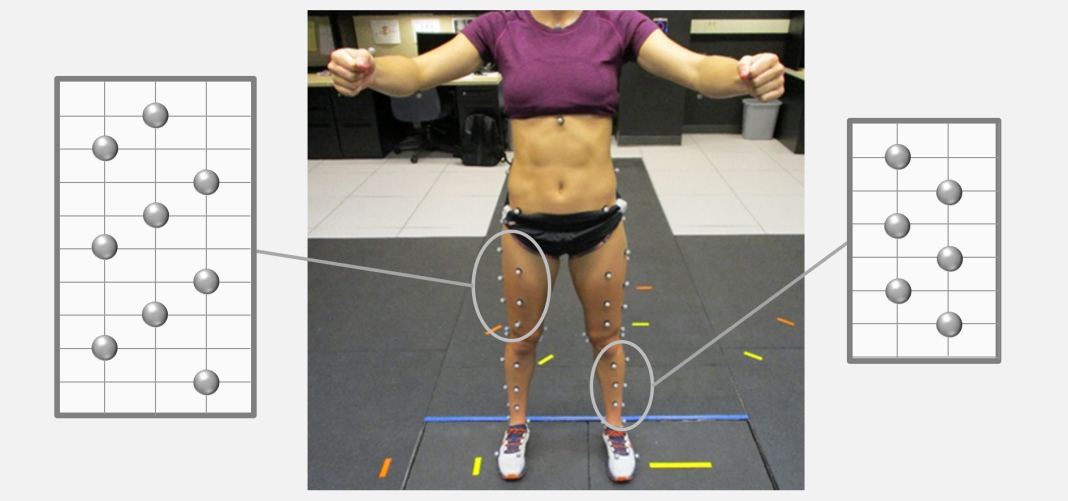

Figure 27: The placement of the 79 retroreflective markers used in the point cluster technique[9].

3.3 Data Processing

The data processed and analyzed using Visual 3D (C-Motion Research Biomechanics; Ontario, Canada). The marker data was filtered using a 15 Hz lowpass butterworth filter. The ISB's recommendations for anatomical coordinate systems were used to define each segment[204]. Unless otherwise noted, the joints in the lower body (hip, knee, and ankle) were constrained to three degrees of rotation and zero degrees of translation[47,122].

3.4 Tasks

Each subject completed a minimum of three trials for each of the tasks listed: 1) vertical drop-jump: Landing Error Scoring System (LESS)[150,151], 2) squat, 3) walking down stairs (DS), 4) lateral reach (LR), 5) walking, 6) jogging, 7) 180° pivot turn (pivot).

The subjects performed each task at least three times for a minimum of three complete trials. A trial was considered complete when the subject correctly landed or stepped onto the force plate and completed each task correctly. The subjects were given minimal directions to perform each task, so that the performance was influenced as little as possible by the researchers.

3.4.1 Landing Error Scoring System

The LESS test is a standard drop jump analysis tool, the details of which can be found in the work of Padua et al.[151]. The subject jumps from the top of a 12" box to a distance that is 50% of their height which was designated by tape on the floor. The layout of this test can be seen in Figure 28. The test was considered to have failed if the subjected did not reach the 50% distance and failed tests were discarded from the data set.

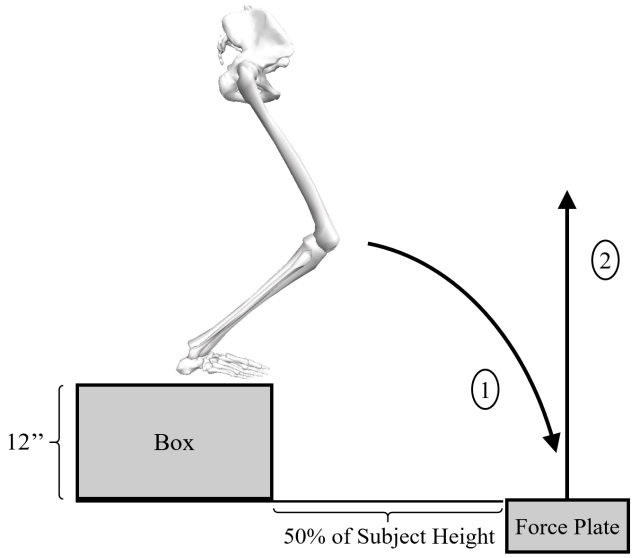

Figure 28: Landing Error Scoring System (LESS) drop-jump[150,151]. 1) flight phase and 2) vertical jump.

3.4.2 Squatting

The squat was performed by instructing the subjects to stand at the width they would typically stand to perform a squat with one foot placed on each force plate. The subjects were then given a light weight polyvinyl chloride (PVC) pipe to hold directly in front of them while they squatted in such a way so as to not obscure markers and to allow for a counter balance to replicate lifting patterns experienced during their regular workout routines.

3.4.3 Walking down stairs

The walking down stairs task (DS) was completed by the subject walking down steps at a standard step height and length. The subject began the task standing on a 14" tall box then stepping down to a 7" box, then to the floor. The box on the force plate was a standard stair tread depth of 11"; the dimensions of the boxes used for the stair test can be seen in Figure 29. The left leg of the subject stepped down first and was analyzed while the foot was on the force plate. The subject was instructed to take a couple steps forward once on the floor plane.

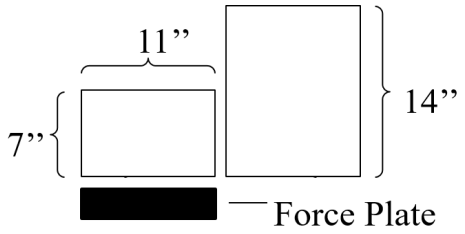

Figure 29: Walking down stairs (DS).

3.4.4 Lateral reach

For the lateral reach (LR), the subjects stood on one leg with hands on their hips and reached out with their free leg in five different directions. The subjects were instructed to bend their standing leg and reach as far out as they could then to tap the floor with their contralateral without shifting their weight. The leg reaches started at the front and moved to the back in the following five locations: (1) front, (2) 45-degrees from the front, (3) side, (4) 45-degrees from the back, and (5) directly back (Figure 30). Tape was placed on the floor in order to give the subjects direction on where to reach; the placement of the tape can be seen in Figure 30. The angles were calculated during the LR at maximum knee flexion when the subject was reaching to the side, position 3, shown in Figure 30. The test was considered a failed test if the subject removed their hands from their waist in order to prevent falling or shifted their weight onto the extend leg. Additionally, the test was considered to have failed if the subject lost balance and

fell off of their supporting foot.

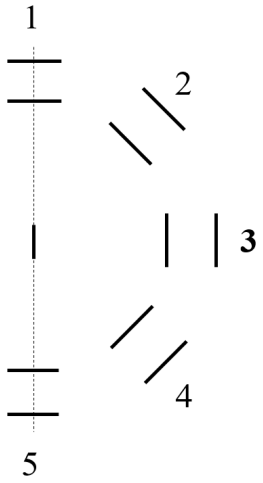

Figure 30: Lateral reach (LR) for a subject standing on their left leg and reaching with their right leg.

3.4.5 Walk

The subject walked a distance of 25 feet at a self-selected pace. The walking test was positioned such that the motion-capture image volume and force plates were in the middle of their walk (at 25/2 feet). Only one foot was on the force plates at a time (i.e. no split stance on the force plates).

3.4.6 Jog

The subject jogged a distance of 25 feet at a self-selected pace. The jogging test was positioned such that the motion capture volume and force plates were in the middle of their walk (at 25/2 feet).

3.4.7 Pivot

The subject jogged approximately 12 feet towards the force plate embedded in the ground (Figure 31.1) before planting their foot on a force plate and pivoting 180-degrees (Figure 31.2), and then jogged directly back from where they started the task (Figure 31.3). The pivot test was

considered to be a failed test if the subject jogged in a circular pattern to make the 180-degree turn, rather than planting the foot and pivoting.

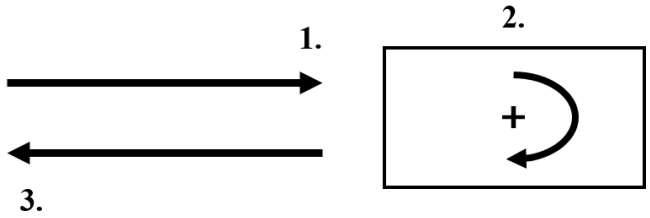

Figure 31: Pivot turn test: 1) Approach to the force plate, 2) 180° rotation, 3) Return jog.

3.5 Angles

Each angle was measured and calculated at maximum knee flexion during the stance phase. The priority of this study was to measure the relationship between different mathematical models and tasks. Therefore, the same leg, the left in this case, was measured for all subjects across all tasks. Five distinct angles were calculated for this study: 1) knee flexion 2) knee abduction 3) KVA measured in three dimensions using the global coordinate system (KVA 3G), 4) KVA 2G using the global coordinate system (KVA 2G), and 5) KVA in two dimensions using the pelvic coordinate system (KVA 2P). Translation was not measured in this study; however, Grood and Suntay developed a method of calculating translation of the tibia with respect to the femur that can be used. Knee flexion angle, knee abduction angle, KVA 3G, and KVA 2G were calculated as shown in Sections 2.3 and 2.4, and Appendix A. Details of the calculation for the fifth angle, KVA 2P, are shown in the following section.

3.5.1 KVA 2P Calculation

Calculating a knee valgus angle using the pelvis frontal plane and G_Z (KVA 2P) allows for an angle similar to KVA 2G and KVA 3G to be measured in rotating tasks. This modification, though slight, could provide the means to account for a broader range of variability in

movement and could, thus, apply to a broader category of tasks.

To create the modified pelvis coordinate system (MPCS), the lateral pelvis axis (P_X) was crossed with G_Z, shown in Equation 7. Then system was made orthogonal by crossing P'_Y with G_Z as shown in Equation 8. The frontal plane of the MPCS was defined as the P'_X-G_Z plane or the plane perpendicular to P'_Y.

$$P'_Y = \frac{G_Z \times P_X}{\|G_Z \times P_X\|} \tag{7}$$

$$P'_X = \frac{P'_Y \times G_Z}{\|P'_Y \times G_Z\|} \tag{8}$$

The angle was then calculated in the MPCS frontal plane using the same method as KVA 2G. The e_3 axis was projected onto the MPCS frontal plane then the dot product was used between $proj_{P'_Y Plane}$ and G_Z, as shown in Equation 9 and 10. This angle can be seen in Figure 32.

$$proj_{P'_Y Plane}(e_3) = e_3 - proj_{P'_Y}(e_3) = e_3 - \frac{e_3 \cdot P'_Y}{\|P'_Y\|^2} P'_Y \tag{9}$$

$$\cos(KVA\,2P) = G_Z \cdot proj_{P'_Y Plane}(e_3) \tag{10}$$

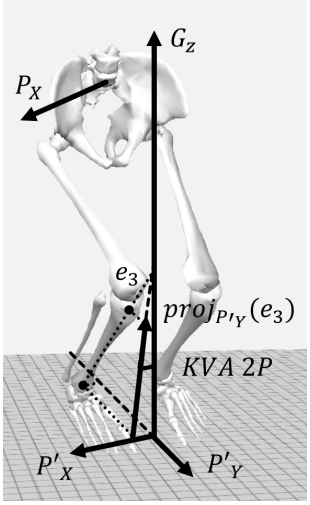

Figure 32: KVA measured in two dimensions on the pelvis frontal plane of the MPCS (KVA 2P) between the shank (e_3) and the global vertical axis (G_Z). P_X is the lateral axis of the pelvis, P'_Y defines the pelvis frontal plane, and P'_X is the axis orthogonal to G_Z and P'_Y.

3.6 Joint Constraint Models

Four models were made to analyze three angles at maximum knee flexion: 1) knee flexion, 2) knee valgus angle in global two dimensional (KVA 2G), and 3) knee valgus angle in global three dimensions (KVA 3G). Three joints were manipulated to create the models for analysis of the hip, knee, and ankle. Four models were created to compare with each other and are listed in Table 11. The first model has six degrees of freedom (three rotations and three translations) in the hip, knee, and ankle (666), Table 11. The second model has three degrees of freedom (three rotations) in the hip, knee, and ankle (333), Table 11. The third model has three degrees of freedom (three rotations) in the hip and knee and two degrees of freedom (flexion and abduction) in the ankle (332), Table 11. The fourth model has three degrees of freedom (three rotations) in the hip and two degrees of freedom (flexion and abduction) in the knee and ankle (332), Table 11. Table 11 shows the four models and the associated DOF, and Figure 33 depicts the rotations and translations used to build each model.

Table 11: The DOF for each of the four models.

		Rotations			Translations		
	Model	Hip	Knee	Ankle	Hip	Knee	Ankle
1)	666	3	3	3	3	3	3
2)	333	3	3	3	0	0	0
3)	332	3	3	2*	0	0	0
4)	322	3	2*	2*	0	0	0

* Rotation in flexion (α) and abduction (β). No internal rotation (γ).

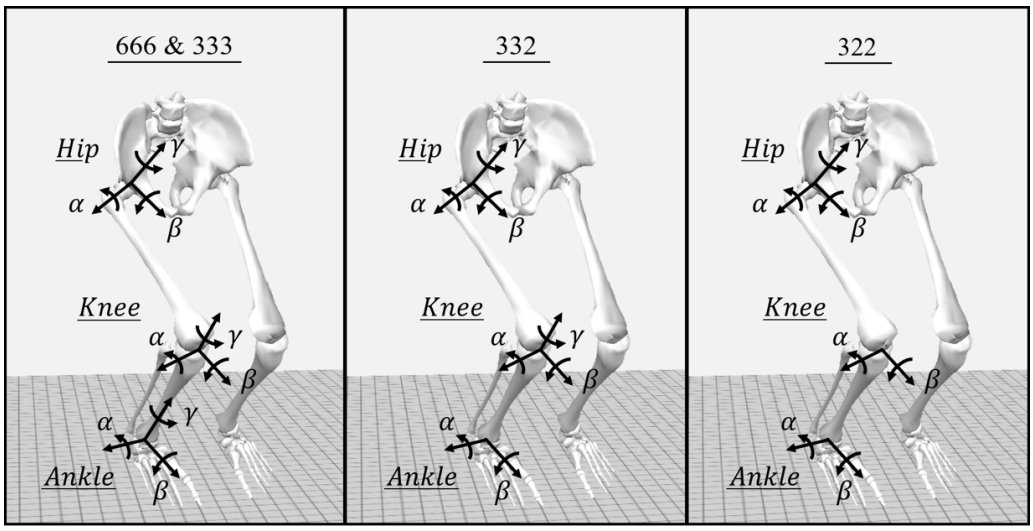

Figure 33: DOF of each model for the hip, knee, and ankle joints.

3.7 Statistical Analysis

The angles were averaged over three successful trials of each task, resulting in one value for each task. Details for the statistical analysis of each study can be found in the Statistical Analysis section of each study.

4 Study 1: Comparative Analysis of Medial Knee Alignment Definitions in Female Athletes

Study 1 Hypothesis: Measures of KVA are equivalent despite changes in measurement calculations methods and movement task.

4.1 Abstract

KVA with respect to a global reference frame in three dimensions (KVA 3G) during drop jumps has been shown to correlate with subsequent ACL injury. KVA 3G and other mathematical evaluations of KVA (namely a 2D KVA and local coordinate system method referred to as abduction) are often used as equivalent angles. This study aims to elucidate the differences between the angles within and across tasks.

The kinematics of 23 female athletes, D1 soccer, D1 basketball, and club soccer (height $= 171.2 \pm 88.9cm$, weight $= 66.3 \pm 8.6kg$, age $= 19.8 \pm 1.9yrs$), was analyzed using a motion capture system during tasks related to their sport and daily living.

The knee abduction angle, measured using body fixed axes, only correlated to the two-dimensional global reference frame angle (KVA 2G) in three of the six tasks (walking, squatting, and walking down stairs), and one out of six tasks in the 3D measurements (jogging). This suggests that the knee abduction angle does not always relate to other versions of KVA.

The KVA with reference to the pelvis coordinate system (KVA 2P) correlated to the KVA 2G in six out of six tasks (r$= 0.734 \pm 0.037$, P$\ll 0.001$), suggesting the pelvis can be utilized as a reference plane during rotating tasks, such as run-to-cut, when a fixed global system is less meaningful. Not all measures of KVA are equivalent and should be considered individually. A thorough understanding of the equivalence or non-equivalence of various measures of KVA is essential in understanding ACL injury risk.

4.2 Methods

4.2.1 Statistical Analysis

The KVA 2G, 3GC, 2P, and knee abduction angle in each of the six tasks were compared with KVA 2G, 3GC, 3GA, 2P, and knee abduction angle in each of the respective tasks. In addition, the angles KVA 2G, 3GC, 2P, and knee abduction measured during the LESS task were compared with the same angles measured during each of the six different tasks. The data was statistically analyzed with a two-tailed Pearson Correlation test using Statistical Package for the Social Sciences (SPSS; SPSS Inc, Chicago, Illinois). The results are considered significant when the Pearson correlation coefficient, r, is less than 0.05.

4.3 Results

The results of the analysis can be seen in Table 12 where the mean and standard deviation of each task and angle are listed.

Table 12: The average and standard deviation (SD) for each of the angles and tasks measured. Angles are given in degrees.

	LESS		**Squat**		**DS**		**LR**		**Walk**		**Jog**		**Pivot**	
Angle	Mean	SD	Mean	SD	Mean	SD	Mean	SD	Mean	SD	Mean	SD	Mean	SD
Flexion	93.86	24.71	122.50	14.45	25.15	9.82	74.01	10.12	16.23	5.82	41.02	13.95	56.53	14.21
KVA 2G	-0.01	0.11	0.08	0.08	0.06	0.04	0.00	0.09	0.08	0.04	0.12	0.04		
KVA 3GC	-0.03	0.70	0.46	0.43	0.31	0.17	-0.19	0.70	0.08	0.04	0.48	0.04	N/A	
KVA 3GA	-0.03	0.70	0.62	0.09	0.35	0.06	-0.19	0.70	0.21	0.07	0.48	0.04		
KVA 2P	-0.03	0.13	0.05	0.14	0.08	0.06	-0.24	0.17	0.06	0.03	0.19	0.09	-0.36	0.23
Abduction	-0.37	6.06	-5.02	5.14	-0.08	4.11	-10.85	5.64	1.91	3.16	-0.44	3.88	-8.32	6.45

Tables 13 - 17 list the comparisons between the angles (abduction, KVA 2G, KVA 3GC, KVA 3GA, and KVA 2P) and the tasks (LESS, squat, DS, LR, walk, jog, and pivot). More specifically, Tables 13, 14, and 15 describe the relationship between the KVA 2G, KVA 2P, and

knee abduction angle measured during the each task compared to other mathematical measures during the same task. KVA 3GC measured during each task compared to other mathematical measures during the same task can be found in Appendix C. Table 17 compares each of the angles measured during the LESS task to the KVA 2G of each task. The measure of the LESS task compared to KVA 3GC, KVA 2P, and knee abduction angle can be found in Appendix B.

Table 13: The KVA 2G measured for each task compared to other measures of the same task.

			KVA 2G						
	Angle	†	LESS	Squat	DS	LR	Walk	Jog	Pivot
Respective Task	KVA 3GC	r	**0.857**	**0.627**	0.399	**0.680**	0.050	0.108	N/A
		P	**≪0.001**	**0.001**	0.073	**≪0.001**	0.820	0.642	
	KVA 3GA	r	**0.857**	0.184	-0.048	**0.680**	**0.762**	0.108	
		P	**≪0.001**	0.400	0.836	**≪0.001**	**≪0.001**	0.642	
	KVA 2P	r	**0.782**	**0.731**	**0.722**	**0.708**	**0.773**	**0.689**	
		P	**≪0.001**	**≪0.001**	**≪0.001**	**≪0.001**	**≪0.001**	**0.001**	
	Knee Abduction	r	0.324	**0.427**	**0.587**	0.159	**0.800**	0.192	
		P	0.141	**0.042**	**0.005**	0.468	**≪0.001**	0.416	

†Where r is the Pearson correlation coefficient and P is the significance

Table 14: The KVA 2P measured for each task compared to other measures of the same task.

			KVA 2P						
	Angle	†	LESS	Squat	DS	LR	Walk	Jog	Pivot
Respective Task	KVA 2G	r	**0.782**	**0.731**	**0.722**	**0.708**	**0.773**	**0.689**	N/A
		P	**≪0.001**	**≪0.001**	**≪0.001**	**≪0.001**	**≪0.001**	**≪0.001**	
	KVA 3GC	r	**0.689**	**0.821**	0.363	0.267	-0.200	0.031	
		P	**≪0.001**	**≪0.001**	0.106	0.218	0.359	0.895	
	KVA 3GA	r	**0.689**	0.150	-0.105	0.267	**0.424**	0.031	
		P	**≪0.001**	0.496	0.651	0.218	**0.044**	0.895	
	Knee Abduction	r	0.192	0.121	0.359	0.128	**0.527**	0.041	-0.021
		P	0.391	0.581	0.110	0.562	**0.010**	0.863	0.927

†Where r is the Pearson correlation coefficient and P is the significance

Table 15: The knee abduction angle measured for each task compared to other measures of the same task.

			Knee Abduction Angle						
	Angle	†	LESS	Squat	DS	LR	Walk	Jog	Pivot
Respective Task	KVA 2G	r	0.324	**0.427**	**0.587**	0.159	**0.800**	0.192	
		P	0.141	**0.042**	**0.005**	0.468	**≪0.001**	0.416	
	KVA 3GC	r	0.382	0.099	0.259	0.249	0.073	**-0.568**	N/A
		P	0.079	0.653	0.257	0.252	0.741	0.009	
	KVA 3GA	r	0.382	0.087	-0.313	0.249	**0.576**	**-0.568**	
		P	0.079	0.695	0.167	0.252	**0.004**	**0.009**	
	KVA 2P	r	0.192	0.121	0.359	0.128	**0.527**	0.041	-0.021
		P	0.391	0.581	0.110	0.562	**0.010**	0.863	0.927

†Where r is the Pearson correlation coefficient and P is the significance

Table 16: The KVA 3GC compared to KVA 3GA across all tasks.

			KVA 3GC						
	Angle	†	LESS	Squat	DS	LR	Walk	Jog	Pivot
Respective Task	KVA 3GA	r	**1.000**	0.353	0.373	**1.000**	0.025	**1.000**	N/A
		P	**≪0.001**	0.099	0.096	**≪0.001**	0.910	**≪0.001**	

†Where r is the Pearson correlation coefficient and P is the significance

Table 17: Each angle measured during the LESS tasks compared to the KVA 2G angle of the other six tasks.

			LESS				
	Task	†	KVA 2G	KVA 3GC	KVA 2GP	KVA 2P	Abduction
KVA 2G	Squat	r	0.402	0.282	0.282	**0.481**	0.137
		P	0.064	0.203	0.203	**0.023**	0.544
	DS	r	0.077	0.042	0.042	0.294	-0.111
		P	0.747	0.862	0.862	0.208	0.641
	LR	r	-0.114	-0.174	-0.174	0.173	0.149
		P	0.612	0.440	0.440	0.442	0.508
	Walk	r	0.179	0.211	0.211	0.332	-0.176
		P	0.426	0.347	0.347	0.131	0.433
	Jog	r	-0.062	0.071	0.071	0.124	-0.200
		P	0.796	0.765	0.765	0.602	0.398
	Pivot	r	N/A				
		P					

†Where r is the Pearson correlation coefficient and P is the significance

4.4 Discussion

The purpose of this study is to demonstrate how the KVAs are not necessarily the same when different calculation methods are used and when it is measured in different tasks. Additionally, this study determined certain correlations between types of KVA and KVA measured in different movement tasks. Some of the comparisons are shown in the Results section, Tables 12-17; additional comparisons are shown in Appendix B. Not only does the chosen mathematical model of the KVA have the potential to change the value of the KVA measured, as one would expect, the value of the angle in one task does not necessarily correlate to other tasks completed by the same subject, which is less obvious. Even with the differences in angles

within and between tasks, there are correlations that have affected previous and may influence future studies on ACL biomechanics.

The KVA 2G is highly correlated to both the KVA 3GC and 3GA, but only in some tasks (Table 13). KVA 2G related to KVA 3GC in LESS, squatting, and LR tasks, but not the DS, walking, or jogging tasks (Table 13). The KVA 2G related to KVA 3GA in LESS, LR, and walking, but not the squatting, DS, or jogging tasks (Table 13). This indicates how changing between the two- and three-dimensional calculation of this angle is only related in some tasks.

Unsurprisingly, the 3GC and 3GA are related to each other; the sign is the only difference between them (Table 16). However, only some tasks have a one-to-one relationship with strong significance, LESS, LR, and jogging ($r = 1.000$, $P \ll 0.001$). Squatting, DS, and walking, half of the tasks studied, did not significantly relate to each other (Table 16). This indicates that for some tasks the sign convention does not have a great influence over the results, but in other tasks the outcome of the analysis can be different.

The pivot turn is denoted with a 'N/A' when correlated with an angle that requires the global reference frame, because the global reference frame is no longer representing the frontal plane. This should be taken into consideration when choosing tasks and angles to measure as the KVA 2G, 3GC, and 3GA angles cannot meaningfully be measured during rotating tasks.

In order to measure the 2G, 3GC, and 3GA during rotating tasks, the pelvis coordinate system was analyzed to see if it could serve as a substitute during rotating tasks (Table 14). The analysis indicates that the relationship between KVA 2P and KVA 2G is the most consistent across all tasks, more so than any other two angles. Even though there is not a one-to-one relationship between these angles, the Pearson correlation coefficient ranges from 0.689 to 0.782. While the relationship between these angles is notable in this work, more tasks will need to be measured and compared in order to ascertain if this relationship remains the same regardless

of the task. This preliminary observation of a consistent relationship between six angles does suggest that KVA 2P can be used as a substitute for angles that use a global reference frame.

Not only is there a relationship between the KVA 2G and KVA 2P, but both have similar significant relationships to the three-dimensional tasks (Tables 13 and 14). In the LESS task both KVA 2G and 2P relate to KVA 3GC and 3GA (Tables 13 and 14). However, in the squatting tasks, they both only relate to KVA 3GC and not to 3GA (Tables 13 and 14). Neither of the angles related in the DS tasks. In the LR tasks, KVA 2G relates to both three-dimensional angles, but KVA 2P only relates to one (Tables 13 and 14). The consistent relationship between KVA 2G and 2P is another indicator that they may be useful substitutes. However, the inconsistency in the LR task should be further explored as it may imply which tasks are not suitable for this substitution.

The LESS task had the most consistent correlations between angles in comparison to the rest of the tasks, with the exception of the knee abduction angle, shown in Table 13 and 14. As much of the literature on the relationship between KVA and ACL injuries focuses on the measurement of KVA during drop-jumps, the difference between these definitions may not greatly influence this conclusion. However, the knee abduction angle was not correlated with any of the other measures for KVA during the LESS task. As a result, ambiguity between the knee abduction and other KVAs could greatly affect the reader's understanding of the analysis and conclusion. The confusion of these angles becomes even more pronounced when attempting to draw conclusions between papers that do not clearly define whether knee abduction angle or other KVAs were used.

The knee abduction angle correlated with the KVA 2G in some tasks (squatting, DS, walking) but not in the LR or jogging task (Table 15). Walking exhibited the largest relationship between the knee abduction angle and the other angles over the other tasks (Table 15). In the

jogging task, the knee abduction angle related to the three-dimensional measures, KVA 3GC and 3GA, but not the two-dimensional measures, KVA 2G and 2P (Table 15).

To highlight how the different angles and tasks affected the results and subsequent conclusions, Table 17 shows angles measured during the LESS task compared to the KVA 2G measured in all the tasks. This comparison resulted in minimal correlations; only the LESS KVA 2P and squat KVA 2G ($r = 0.481$, $P = 0.023$) correlated. Additional tables similar to 17 can be found in Appendix B. While this analysis does not prove insignificance, it does illustrate some of the limitations of the relationship between tasks and the mathematical angles and can raise awareness amongst researchers of KVA as to how this may affect their results.

5 Study 2: Multivariable Analysis of Lower Limb Joint Angles and Knee Valgus Angles in Female Athletes

Study 2, Hypothesis A: Lower extremity joint angles can predict the KVA and knee abduction angle given different joint constraints and movement tasks, and **Hypothesis B:** An angle or combination of angles can be found that contribute the most to KVA.

5.1 Abstract

Individual joint angles can be combined with one another in different ways to achieve the same overall knee valgus angle (KVA). Being able to determine how the lower extremity joint angles interact with one another to develop the KVA would progress the understanding of KVA. Walking, jogging, and drop-jumps of 23 female athletes (height $= 171.2 \pm 88.9cm$, weight $= 66.3 \pm 8.6$kg, age $= 19.8 \pm 1.9$yrs) were measured using a motion capture system. Flexion, abduction, and internal rotation angles of the ankle, knee, and hip was analyzed along with knee valgus angle measured with respect to a global reference frame. A multivariable anlaysis was used to determine how the individual joint angles interacted to predict the KVA and knee abduction angle. It was determined that the KVA and knee abduction could be predicted from individual joint angles. Additionally, it was observed that in some cases ankle and knee internal rotation angles contributed to the resulting evaluation despite the traditionally low accuracy reported in these angles. Evaluating the KVA by considering the complexity of the lower extremity joint interactions as well as the individual joint angle contributions to the overall KVA will give insight to the complexity of the lower extremity joint interactions that might have been otherwise overlooked.

5.2 Statistical Analysis

A multiple linear regression was run to predict KVA 2G and KVA 3G from flexion, abduction, and internal rotation angles of the ankle, knee, and hip. This regression was run for all tasks (LESS, jog, and walk). The same test was also run to predict the knee abduction angle from flexion, abduction, and internal rotation angles of the ankle and hip as well as knee flexion and internal rotation angles. These nine regressions (predicting the KVA 2G, KVA 3G, and knee abduction angles during LESS, jogging, and walking) were analyzed with three data sets. The first the data set was processed with the 333 kinematic model and including all lower extremity joint angles as independent variables. The second data set was processed with the 333 kinematic model and only including ankle and knee flexion and internal rotation, and hip flexion, abduction, and internal rotations as independent variables. The third data set was processed with the 322 kinematic model and including ankle and knee flexion and internal rotation, and hip flexion, abduction, and internal rotation as independent variables. The result was considered significant when $p < 0.05$.

6 Results

The nine variables (flexion, abduction, and internal rotation angles of the ankle, knee, and hip) significantly predicted KVA 2G in the LESS, walk, and jog tasks. The results of the analysis are as follows: LESS: $F(9,12) = 3.34$, $p < .05$, $R^2 = 0.73$; jog: $F(9,11) = 5.94$, $p < 0.005$, $R^2 = 0.84$; and walk: $F(9,13) = 4.67$, $p < 0.005$, $R^2 = 0.78$. In the following tables (Tables 18-23), β is the coefficient and p is the significance.

Table 18: Multivariable analysis of KVA 2G of the ankle, knee, and hip flexion, abduction, and internal rotation using the 333 kinematic model.

KVA 2G, 333	LESS		Jog		Walk	
R Square	**0.732**		0.605		**0.778**	
Significance	**0.032**		0.209		**0.008**	
Angle	Coefficients	P-value	Coefficients	P-value	Coefficients	P-value
Ankle Flexion	0.008	0.343	0.004	0.103	$\ll$0.001	0.847
Ankle Abduction	-0.001	0.810	0.001	0.780	0.001	0.395
Ankle Internal Rotation	0.005	0.346	-0.001	0.698	$\ll$0.001	0.980
Knee Flexion	0.001	0.852	$\ll$0.001	0.880	$\ll$0.001	0.929
Knee Abduction	0.012	0.126	0.009	0.102	**0.009**	$\ll$**0.001**
Knee Internal Rotation	0.003	0.468	$\ll$0.001	0.886	$\ll$0.001	0.887
Hip Flexion	-0.013	0.090	-0.001	0.345	$\ll$0.001	0.966
Hip Abduction	0.001	0.686	$\ll$0.001	0.849	0.004	0.096
Hip Internal Rotation	-0.003	0.592	-0.007	0.015	-0.001	0.469

KVA 2G measured during the LESS condition showed to have significance with the nine independent variables using the 333 kinematic model ($R^2 = 0.732$, $p = 0.032$); however, no one angle contributed to a significant degree (Table 18). KVA 2G measured during the walking condition using the 333 kinematic model also showed to have significance with the nine independent variables ($R^2 = 0.778$, $p = 0.008$). In this case, the knee abduction angle was the only significant contributor, although its' direct contribution can be interpreted as minimal considering the extremely low coefficient ($\beta = 0.009$, $p \ll 0.001$).

Table 19 lists the results of the multivariable analysis for the LESS, jog, and walk tasks between KVA 3G using the 333 kinematic model and including all rotations (flexion, abduction, and internal rotation) as independent variables.

Table 19: Multivariable analysis of KVA 3G using the 333 kinematic model and including all rotations (flexion, abduction, and internal rotation) as independent variables

KVA 3G, 333	LESS		Jog		Walk	
R Square	**0.725**		**0.882**		0.558	
Significance	**0.023**		**0.001**		0.157	
Angle	Coefficients	P-value	Coefficients	P-value	Coefficients	P-value
Ankle Flexion	0.105	0.061	-0.003	0.268	0.002	0.380
Ankle Abduction	0.039	0.280	-0.002	0.448	-0.001	0.609
Ankle Internal Rotation	-0.017	0.530	0.001	0.793	0.001	0.538
Knee Flexion	0.022	0.345	**-0.016**	$\ll$**0.001**	0.001	0.752
Knee Abduction	**0.140**	**0.009**	0.004	0.329	0.007	0.057
Knee Internal Rotation	0.035	0.239	0.001	0.714	$\ll$0.001	0.845
Hip Flexion	**-0.117**	**0.019**	**-0.004**	**0.029**	-0.001	0.797
Hip Abduction	0.024	0.158	0.002	0.352	0.003	0.559
Hip Internal Rotation	0.021	0.539	-0.003	0.129	0.001	0.647

KVA 3G measured during the LESS condition showed to have significance ($R^2 = 0.725$, p= 0.023) with the nine independent variables when using the 333 kinematic model, as shown in Table 19; the knee abduction and hip flexion angles were shown to be a significant contributors ($\beta = 0.140$, p $= 0.009$; and $\beta = -0.117$, p $= 0.019$, respectively). KVA 3G measured during the jogging condition also showed to have significance when using the 333 kinematic model ($R^2 = 0.882$, p= 0.001) with the nine independent variables. In this case, knee flexion and hip flexion were the only significant contributors ($\beta = -0.016$, p $\ll 0.001$; and $\beta = -0.004$, p $= 0.029$, respectively).

Table 20 lists the results of the multivariable analysis for the LESS, jog, and walk tasks for the knee abduction angle using the 333 kinematic model and including all rotations (flexion, abduction, and internal rotation) of the ankle and hip, and flexion and internal rotation of the

knee as independent variables.

Table 20: Multivariable analysis of the knee abduction angle using the 333 kinematic model and including all rotations (flexion, abduction, and internal rotation) of the ankle and hip, and flexion and internal rotation of the knee as independent variables.

Knee Abduction Angle, 333	LESS		Jog		Walk	
R Square	**0.870**		**0.773**		0.400	
Significance	**$\ll$0.001**		**0.006**		0.382	
Angle	Coefficients	P-value	Coefficients	P-value	Coefficients	P-value
Ankle Flexion	-0.453	0.141	0.079	0.701	-0.239	0.218
Ankle Abduction	**-0.505**	**0.007**	-0.200	0.266	-0.097	0.626
Ankle Internal Rotation	0.154	0.351	0.018	0.910	-0.223	0.230
Knee Flexion	-0.156	0.265	**0.488**	**0.022**	-0.304	0.154
Knee Abduction	-	-	-	-	-	-
Knee Internal Rotation	**-0.362**	**0.024**	-0.192	0.185	-0.154	0.336
Hip Flexion	**0.853**	**$\ll$0.001**	0.116	0.376	-0.146	0.436
Hip Abduction	-0.112	0.258	-0.140	0.463	-0.024	0.946
Hip Internal Rotation	**-0.448**	**0.016**	**0.341**	**0.009**	0.179	0.347

The analysis shown in Table 20 used the knee abduction angle as the dependent variable. As such, the knee abduction angle was removed from the independent variable list. The knee abduction angle measured during the LESS and jogging conditions using the 333 kinematic model was significant with the eight independent variables (R^2=0.870, p$\ll 0.001$; R^2=0.773, p$= 0.006$, respectively). The ankle abduction, knee internal rotation, hip flexion, and hip internal rotation angles significantly contributed to the knee abduction angle when measured during the LESS condition ($\beta = -0.505$, p $= 0.007$; $\beta = -0.362$, p $= 0.024$; $\beta = 0.853$, p $\ll 0.001$; and $\beta = -0.448$, p $= 0.016$, respectively). Of these four angles, the hip flexion angle was the largest contributor followed by the ankle abduction, hip internal rotation angles, then knee internal rotation angle. In the jogging task, both knee flexion and hip internal rotation

angles significantly contributed to the the knee abduction angle ($\beta = -0.488$, p $= 0.022$; $\beta = 0.341$, p $= 0.009$, respectively). Of these two angles, the knee flexion angle contributed the most to the dependent variable.

Table 21 lists the results of the multivariable analysis for the LESS, jog, and walk tasks between KVA 2G using the 333 kinematic model but only including flexion and abduction of the ankle and knee, and flexion, abduction, and internal rotation of the hip.

Table 21: Multivariable analysis of KVA 2G using the 333 kinematic model but only including flexion and abduction of the ankle and knee, and flexion, abduction, and internal rotation of the hip.

KVA 2G, 333	LESS		Jog		Walk	
R Square	**0.709**		**0.529**		**0.819**	
Significance	**0.006**		**0.012**		**$\ll$0.001**	
Angle	Coefficients	P-value	Coefficients	P-value	Coefficients	P-value
Ankle Flexion	0.004	0.589	0.004	0.082	0.000	0.476
Ankle Abduction	-0.003	0.314	$\ll$0.001	0.832	0.001	0.360
Knee Flexion	-0.002	0.573	-0.001	0.760	$\ll$0.001	0.921
Knee Abduction	0.010	0.083	**0.011**	**0.001**	**0.009**	**$\ll$0.001**
Hip Flexion	-0.009	0.052	-0.002	0.271	$\ll$0.001	0.946
Hip Abduction	$\ll$0.001	0.912	0.001	0.636	**0.004**	**0.030**
Hip Internal Rotation	-0.006	0.054	**-0.007**	**$\ll$0.001**	-0.001	0.319

When ankle and knee internal rotation was removed from the analysis, KVA 2G measured during all three conditions using the 333 kinematic model showed to have significance (LESS: R^2=0.709, p = 0.006; jog: R^2= 0.529, p = 0.012; and walk: R^2 = 0.819, p $\ll$ 0.001), as shown in Table 21. KVA 2G analyzed in the LESS condition has no one independent variable that significantly contributed to the value of KVA 2G. In the jogging condition, both the knee abduction and hip internal rotation angles contributed to the value of KVA 2G ($\beta = 0.011$, p $= 0.001$; and $\beta = -0.007$, p $\ll 0.001$, respectively). Of these two rotations, the knee abduction angle contributed more than the hip internal rotation angle. In the walking condition,

the knee abduction and hip abduction angles contributed to the value of KVA 2G ($\beta = 0.009$, p $\ll 0.001$; and $\beta = 0.004$, p $= 0.030$, respectively).

Table 22 lists the results of the multivariable analysis for the LESS, jog, and walk tasks of KVA 3G using the 333 kinematic model but only including the flexion and abduction of the ankle and knee, and flexion, abduction, and internal rotation of the hip as independent variables.

Table 22: Multivariable analysis of KVA 3G using the 333 kinematic model but only including the flexion and abduction rotations of the ankle and knee, and flexion, abduction, and internal rotation of the hip as independent variables.

KVA 3G, 333	LESS		Jog		Walk	
R Square	**0.681**		**0.694**		0.513	
Significance	**0.010**		**0.012**		0.0880	
Angle	Coefficients	P-value	Coefficients	P-value	Coefficients	P-value
Ankle Flexion	0.084	0.072	0.004	0.082	0.001	0.408
Ankle Abduction	-0.003	0.868	$\ll$0.001	0.832	$\ll$0.001	0.819
Knee Flexion	0.008	0.655	-0.001	0.760	$\ll$0.001	0.926
Knee Abduction	**0.100**	**0.012**	**0.011**	**0.001**	0.006	0.056
Hip Flexion	**-0.075**	**0.020**	-0.002	0.271	-0.001	0.628
Hip Abduction	0.010	0.413	0.001	0.636	0.003	0.402
Hip Internal Rotation	-0.011	0.539	-0.007	$\ll$0.001	0.002	0.259

When the ankle and knee internal rotation was removed from the analysis, KVA 3G measured during LESS and jogging using the 333 kinematic model were significant (R^2=0.681,p = 0.010 and R^2 = 0.694, p = 0.012, respectively), as shown in Table 22. In the LESS condition, the knee abduction and hip flexion angles significantly contributed to the value of KVA 3G ($\beta = 0.100$, p $= 0.012$; and $\beta = -0.075$, p $= 0.020$, respectively). In the jogging condition, only the knee abduction angle significantly contributed to the value of KVA 3G ($\beta = 0.011$, p $= 0.001$).

Table 23 lists the results of the multivariable analysis for the LESS, jog, and walk tasks

of the knee abduction angle using the 333 kinematic model but only including the flexion and abduction angles of the ankle and knee, and flexion, abduction, and internal rotation angles of the hip as independent variables.

Table 23: Multivariable analysis of the knee abduction angle using the 333 kinematic model but only including flexion and abduction of the ankle and knee, and flexion, abduction, and internal rotation of the hip as independent variables.

Knee Abduction Angle, 333	LESS		Jog		Walk	
R Square	0.327		0.158		0.318	
Significance	0.351		0.841		0.337	
Angle	Coefficients	P-value	Coefficients	P-value	Coefficients	P-value
Ankle Flexion	-1.064	0.105	0.229	0.544	-0.119	0.265
Ankle Abduction	-0.477	0.081	0.039	0.904	-0.543	0.069
Knee Flexion	-0.626	0.245	-0.306	0.535	-0.625	0.100
Knee Abduction	-	-	-	-	-	-
Hip Flexion	0.489	0.273	-0.160	0.499	-0.258	0.361
Hip Abduction	-0.187	0.323	-0.231	0.409	0.350	0.466
Hip Internal Rotation	0.117	0.675	0.143	0.608	0.390	0.063

The analysis shown in Table 23 used the knee abduction angle as the dependent variable. As a result, the knee abduction angle was removed from the independent variable list. The knee abduction angle using the 333 kinematic model was not significant in any of the three conditions tested.

Table 24 lists the results of the multivariable analysis for the LESS, jog, and walk tasks between KVA 2G using the 322 kinematic model and including flexion and abduction of the ankle and knee, and flexion, abduction, and internal rotation of the hip as independent variables.

Table 24: Multivariable analysis of KVA 2G using the 322 kinematic model and including flexion and abduction of the ankle and knee, and flexion, abduction, and internal rotation of the hip as independent variables.

KVA 2G, 322	LESS		Jog		Walk	
R Square	**0.705**		0.481		**0.823**	
Significance	**0.006**		0.230		**≪0.001**	
Angle	Coefficients	P-value	Coefficients	P-value	Coefficients	P-value
Ankle Flexion	0.010	0.209	≪0.001	0.952	**-0.004**	**0.005**
Ankle Abduction	-0.003	0.277	-0.001	0.742	0.000	0.990
Knee Flexion	0.002	0.549	-0.001	0.670	**-0.002**	**0.003**
Knee Abduction	0.009	0.078	0.009	0.151	**0.009**	**≪0.001**
Hip Flexion	0.002	0.258	-0.003	0.240	-0.001	0.085
Hip Abduction	-0.002	0.608	0.006	0.075	0.002	0.350
Hip Internal Rotation	-0.014	0.011	-0.007	0.055	-0.002	0.019

KVA 2G measured during the LESS condition using the 322 kinematic model showed to have significance with the nine independent variables ($R^2 = 0.705$, $p = 0.006$); however, no one angle contributed to a significant degree (Table 24). KVA 2G measured during the walking condition using the 322 kinematic model also showed to have significance with the nine independent variables (R^2 = 0.823, p ≪0.001). In this case, the ankle flexion, knee abduction, and knee abduction angles significantly contributed, although their direct contribution can be interpreted as minimal considering the extremely low coefficient.($\beta = -0.004$, p=0.005; $\beta = -0.002$, p=0.003; $\beta = 0.009$, $p \ll 0.001$, respectively).

Table 25 lists the results of the multivariable analysis for the LESS, jog, and walk tasks of KVA 3G using the 322 kinematic model and including flexion and abduction of the ankle and knee, and flexion, abduction, and internal rotation of the hip as independent variables.

Table 25: Multivariable analysis of KVA 3G using the 322 kinematic model and including flexion and abduction of the ankle and knee, and flexion, abduction, and internal rotation of the hip as independent variables.

KVA 3G, 322	LESS		Jog		Walk	
R Square	**0.827**		0.606		**0.933**	
Significance	**$\ll$0.001**		0.067		**$\ll$0.001**	
Angle	Coefficients	P-value	Coefficients	P-value	Coefficients	P-value
Ankle Flexion	-0.006	0.159	-0.006	0.380	**-0.016**	**0.002**
Ankle Abduction	0.000	0.842	0.002	0.598	0.002	0.228
Knee Flexion	**0.008**	**$\ll$0.001**	-0.014	0.024	-0.010	$\ll$0.000
Knee Abduction	0.000	0.863	-0.003	0.804	0.004	0.433
Hip Flexion	**0.004**	**$\ll$0.001**	-0.008	0.077	**-0.009**	**0.006**
Hip Abduction	0.002	0.434	0.008	0.184	-0.004	0.575
Hip Internal Rotation	-0.001	0.793	$\ll$0.001	0.953	-0.003	0.283

KVA 3G measured during LESS and walking using the 322 kinematic model were significant (R^2=0.827,p $\ll$ 0.001 and R^2 = 0.933, p $\ll$0.001, respectively), as shown in Table 25. In the LESS condition, the knee flexion and hip flexion angles significantly contributed to the value of KVA 3G ($\beta = 0.008$, p $\ll 0.001$; and $\beta = -0.004$, p $\ll 0.001$, respectively). In the walking condition, the ankle flexion and hip flexion angles significantly contributed to the value of KVA 3G ($\beta = -0.016$, p $= 0.002$; $\beta = -0.009$, p $= 0.006$, respectively).

Table 26 lists the results of the multivariable analysis for the LESS, jog, and walk tasks of the knee abduction angle using the 322 kinematic model and including flexion and abduction of the ankle and knee, and flexion, abduction, and internal rotation of the hip as independent variables.

Table 26: Multivariable analysis of the knee abduction angle using the 333 kinematic model but only including flexion and abduction of the ankle and knee, and flexion, abduction, and internal rotation of the hip as independent variables.

Knee Abduction Angle, 322	LESS		Jog		Walk	
R Square	**0.808**		**0.864**		**0.651**	
Significance	**$\ll$0.001**		**$\ll$0.001**		**0.011**	
Angle	Coefficients	P-value	Coefficients	P-value	Coefficients	P-value
Ankle Flexion	-0.014	0.972	-0.173	0.348	0.206	0.395
Ankle Abduction	-0.236	0.089	0.049	0.625	-0.119	0.235
Knee Flexion	-0.006	0.972	**0.279**	**0.036**	0.184	0.096
Knee Abduction	-	-	-	-	-	-
Hip Flexion	0.081	0.371	0.150	0.141	0.062	0.694
Hip Abduction	-0.024	0.908	**-0.083**	**0.569**	-0.037	0.926
Hip Internal Rotation	**0.811**	**$\ll$0.001**	**0.441**	**$\ll$0.001**	0.200	0.172

KVA 3G measured during LESS, jogging, and walking using the 322 kinematic model were significant (R^2=0.808,p$\ll 0.011$; R^2 = 0.864, p $\ll 0.011$; R^2 = 0.651, p=0.011, respectively), as shown in Table 26. In the LESS condition, the hip internal rotation angles significantly contributed to the value of KVA 3G ($\beta = 0.811$, p $\ll 0.001$). In the jogging condition, the knee flexion, hip abduction, and hip internal rotation angles significantly contributed to the value of KVA 3G ($\beta = 0.279$, p $= 0.0.36$; $\beta - 0.083$, p $= 0.569$; $\beta 0.441$, p $\ll 0.001$, respectively).

6.1 Discussion

It might be assumed that if one angle has a large influence on KVA 2G in one task, then it will have a similar KVA in other tasks. However, Tables 18 through 23 show that significance does not necessarily repeat itself across all tasks as each task has a unique combination of lower body joint angles that contribute to the final position of the subject.

KVA 2G analyzed during the LESS condition for both the nine angles and seven angles

(Table 18 and 21) was found to be significant. However, no one independent variable was found to be individually significant. This is unusual for multivariable analyses, where individual independent variables are typically significantly related to the dependent variable as well.

The knee abduction was found to be significant in KVA 2G analyzed during the walking condition (Table 21). However, the coefficient of knee abduction was small (0.009), indicating that the knee abduction angle contributed significantly, but only a small amount per unit. In Study 1, the knee abduction angle was also calculated to have significance (Pearson correlation coefficient at 95% confidence) the squatting and DS conditions, but not for the LESS, LR, jogging, or pivot condition, where KVA 2P was used for the pivot condition (Table 13).

THe KVA 3G analyzed during the LESS condition for both the nine angles and seven angles (Table 18 and 21) found knee abduction to be significant. However, when KVA 3G was tested in Study 3 (with the same data set and processing methods) using the Pearson correlation coefficient, knee abduction was shown to not have significance (r$= 0.382$, P$= 0.079$). In the multivariable analysis, knee abduction with nine independent variables was slightly more significant (P=0.009) with a higher coefficient (0.140) (Table 19), where the results for the multivariable analysis with seven variables for knee abduction was P$= 0.012$ and a coefficient of 0.100 (Table 22).

In Table 20, the knee internal rotation angle showed to play a significant role in the dependent variable (knee abduction) in the LESS condition. This is notable because some studies restrict the internal rotation the kinematic models during data processing.

7 Study 3: The Effect of Varying Joint Constraints on Multiple Knee Valgus Angles in Female Athletes

Study 3 Hypothesis: Calculating KVA using different lower extremity joint constraints will result in KVAs that are not correlated.

7.1 Abstract

Intro: Soft tissue artifacts (STAs) influence the kinematic measurement of movement when using retroreflective markers on the skin. This study analyzes the differences between lower body joint constraint models across and within multiple tasks.

Methods: The kinematics of 23 (D1 soccer, D1 basketball, and club soccer (height $=$ 171.2 ± 8.9cm, weight $=$ 66.3 ± 8.6kg, age $=$ 19.8 ± 1.9yr)) female athletes were analyzed using a 10-camera VICON motion capture system. Four analysis models were designed by varying the degrees of freedom (DOF) in the hip, knee, and ankle: 1) six, 2) three, 3) three-three-two, and 4) three-two-two DOF, respectively. Three angles were measured at maximum knee flexion: 1) knee flexion, 2) knee valgus in 2D, and 3) knee valgus in 3D. The models were compared across three tasks: 1) walking, 2) jogging, and 3) drop-jumping.

Hypothesis: Angles will vary more between models during high-impact tasks than lower impact tasks.

Results: Angles correlated more between models during the high-impact task (drop-jump) than the lower impact task (walking) at maximum knee flexion.

Conclusion: At maximum knee flexion, high-impact tasks may have reduced STA influence on measured angles than lower impact tasks.

7.2 Methods

7.2.1 Statistical Analysis

Three angles (knee flexion, KVA 2G, and KVA 3G) were measured at maximum knee flexion for each model (666, 333, 332, and 322) then compared with one another. Additionally all the angles and models were measured during walking, jogging, and LESS. The data was statistically analyzed with a two-tailed Pearson Correlation test using SPSS (SPSS Inc, Chicago, Illinois). The data was tested at a 95% confidence level, and the results are considered significant when the Pearson correlation coefficient, r, with a corresponding p value of $< .05$.

7.3 Results

The following tables show the correlation between different models and tasks between each subject's tasks. Table 27 shows the correlations between the tasks and models for knee flexion, Table 28 shows the correlations between the tasks and models for KVA 2G, and Table 29 shows the correlation between the tasks and models for KVA 3G.

Table 27: Comparing the maximum knee flexion angle during stance phase of the same subject during each task, walking, jogging, and LESS, between the four models.

		Walking				**Jogging**				**LESS**			
Model		666	333	332	322	666	333	332	322	666	333	332	322
666	r	**1.000**	0.350	0.391	0.157	**1.000**	**0.476**	**0.557**	**0.514**	**1.000**	**0.965**	**0.897**	**0.902**
	P	**0.000**	0.110	0.072	0.497	**0.000**	**0.034**	**0.013**	**0.020**	**0.000**	**<0.001**	**<0.001**	**<0.001**
333	r	0.350	**1.000**	**0.956**	0.274	**0.476**	**1.000**	**0.612**	**0.985**	**0.965**	**1.000**	**0.892**	**0.900**
	P	0.110	**0.000**	**<0.001**	0.229	**0.034**	**0.000**	**0.004**	**<0.001**	**<0.001**	**0.000**	**<0.001**	**<0.001**
332	r	0.391	**0.956**	**1.000**	0.300	**0.557**	**0.612**	**1.000**	**0.554**	**0.897**	**0.892**	**1.000**	**0.998**
	P	0.072	**<0.001**	**0.000**	0.187	**0.013**	**0.004**	**0.000**	**0.014**	**<0.001**	**<0.001**	**0.000**	**<0.001**
322	r	0.157	0.274	0.300	**1.000**	**0.514**	**0.985**	**0.554**	**1.000**	**0.902**	**0.900**	**0.998**	**1.000**
	P	0.497	0.229	0.187	**0.000**	**0.020**	**<0.001**	**0.014**	**0.000**	**<0.001**	**<0.001**	**<0.001**	**0.000**

Where r is the Pearson correlation coefficient and P is the significance

The bolded values in Table 27 show the correlation between models of each task for knee flexion. For this angle and walking task, only the models 332 and 333 were correlated to one another. However, during jogging and the LESS test, all of the models correlated with one another. Additionally, the probability that different models would produce different knee flexion values for the highest impact task (LESS) was less than 0.001 for all models.

Table 28: Comparing the KVA 2G of the same subject for each task, walking, jogging, and LESS, between the four models.

		Walking				**Jogging**				**LESS**			
Model		666	333	332	322	666	333	332	322	666	333	332	322
666	r	**1.000**	**0.865**	**0.902**	0.336	**1**	**0.550**	**0.714**	**0.649**	**1.000**	**0.886**	**0.919**	**0.784**
	P	**0.000**	**<0.001**	**<0.001**	0.127	**0.000**	**0.012**	**<0.001**	**0.002**	**0.000**	**<0.001**	**<0.001**	**<0.001**
333	r	**0.865**	**1.000**	**0.779**	0.383	**0.550**	**1**	**0.744**	**0.505**	**0.886**	**1.000**	**0.858**	**0.736**
	P	**<0.001**	**0.000**	**<0.001**	0.086	**0.012**	**0.000**	**<0.001**	**0.028**	**<0.001**	**0.000**	**<0.001**	**<0.001**
332	r	**0.902**	**0.779**	**1**	0.347	**0.714**	**0.744**	**1.000**	**0.894**	**0.919**	**0.858**	**1.000**	**0.916**
	P	**<0.001**	**<0.001**	**0.000**	0.113	**0.001**	**<0.001**	**0.000**	**<0.001**	**<0.001**	**<0.001**	**0.000**	**<0.001**
322	r	0.336	0.383	0.347	**1.000**	**0.649**	**0.505**	**0.894**	**1.000**	**0.784**	**0.736**	**0.916**	**1.000**
	P	0.127	0.086	0.113	**0.000**	**0.002**	**0.028**	**<0.001**	**0.000**	**<0.001**	**<0.001**	**<0.001**	**0.000**

Where r is the Pearson correlation coefficient and P is the significance

The bolded values in Table 28 show the correlation between models of each task for KVA 2G. For walking, each of the models except, for 322, were significantly similar to one another, and as a result the value for KVA 2G is not dependent on processing the data with the 666, 333, or 332 models. Similarly, the walking and LESS tasks were not dependent on the difference between the 666, 333, or 332. However, for these two tasks, the 322 model was also correlated with the other models, so any of the four models can be chosen and will produce similar KVA 2G angle. Similar to the knee flexion angle, the probability that different models would produce different KVA 2G values for the highest impact task (LESS) was less than 0.001 for all models. Once again, the difference in joint DOF constraints did not significantly change the resultant

KVA 2G value.

Table 29: Comparing the KVA 3G of the same subject for each task, walking, jogging, and LESS, between the four models.

		Walking				**Jogging**				**LESS**			
Model		666	333	332	322	666	333	332	322	666	333	332	322
666	r	**1.000**	0.054	0.185	0.053	**1.000**	**0.586**	0.164	**0.479**	**1.000**	**0.849**	**0.731**	-0.190
	P	**0.000**	0.812	0.411	0.819	**0.000**	**0.007**	0.503	**0.033**	**0.000**	**<0.001**	**<0.001**	0.397
333	r	0.054	**1.000**	**0.816**	0.101	**0.586**	**1.000**	**0.579**	**0.722**	**0.849**	**1.000**	**0.781**	-0.084
	P	0.812	**0.000**	**<0.001**	0.664	**0.007**	**0.000**	**0.007**	**0.000**	**<0.001**	**0.000**	**<0.001**	0.711
332	r	0.185	**0.816**	**1.000**	0.192	0.164	**0.579**	**1.000**	**0.539**	**0.731**	**0.781**	**1.000**	-0.142
	P	0.411	**<0.001**	**0.000**	0.404	0.503	**0.007**	**0.000**	**0.017**	**<0.001**	**<0.001**	**0.000**	0.528
322	r	0.053	0.101	0.192	**1.000**	**0.479**	**0.722**	**0.539**	**1.000**	-0.190	-0.084	-0.142	**1.000**
	P	0.819	0.664	0.404	**0.000**	**0.033**	**<0.001**	**0.017**	**0.000**	0.397	0.711	0.528	**0.000**

Where r is the Pearson correlation coefficient and P is the significance

The models for the KVA 3G angle, Table 29, also had correlations with one another. For walking, only the 332 and 333 models were correlated. More models related to each other for jogging and LESS. For jogging all except 666 to 332 correlated, and for LESS all except 322 to 666, 333, and 332 correlated. These correlations suggest, as well, that similar angles can be found despite the different uses in models.

7.4 Discussion

The results were contrary to the hypothesis that increasing the impact of tasks will yield significant differences in the measured angles across the lower body kinematic models. The findings in this study showed that the models were correlated despite the increased impact during jogging and jumping (Tables 27, 28, and 29). This suggests that angles measured during walking, jogging, and jumping will be similar regardless of the kinematic model used.

Marker position is affected by the local placement of soft tissue. Despite the hypothesis

that the markers would move more with higher impact tasks and therefore increase variability in angles, the results showed that in some cases, the tasks with increased forces were correlated. One explanation could be that during higher impact tasks, the markers are translated similarly as the markers move in the same direction due to the increased force applied to each segment. During lower impact tasks, the soft tissue position is less controlled by momentum and more dependent on the frequency of the tissue. Therefore, the marker movement is not dependent on the overall position of the limbs.

The differences in model correlations between tasks could also be a result of limb geometry. The correlations between models in knee flexion angle, Table 27, increases between walking, to jogging, to the LESS drop jump. It could be said that the increased flexion tightens the soft tissue of the thigh, thereby reducing artifacts on that limb. This is unlikely given that a highly unusual amount of translation in the thigh segment during the drop jump when the knee translations are not fixed, suggesting that the soft tissue is moving along the segment. Without further analysis, the cause of this phenomenon cannot be known in its entirety.

It is only shown that the models correlate with each other at maximum knee flexion. These correlations may not necessarily be the same if the angles were measured at a different point during the trial. Additional analysis should be done to determine if the models continue to keep the same correlations over a period of time rather than just at the maximum knee flexion position.

Analyzing individual marker movements as a result of STAs could indicate the best marker placements. In addition to placing markers on bony landmarks, markers can be placed on sections of limbs that have the least amount of soft tissue movement. As a result, the STAs that cause improper marker movement would be reduced. Additionally, learning more about patterns of soft tissue movement for specific tasks could inform how much STAs affect different

movements. This could help determine which tasks should be tested and, as a result, reduce the influence of STAs on the final data.

The relationships between the test population and the greater population may not fully relate as the subjects train regularly and were familiar with the tasks tested. Increasing the number of subjects tested would reduce the amount of variability. Some athletes had previous knee injuries, which may have influenced the outcome, even though the tests were compared between subjects. There was not a golden standard that the models were compared to; rather, the subject data were compared to determine trends.

The knee flexion angle was not controlled during the collection of data. Therefore, the magnitude of this confounder is unknown. It can be assumed the influence of this variable is small compared to the change in other variables because of the varying and irregular pattern in the change in knee flexion between tasks. Additionally, many angles in the lower body contribute to each knee valgus angle, including the hip, all of which cannot be controlled.

8 Conclusion

Focusing on a single joint or task gives focus to testing protocols and rehabilitation programs, but that focus should be based on correlations that exist rather than extrapolating correlations beyond what has been statistically confirmed. Even though it can be helpful to focus and simplify the connection between joint angles and KVA, researchers and clinicians should be wary of neglecting the complexity of the human system. A single joint angle is only one of many contributing factors to a KVA or lower extremity orientation rather than being solely responsible for any particular angle. Additionally, changing the kinematic joint constraints may assist in reducing STAs, but generally, the different KVA angles were found to be similar even when different joint constraint models were used to process the motion capture data.

Study 1: Comparative Analysis of Medial Knee Alignment Definitions in Female Athletes

Lower extremity joint angles and the different KVAs should be considered individually, and the statistical significance between the angles should be considered before assuming the angles are significantly related. Many of the correlations lack significance. However, the relatively small number of subjects (23 subjects) warrants caution when making conclusions on the angles not to be certainly correlated to one another. What can be concluded from the data is that just because one angle has a relationship with ACL injury does not necessarily mean that same angle will have the same relationship when measured during a different task.

Different mathematical models measured during one type of task did not result in true equivalence between these angles (r = 1.000 and P = 0.000). However, some of the different KVAs and lower extremity joint angles did have high correlation within each task even between different movement tasks. Specifically, the KVA 2P and 2G had strong significance ($P \ll 0.001$) and a similar Pearson value correlation coefficient for each of the tasks. This suggests

the KVA 2P can be used during rotating tasks where the KVA 2G is limited by the global reference frame. However, more tasks will need to be considered to determine if this substitute can be trusted.

Each of the lower extremity joint angles and different KVAs analyzed have distinct applications in biomechanics and will continue to have individual purpose. Therefore, it is impossible to choose one angle that is objectively better and which should always be used. It is more important that an author be informed of the types of angles, so that they can make an knowledgeable decision when choosing measuring techniques. Researchers and clinicians should be informed of the various types of angles so that they are able to determine the best angle for their purpose.

Study 2: Multivariable Analysis of Lower Limb Joint Angles and Knee Valgus Angles in Female Athletes

Some angles (independent variables) influence the value of the KVA 2G, KVA 3G, and the knee abduction angle more than others, but all the angles of the lower body work together and contribute to the final position of the subject. Analyzing the importance of the rotations of the ankle, knee, and hip (flexion, abduction, and internal rotation) to various forms of KVA helps prioritize individual angles when attempting to reduce a KVA. However, all angles should be considered before simplifying the system and exclusively focusing on one angle.

The human body is a complex system that can not be easily simplified. Simplifying the complexities of biological systems is helpful, if not required, to make advances in medicine, performance, et., but should be recognized as simplifications and not an exact representation of the system.

Study 3: The Effect of Varying Joint Constraints on Multiple Knee Valgus Angles in Female Athletes

It was found that changing the lower extremity kinematic joint constraint model did not generally change the value of the different KVAs, especially in higher impact tasks. This was contrary to the hypothesis that the angles calculated based on the different kinematic models would be significantly related during low-impact tasks but not higher impact tasks. There were exceptions to this conclusion though, namely KVA 2G-walking, knee flexion-walking, and KVA 3G-walking. However, the similarity between most of the angles suggests that changing the kinematic model used to process motion capture data does modify the data enough to significantly change most angles, even in higher impact tasks.

9 Future Study I: A Comparative Analysis of Knee Valgus Angles in MRI and Motion Capture

9.1 Introduction

In both imaging (particularly magnetic resonance imaging, MRI) and movement analysis (particularly video motion capture), the KVA is commonly measured to determine ACL injury risk and to assess chronic conditions such as knee osteoarthritis. MRI angles are also used for surgery planning in ACL reconstruction and knee replacement to facilitate normal kinematic functioning of the knee. Knowing how knee angles measured using MRI relates to angles measured during gait, using motion analysis, may help customize knee alignment in total knee replacement surgeries or other repairs. The purpose of this study would be to test the hypothesis that multiple knee angles measured with motion capture are related to similar angles measured via MRI in order to better understand how surgical alignment of the knee might impact subsequent gait kinematics.

9.2 Background

The goal in knee replacement, ACL reconstruction, or other knee-related surgeries is to allow the individual to safely perform tasks of daily living or higher performing tasks without pain and in a manner that reduces future injuries. When joint replacement surgeries were first being performed, there was little consideration of joint mechanics. Over time, though, surgeries concerning the joint (including ACL reconstructive surgeries) considered not only joint impact loads, but the angles in the joint required to perform a gait pattern as close as possible to the pre-injury gait. This excludes unique cases where bone modification is required to allow the individual to walk in a safe manner, including valgus deformity of the knees[33,164,180].

The combination of movement studies (motion capture) and imaging (such as MRI) provide

essential information in how to improve the success of surgeries. As the individual is lying on the table, instead of upright like in a movement analysis with motion capture, a surgeon working on the knee has the local coordinates of the shank and thigh as well as the plane in reference to the table. In an MRI, the surgeon is provided with less information. Not only is there no reference in the image to the global plane, but the shank and the femur are segmented and only the portion of the bone at the knee joint is able to be imaged. ISB recommendations on building local coordinate systems on segments of the body require the full segment to make the local coordinate system and to create the long axis of segments through the mechanical joint centers[205]. The small capture volume of MRI prevents the measurement of the ankle and hip joint centers and requires the shaft of the long bone to be used for the axis reference. As a result, alternative methods are used to create local coordinate systems for the thigh segments, namely using the anatomic axis (axis along the shaft) instead of the mechanical axis (axis from the knee joint center to the hip joint center). The femoral mechanical anatomic angle (FMA) or the anatomical-mechanical angle (AMA), which is the angle between the anatomic and mechanical axes, has been well documented in imaging research and has even been found to correlate with valgus OA[33–35,80,85,104,137,138,169,178,184,200]. Surgeons have even been advised to consider FMA angle when planning total knee arthroplasty[35]. Miranda et al. developed a method to identify local coordinates on segmented limbs with a computed tomography (CT) scan using cylindrical shapes over the shaft of the tibia and femur to calculate the anatomic axes. MRI scans have smaller capture volumes than CT-scans. Therefore matching cylindrical shapes to the shafts is too arbitrary for repeatability given the shape of the bones when cut short.

9.3 Methods

9.3.1 Participants

Preliminary testing (for biomechanics and MRI) was collected for 9 female student soccer athletes from Auburn University (height = 171.2 +/- 8.9 cm, weight = 66.3 +/- 8.6, kg age = 19.8 +/- 1.9 yr). Athletes were not excluded based on prior injuries or surgeries.

9.3.2 Instrumentation

The subjects were be fitted with 79 retroreflective markers using the point cluster technique shown in Figure 27[9]. Kinematic and kinetic data will be captured with a 10-camera motion capture system (Vicon, Vantage V5 Wide Optics cameras with 22 high-powered IR LED strobe at 85 nm) and two force plates embedded in the floor (AMTI BP400600, 2000 lb. capacity). The cameras were configured so that the motion capture volume (the volume at which three or more cameras can view a single marker) was be directly above the force plates embedded in the floor. Data from the Vicon system and force plates was collected using Nexus software (Version 2.6.1; Vicon Motion Systems Ltd, Oxford Industrial Park, Oxford, UK).

9.3.3 Data Processing

The marker data was filtered using a 15 Hz lowpass butterworth filter, then processed and analyzed using Visual 3D. The ISB recommendations for anatomical coordinate systems was used for each segment[204]. The subjects performed each task at least three times for a minimum of three complete trials. The subjects were given minimal directions to perform each task, so that the task was performed with as little influence from the researchers as possible.

9.3.4 Tasks

For the motion capture portion of the study, each subject completed a minimum of three trials for each of the tasks listed: 1) vertical drop jump: LESS[150,151], 2) squat, 3) walking down stairs (DS), 4) lateral reach (LR), 5) walking, 6) jogging, 7) 180° pivot turn (pivot). These tasks are described in detail in Section 3.4.

9.3.5 Angles

The angles described in Section 3.5 were measured in this study. However, only knee flexion and abduction angle were measured on the MRI models.

9.3.6 MRI

A 7-Tesla MRI machine was used to image both right and left knees using a true fast imaging (TRUFI) sequence. The subjects were instructed to self-align themselves in a comfortable, supine position, and their knees were braced to prevent movement during the scan. The TRUFI images were segmented in Amira and reconstructed to form a 3D rendering of the femur and tibia structures as well as their alignment (Mercury Computer Systems, Inc.; Chelmsford, US). The Laplacian Smooth function was used in MeshLab to smooth irregularities from the segmentation.

In the preliminary data collection, local reference frames were fixed to the femur and tibia using similar method as Miranda et al.[123]; however, adjustments had to be made due to differences in instrumentation. Because a CT-scan (computed tomography scan) produced the knee images in the work done by Miranda et al.[123], a larger portion of the bone shaft length was available than what the MRI scans produce. As a result, the inertial axis of the diaphysis used to calculate the anatomic axis of the bones of the CT-scan is not a reliable method for calculating the anatomic axis of MRIs.

The tibial longitudinal axis was defined by the centroid of a cross-section of the tibial plateau and the centroid of the cross-sectional area of the distal-most part of the tibial shaft. The lateral axis of the tibia was defined by the most medial and lateral points of the tibial plateau cross-section. The femur longitudinal axis was defined by the shaft inertial axis and the centroid of the cross-sectional area of the proximal-most part of the femur shaft. The lateral axis was identified by fitting a cylinder to the femoral condyles. The lateral axis was defined by the farthest medial and lateral points along the centerline of the cylinder. The cross product was used with the distal axes and proximal axes to create the orthogonal coordinate systems. Blender (V2.4.9; Stitching Blender Foundation, Amsterdam, Netherlands) was used to select the points that identified the local reference frames.

9.3.7 Statistics

The pilot data compared knee angles measured with MRI scans to knee angles measured with motion capture technology during movement tasks. The following angles were measured at maximum knee flexion during the stance phase of LESS, walking, and jogging: knee flexion, knee abduction, knee internal rotation angles, KVA 2G, and KVA 3G. The following angles were calculated from the 2D femur and tibia MRI rendering: knee flexion, abduction, and internal rotation angles. All the angles from MRI and motion capture were then compared using a two-tailed Pearson Correlation test with a 95% confidence interval.

The pilot results of this study support the hypothesis that knee angles measured from MRI are related to angles measured using motion capture data

9.4 Results

The following are the results from the pilot data for the nine female athletes. A rendering of the 3D femur and tibia structures and their alignment is shown in Figure 34.

Figure 34: A rendering of the 3D femur and tibia structures and their alignment from the MRI pilot data using Amira and Blender.

Table 30: Values of knee flexion angle, knee abduction angle, and KVA 2G measured during walking with motion capture, as well as the knee flexion and abduction angles measured with MRI.

Task	**Knee Angle**	**Mean (°)**	**SD**
Walking (Motion Capture)	Flexion	1.10	2.49
	Abduction	14.46	6.38
	KVA 2G	0.09	0.04
MRI	Flexion	3.09	6.02
	Abduction	0.32	1.98

Table 31: MRI knee flexion compared to the knee abduction angle and KVA 2G measured during walking with motion capture.

Walking	MRI Knee Flexion Angle	
Knee Angle	r	P
Abduction	**0.70**	**0.036**
KVA 2G	**0.767**	**0.016**

9.5 Discussion

The pilot results of this study support the hypothesis that knee angles measured from MRI are related to angles measured using motion capture data. More specifically, the results show a correlation between the resting KF angle measured with MRI and KVA at maximum KF measured from motion capture during the gait cycle. Therefore, KF angle in MRI gives insight into KVA and KA measured with motion capture. This may allow physicians to better understand how surgical alignment of the knee impacts subsequent gait kinematics. The fact that the MRI KF is highly correlated with KVA from motion capture shows that using static measurements for reconstruction alignment is beneficial for the dynamic functions of the knee.

10 Future Study II: A Comparative Analysis of Knee Valgus Angles in Drop-Jump Variations

10.1 Introduction and Background

Multiple variations of drop jumps can be found in the research literature that focuses on knee alignment, from drop-vertical jump to drop-forward jump: these tasks vary in methodology and execution [3,10,13,15,23,27,28,31,38,50,62,78,87,88,98,109,111,112,115,119,125,126,133,140,142,150,151,176,187,190,195,197,198,203]. In Study 1, the findings showed that different tasks resulted in different joint angles of the lower body. Angles measured across the tasks (walking, jogging, LESS, DS, LR, squatting, and pivot turn) were not always significantly related to one another. However, many studies do not distinguish between the type of drop jump executed by the test subjects. Some standard developments of drop-jumps for ACL testing have been developed, such as the landing error scoring system; however, many of these are associated with point systems for grading performance rather than being used in motion capture research programs [150]. Accordingly, one potentially useful study to be conducted in the future would be to determine the similarities and differences in knee angles measured during different types of drop jumps. This would allow researchers to effectively compare data across studies, preventative measurement programs, and rehabilitation programs.

This study would test multiple types of drop jumps (drop-vertical jump, drop-forward jump, etc.). The purpose of such study would not be to determine which drop-jump method is best, but to determine how the drop jump tests are to be compared across studies.

This study would also expand the work done in a previous study by Cruz et al.,"The Effects of Three Jump Landing Tasks on Kinetic and Kinematic Measures: Implications for ACL Injury Research" [31]. This study found that there were minor variations between jump landing tasks, which resulted in varying kinematics and kinetics differences. This study measured and compared the knee abduction angle as measured in the JCS [31,57].

The proposed hypothesis for this study would be similar to that of the Cruz et al. study but with a goal of identifying similarities, not just differences, between the squatting, dropping, drop-jumping, and jumping tasks. It is important not only to know if the tasks are different, but to know which tasks and which parts of those tasks are equivalent in order to compare studies using these methods.

Hypothesis: There are equivalent joint angles, knee valgus angles, joint kinetics, and GRF between squatting, dropping, drop-jumping, and jumping tasks.

10.2 Methods

10.2.1 Instrumentation

The subjects will be fitted with 79 retroreflective markers using the point cluster technique shown in Figure 27[9]. Kinematic and kinetic data will be captured with a 10-camera motion capture system (Vicon, Vantage V5 Wide Optics cameras with 22 high-powered IR LED strobe at 85 nm) and two force plates embedded in the floor (AMTI BP400600, 2000 lb. capacity). The cameras will be configured so that the motion capture volume (the volume at which three or more cameras can view a single marker) will be directly above the force plates embedded in the floor. Data from the Vicon system and force plates will be collected using Nexus software (Version 2.6.1; Vicon Motion Systems Ltd, Oxford Industrial Park, Oxford, UK).

10.2.2 Data Processing

The marker data will be filtered using a 15 Hz lowpass butterworth filter, then processed and analyzed using Visual 3D. The ISB recommendations for anatomical coordinate systems will be used for each segment[204]. The subjects will perform each task at least three times for a minimum of three complete trials. The subjects will be given minimal directions to perform each task, so that the task will be performed with as little influence from the researchers as

possible.

10.2.3 Tasks

Eleven tasks will be tested in this study: squatting, vertical jump, drop-landing, drop-vertical jump, and drop-forward jump. The drop-landing, drop-vertical, and drop-forward jumps will each be tested at three different distances.

Squat

For the squat, the subjects will be instructed to stand at the width they would typically stand to perform a squat with one foot placed on each force plate. The subjects will be given a light weight PVC-pipe to hold directly in front of them while they squat so as to not obscure markers while allowing for a counter balance to replicate lifting patterns experienced during their regular workout routines. This task is shown in Figure 35.

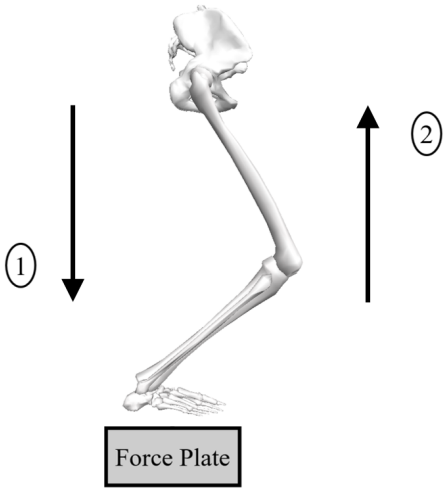

Figure 35: Squatting on a force plate. 1) downward motion from neutral, 2) return to neutral.

Vertical Jump

The subjects will be instructed to stand on the force plates with their feet at a comfortable distance apart. They will then be instructed to perform a countermovment and to jump vertically for maximum height. This task is shown in Figure 36.

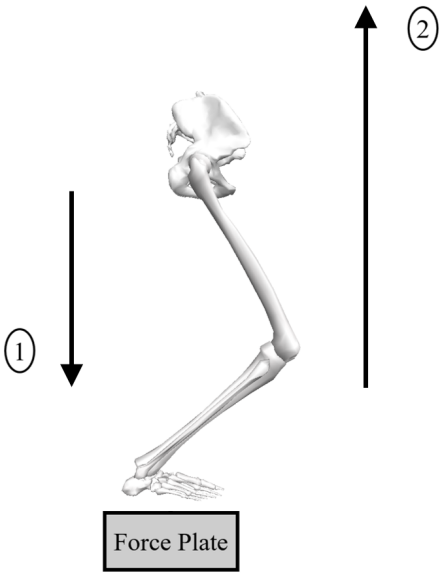

Figure 36: Vertical jump from standing on a force plate. 1) downward counter-movement from neutral, 2) vertical jump for maximum height.

Drop Landing, Vertical Jump, and Forward Jump

In each of the following tasks, the subject will jump from the top of a 12" box onto the two force plates previously described in Section 10.2.1. Nine versions of the jump will be tested. Three jump ranges with distances of 0% of the subject's height (Figure 37), 25% of the subject's height (Figure 38), and 50% of the subject's height (Figure 39). The subjects will also perform three types of jumps: a drop landing (Figures 37a, 38a, and 39a), a drop vertical jump (Figures 37b, 38b, and 39b), and a drop forward jump (Figures 37c, 38c, and 39c). The vertical jump will be for maximum height and the forward jump will be for maximum distance.

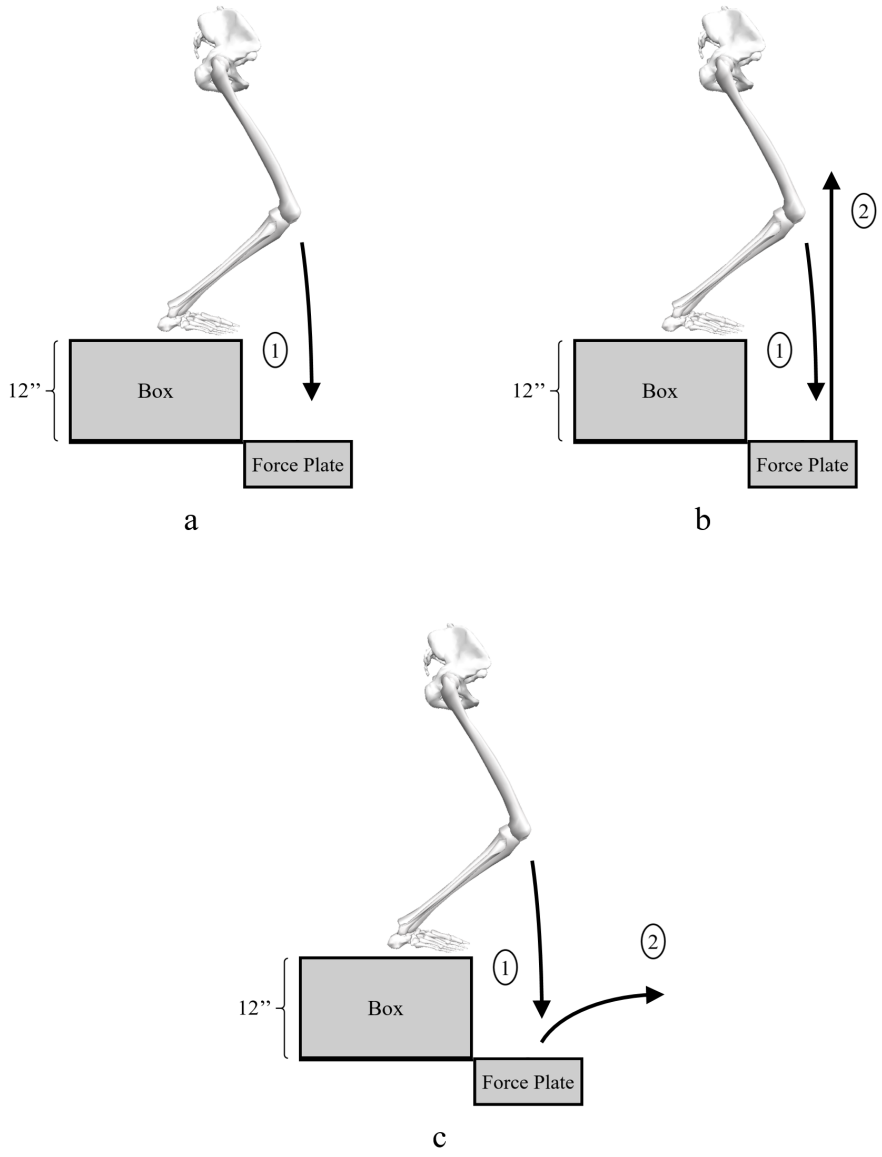

Figure 37: Configuration of the drop task with the landing position (force plate) a distance of 0% subject height away from a 12” tall box: a) drop landing, b) drop vertical jump for maximum height, and c) drop forward jump for maximum distance.

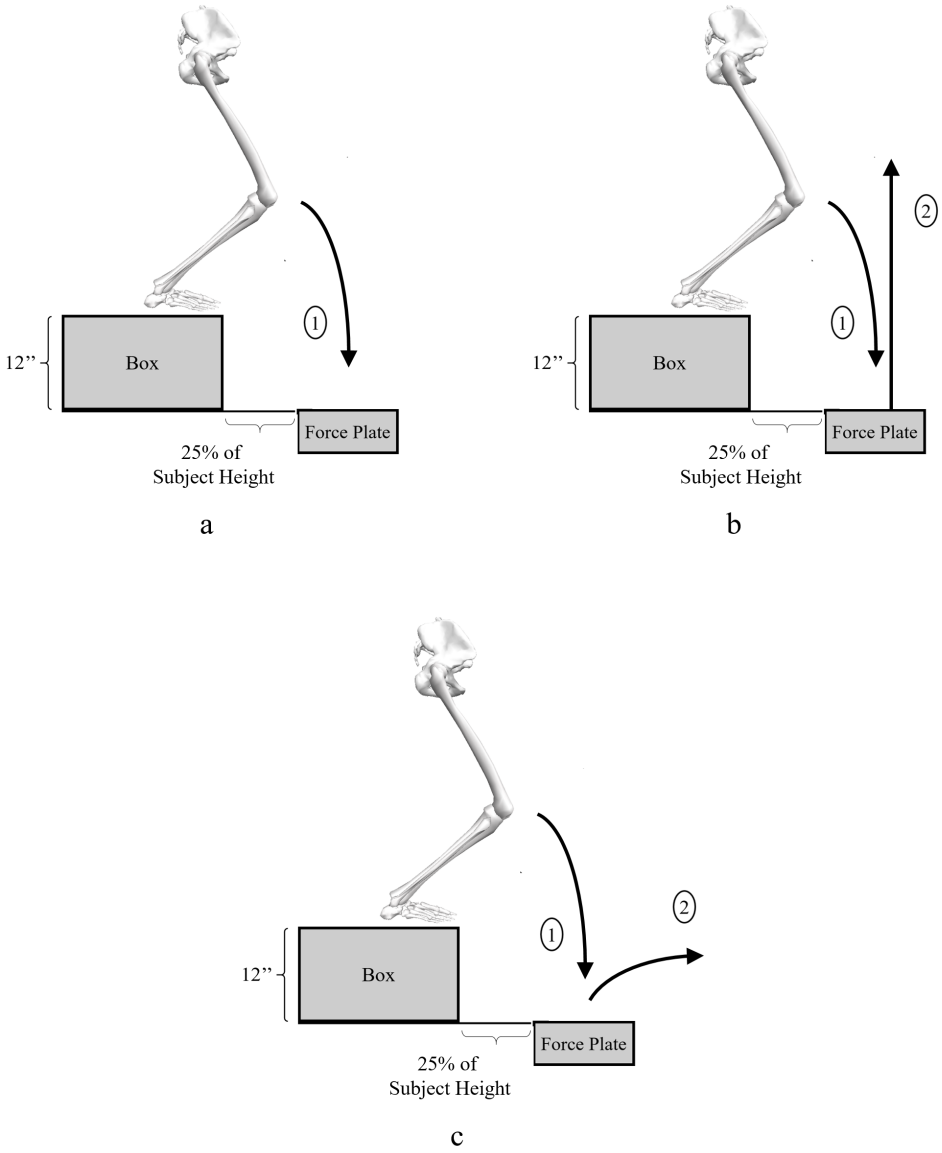

Figure 38: Configuration of the drop task with the landing position (force plate) a distance of 25% subject height away from a 12” tall box: a) drop landing, b) drop vertical jump for maximum height, and c) drop forward jump for maximum distance.

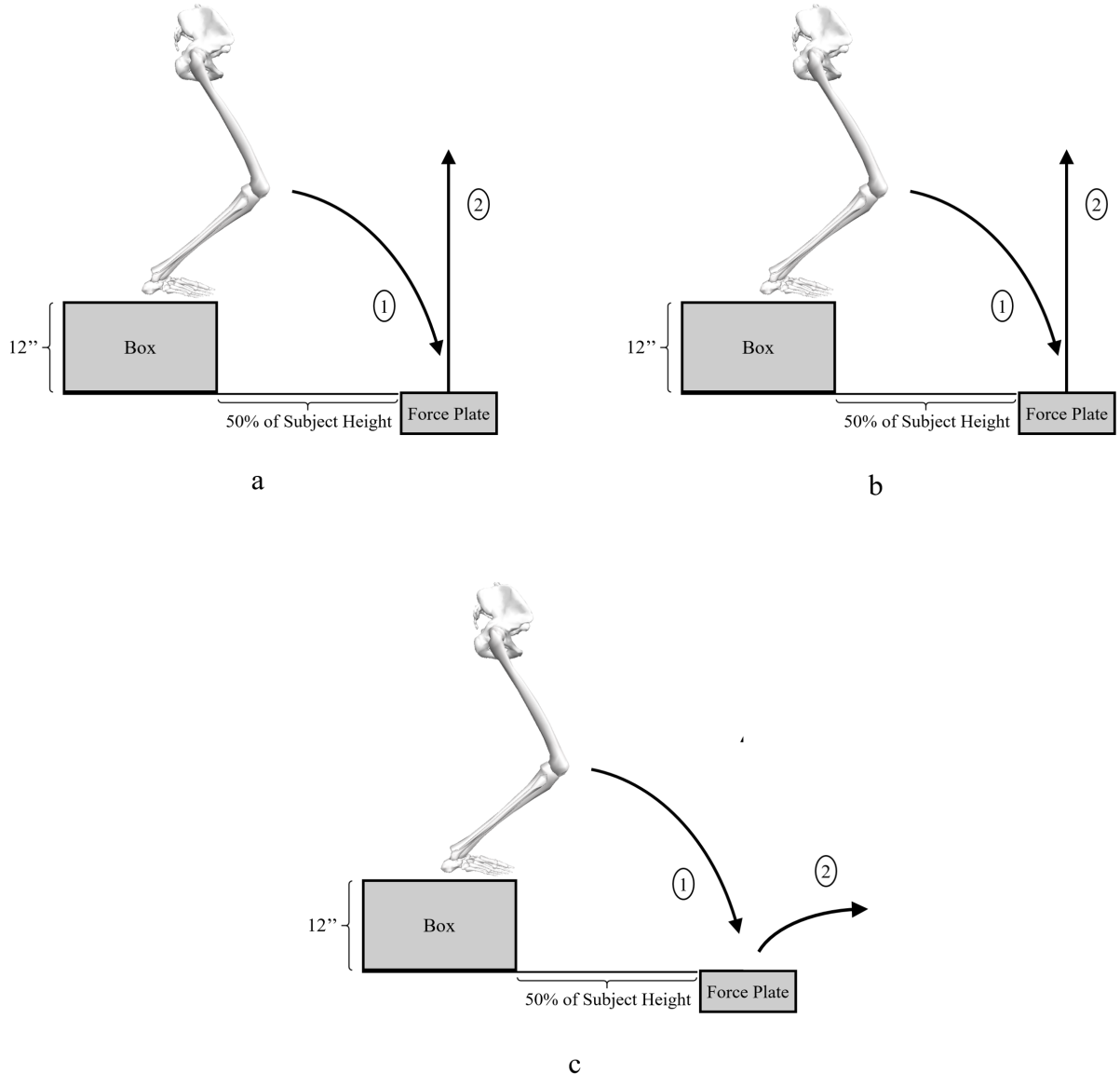

Figure 39: Configuration of the drop task with the landing position (force plate) a distance of 50% subject height away from a 12” tall box: a) drop landing, b) drop vertical jump for maximum height, c) drop forward jump for maximum distance.

10.2.4 Angles

The angles described in Section 3.5 will be measured in this study.

10.2.5 Statistical Analysis

A Pearson Correlation Coefficient Test and a paired T-test will be run with the angles of interest (ankle, knee, and hip flexion, abduction, and internal rotation, as well as KVA 2G and KVA

3G) to determine if any of the angles can be treated equivalently. Evidence of equivalent angles across differing bodies will allow researchers to more accurately and confidently connect discussions of these angles across the research literature.

11 Future Study III: A Comparative Analysis of Knee Valgus Angles and Moments between Multiple Tasks

11.1 Introduction

The kinematics of a subject during a movement task are important because they are a component affecting forces of the joints that is tangible. However, it is the force at local joints that cause injuries, such as ACL ruptures. Study 1 found that some angles were correlated across tasks, but that a correlation was not necessarily the case. Further study would determine if the same joint moments have correlations between tasks. The purpose of this study is to test the hypothesis that an individual who has a large peak vGRF during a drop jump will have a similarly high peak vGRF in other tasks.

11.2 Background

Forces in the knee play a large role in the health of the ACL. As a result, understanding the forces related to the knee during tasks related to daily living, as well as tasks that would be seen in high level sports and military personnel, is essential in developing preventative training programs and rehabilitation programs, and identifying risk factors.

Consequently, forces and moments of the knee have been considered as identifiable risk factors for future ACL ruptures[108,109,151,179]. In fact, peak vertical ground reaction force (vGRF) during vertical drop jumps has been shown to be associated with later ACL ruptures[109].

The position of the individual and joint angles influence how and where the forces and moments are applied in the body. In Study 1, the lower limb angles were not necessarily similar between different tasks. Because of the connection between positions and orientation with the kinematics, differences in forces will most likely be seen between the different tasks in this future study.

11.3 Methods

11.3.1 Instrumentation

The subjects will be fitted with 79 retroreflective markers using the point cluster technique shown in Figure 27,[9]. Kinematic and kinetic data will be captured with a 10-camera motion capture system (Vicon, Vantage V5 Wide Optics cameras with 22 high-powered IR LED strobe at 85 nm) and two force plates embedded in the floor (AMTI BP400600, 2000 lb. capacity). The cameras will be configured so that the motion capture volume (the volume at which three or more cameras can view a single marker) will be directly above the force plates embedded in the floor. Data from the Vicon system and force plates will be collected using Nexus software (Version 2.6.1; Vicon Motion Systems Ltd, Oxford Industrial Park, Oxford, UK).

11.3.2 Data Processing

The marker and force plate data will be filtered using a 15 Hz lowpass butterworth filter. The marker data will then be processed and analyzed using Visual 3D. The ISB recommendations for anatomical coordinate systems will be used for each segment[204]. The subjects will perform each task at least three times for a minimum of three complete trials. The subjects will be given minimal directions to perform each task, so that the task will be performed with as little influence from the researchers as possible.

11.3.3 Tasks

Each subject will complete a minimum of three trials for each of the tasks listed: 1) vertical dropjump: LESS[150,151], 2) squat, 3) walking down stairs (DS), 4) lateral reach (LR), 5) walking, 6) jogging, 7) 180° pivot turn (Pivot). These tasks are described in detail in Section 3.4.

11.3.4 Statistics

The force data will be compared using a Pearson's Correlation Test. The three force variables tested will be peak the knee abduction moment, peak knee flexion moment, and peak vGRF. Significance will be at a 95% confidence interval.

For the hypothesis tested in this study, the r value is not expected to be large, since the value of knee abduction moment, knee flexion moment, and vGRF will inevitably have different ranges of magnitudes for each of the tasks. It is the strength of the r value in its statistical significance (p-value) that will provide information on the ratio of increased peak knee abduction moment, knee flexion moment, and vGRF between the tasks tested. This will determine if there is a pattern of peak values between the tasks.

References

[1] (2018). Valgus. (n.d.). *Merriam-Webster Dictionary Online*.

[2] (2018). Valgus. (n.d.). *Merriam-Webster Dictionary Online*.

[3] Afifi, M. and R. N. Hinrichs (2012). A mechanics comparison between landing from a countermovement jump and landing from stepping off a box. *Journal of Applied Biomechanics 28*(1), 1–9.

[4] Akins, J. S., P. F. Longo, M. Bertoni, N. C. Clark, T. C. Sell, G. Galanti, and S. M. Lephart (2013). Postural stability and isokinetic strength do not predict knee valgus angle during single-leg drop-landing or single-leg squat in elite male rugby union players. *Isokinetics and Exercise Science 21*(1), 37–46.

[5] Alentorn-Geli, E., G. D. Myer, H. J. Silvers, G. Samitier, D. Romero, C. Lázaro-Haro, and R. Cugat (2009). Prevention of non-contact anterior cruciate ligament injuries in soccer players. Part 1: Mechanisms of injury and underlying risk factors. *Knee Surgery, Sports Traumatology, Arthroscopy 17*(7), 705–729.

[6] Almeida, G. P. L., F. J. R. França, M. O. Magalhães, T. N. Burke, and A. P. Marques (2016, mar). Q-angle in patellofemoral pain: relationship with dynamic knee valgus, hip abductor torque, pain and function. *Revista Brasileira de Ortopedia (English Edition) 51*(2), 181–186.

[7] Ambegaonkar, J., S. Shultz, D. Perrin, R. Schimtz, T. Ackerman, and M. Schulz (2008). ACL injuries - The gender bias. *Journal of Athletic Training 43*(5), 543–560.

[8] Andersen, M. S., D. L. Benoit, M. Damsgaard, D. K. Ramsey, and J. Rasmussen (2010).

Do kinematic models reduce the effects of soft tissue artefacts in skin marker- based motion analysis? An in vivo study of knee kinematics. *Journal of Biomechanics 43*(2), 268–273.

[9] Andriacchi, T. P., E. J. Alexander, M. K. Toney, C. O. Dyrby, and J. a. Sum (1998). A point cluster method for in vivo motion analysis: applied to a study of knee kinematics. *Journal of biomechanical engineering 120*(6), 743.

[10] Arai, T. and H. Miaki (2013). Influence of static alignment of the knee, range of tibial rotation and tibial plateau geometry on the dynamic alignment of "knee-in" and tibial rotation during single limb drop landing. *Clinical Biomechanics 28*(6), 642–648.

[11] Asay, J. L., J. C. Erhart-Hledik, and T. P. Andriacchi (2018). Changes in the total knee joint moment in patients with medial compartment knee osteoarthritis over 5 years. *Journal of Orthopaedic Research 36*(9), 2373–2379.

[12] Bates, N. A., A. L. McPherson, R. J. Nesbitt, J. T. Shearn, G. D. Myer, and T. E. Hewett (n.d.). Robotic simulation of identical athletic -task kinematics on cadaveric limbs exhibits a lack of differences in knee mechanics between contralateral pairs. *JOURNAL OF BIOMECHANICS 53*, 36 – 44.

[13] Bates, N. A., R. J. Nesbitt, J. T. Shearn, G. D. Myer, and T. E. Hewett (2015). Relative Strain in the Anterior Cruciate Ligament and Medial Collateral Ligament during Simulated Jump Landing and Sidestep Cutting Tasks: Implications for Injury Risk. *American Journal of Sports Medicine 43*(9).

[14] Battaglia, M. J., M. W. Lenhoff, J. R. Ehteshami, S. Lyman, M. T. Provencher, T. L. Wickiewicz, and R. F. Warren (2009). Medial Collateral Ligament Injuries and Subsequent Load on the Anterior Cruciate Ligament. *The American Journal of Sports Medicine 37*(2), 305–311.

[15] Beaulieu, M. L. and R. M. Palmieri-Smith (2014). Real-time feedback on knee abduction moment does not improve frontal-plane knee mechanics during jump landings. *Scandinavian Journal of Medicine and Science in Sports 24*(4).

[16] Benoit, D. L., D. K. Ramsey, M. Lamontagne, L. Xu, P. Wretenberg, and P. Renström (2006). Effect of skin movement artifact on knee kinematics during gait and cutting motions measured in vivo. *Gait and Posture 24*(2), 152–164.

[17] Boling, M. C., D. A. Padua, S. W. Marshall, K. Guskiewicz, S. Pyne, and A. Beutler (2009). A prospective investigation of biomechanical risk factors for Patellofemoral pain syndrome: The joint undertaking to monitor and prevent acl injury (JUMP-ACL) Cohort. *American Journal of Sports Medicine 37*(11), 2108–2116.

[18] Brent, J. L., G. D. Myer, K. R. Ford, and T. E. Hewett (2013). The Effect of Sex and Age on Isokinetic Hip-Abduction Torques. *J ournal of Sport Rehabilation 22*(1), 41–46.

[19] Butler, R., J. Barrios, T. Royer, and I. Davis (2011). Frontal-Plane Gait Mechanics in People With Medial Knee Osteoarthritis Are Different From Those in People With Lateral Knee Osteoarthritis. *Physical Therapy 91*(8), 1235–1243.

[20] Camomilla, V., R. Dumas, and A. Cappozzo (2017). Human movement analysis: The soft tissue artefact issue. *Journal of Biomechanics 62*, 1–4.

[21] Cereatti, A., T. Bonci, M. Akbarshahi, K. Aminian, A. Barré, M. Begon, D. L. Benoit, C. Charbonnier, F. Dal, S. Fantozzi, C.-c. Lin, T.-w. Lu, M. G. Pandy, R. Stagni, A. J. V. D. Bogert, and V. Camomilla (2017). Standardization proposal of soft tissue artefact description for data sharing in human motion measurements. *Journal of Biomechanics 62*, 5–13.

[22] Cereatti, A., T. Bonci, M. Akbarshahi, K. Aminian, A. Barré, M. Begon, D. L. Benoit,

C. Charbonnier, F. Dal Maso, S. Fantozzi, C. C. Lin, T. W. Lu, M. G. Pandy, R. Stagni, A. J. van den Bogert, and V. Camomilla (2017). Standardization proposal of soft tissue artefact description for data sharing in human motion measurements. *Journal of Biomechanics 62*, 5–13.

[23] Cesar, G. M., C. L. Tomasevicz, and J. M. Burnfield (2016). Frontal plane comparison between drop jump and vertical jump: implications for the assessment of ACL risk of injury. *Sports Biomechanics 15*(4).

[24] Charlton, I. W., P. Tate, P. Smyth, and L. Roren (2004). Repeatability of an optimised lower body model. *Gait and Posture 20*, 213–221.

[25] Clément, J., R. Dumas, N. Hagemeister, and J. A. de Guise (2015). Soft tissue artifact compensation in knee kinematics by multi-body optimization: Performance of subject-specific knee joint models. *Journal of Biomechanics 48*(14), 3796–3802.

[26] Cooke, T. D. V., E. A. Sled, and R. A. Scudamore (2007). Frontal plane knee alignment: A call for standardized measurement. *Journal of Rheumatology 34*(9), 1796–1801.

[27] Cortes, N., J. Onate, and B. van Lunen (2011). Pivot task increases knee frontal plane loading compared with sidestep and drop-jump. *Journal of Sports Sciences 29*(1), 83–92.

[28] Cowley, H. R., K. R. Ford, G. D. Myer, T. W. Kernozek, and T. E. Hewett (2006). Differences in Neuromuscular Strategies Between Landing and Cutting Tasks in Female Basketball and Soccer Athletes. *Journal of Athletic Training 41*(1), 67–73.

[29] Creaby, M. W., S. Le Rossignol, Z. J. Conway, E. Ageberg, M. Sweeney, and M. M. Franettovich Smith (2017). Frontal plane kinematics predict three-dimensional hip adduction during running. *Physical Therapy in Sport 27*, 1–6.

[30] Cronin, B., S. T. Johnson, E. Chang, C. D. Pollard, and M. F. Norcross (2016). Greater Hip Extension but Not Hip Abduction Explosive Strength Is Associated With Lesser Hip Adduction and Knee Valgus Motion During a Single-Leg Jump-Cut. *Orthopaedic Journal of Sports Medicine 4*(4).

[31] Cruz, A., D. Bell, M. McGrath, T. Blackburn, D. Padua, and D. Herman (2013). The effects of three jump landing tasks on kinetic and kinematic measures: Implications for ACL injury research. *Research in Sports Medicine 21*(4), 330–342.

[32] Danino, B., R. Rödl, J. E. Herzenberg, L. Shabtai, F. Grill, U. Narayanan, E. Segev, and S. Wientroub (2019). Growth modulation in idiopathic angular knee deformities: Is it predictable? *Journal of Children's Orthopaedics 13*(3), 318–323.

[33] Davis, J. A., C. Hogan, and M. Dayton (2015). Postoperative Coronal Alignment After Total Knee Arthroplasty: Does Tailoring the Femoral Valgus Cut Angle Really Matter? *Journal of Arthroplasty 30*(8), 1444–1448.

[34] Deakin, A. H., P. L. Basanagoudar, P. Nunag, A. T. Johnston, and M. Sarungi (2012). Natural distribution of the femoral mechanical-anatomical angle in an osteoarthritic population and its relevance to total knee arthroplasty. *Knee 19*(2), 120–123.

[35] Deakin, A. H. and M. Sarungi (2014). A comparison of variable angle versus fixed angle distal femoral resection in primary total knee arthroplasty. *Journal of Arthroplasty 29*(6), 1133–1137.

[36] Defrate, L. E., R. Papannagari, T. J. Gill, J. M. Moses, N. P. Pathare, and G. Li (2006). The 6 degrees of freedom kinematics of the knee after anterior cruciate ligament deficiency: An in vivo imaging analysis. *American Journal of Sports Medicine 34*(8), 1240–1246.

[37] Dempsey, A. R., B. C. Elliott, B. J. Munro, J. R. Steele, and D. G. Lloyd (2012). Whole body kinematics and knee moments that occur during an overhead catch and landing task in sport. *Clinical Biomechanics 27*(5), 466–474.

[38] Dingenen, B., B. Malfait, S. Nijs, K. H. Peers, S. Vereecken, S. M. Verschueren, and F. F. Staes (2015). Can two-dimensional video analysis during single-leg drop vertical jumps help identify non-contact knee injury risk? A one-year prospective study. *Clinical Biomechanics 30*(8).

[39] Donnelly, C. J., D. G. Lloyd, B. C. Elliott, and J. A. Reinbolt (2012). Optimizing whole-body kinematics to minimize valgus knee loading during sidestepping: Implications for ACL injury risk. *Journal of Biomechanics 45*(8), 1491–1497.

[40] Dumas, R., V. Camomilla, T. Bonci, L. Cheze, and A. Cappozzo (2014). Generalized mathematical representation of the soft tissue artefact. *Journal of Biomechanics 47*(2), 476–481.

[41] Eberbach, H., J. Mehl, M. J. Feucht, G. Bode, N. P. Südkamp, and P. Niemeyer (2017). Geometry of the Valgus Knee: Contradicting the Dogma of a Femoral-Based Deformity. *American Journal of Sports Medicine 45*(4), 909–914.

[42] Ema, R., T. Wakahara, K. Hirayama, and Y. Kawakami (2017). Effect of knee alignment on the quadriceps femoris muscularity: Cross-sectional comparison of trained versus untrained individuals in both sexes. *PLoS ONE 12*(8), 1–14.

[43] Şener, O. A. and M. Durmaz (2019). Effect of Sport Training and Education on Q Angle in Young Males and Females. *Journal of Education and Training Studies 7*(7), 17.

[44] Englander, Z. A., H. C. Cutcliffe, G. M. Utturkar, W. E. Garrett, C. E. Spritzer, and L. E.

DeFrate (2019). A Comparison of Knee Abduction Angles Measured by a 3D Anatomic Coordinate System Versus Videographic Analysis: Implications for Anterior Cruciate Ligament Injury. *Orthopaedic Journal of Sports Medicine 7*(1), 1–7.

[45] Erhart-Hledik, J. C., C. R. Chu, J. L. Asay, J. Favre, and T. P. Andriacchi (2019). Longitudinal Changes in the Total Knee Joint Moment After Anterior Cruciate Ligament Reconstruction Correlate With Cartilage Thickness Changes. *Journal of Orthopaedic Research 37*(7), 1546–1554.

[46] Ettinger, M., L. Claassen, P. Paes, and T. Calliess (2016). 2D versus 3D templating in total knee arthroplasty. *Knee 23*(1), 149–151.

[47] Fiorentino, N. M., P. R. Atkins, M. J. Kutschke, K. B. Foreman, and A. E. Anderson (2016). In-vivo quantification of dynamic hip joint center errors and soft tissue artifact. *Gait and Posture 50*, 246–251.

[48] Fiorentino, N. M., P. R. Atkins, M. J. Kutschke, J. M. Goebel, K. B. Foreman, and A. E. Anderson (2017). Soft tissue artifact causes significant errors in the calculation of joint angles and range of motion at the hip. *Gait and Posture 55*(December 2016), 184–190.

[49] Ford, K. R., E. J. Hegedus, E. F. Zuk, and J. B. Taylor (2015). An evidence-based review of hip-focused neuromuscular exercise interventions to address dynamic lower extremity valgus. *Journal of Sports Medicine 6*, 291–303.

[50] Ford, K. R., G. D. Myer, and T. E. Hewett (2003). Valgus knee motion during landing in high school female and male basketball players. *Medicine and Science in Sports and Exercise 35*(10), 1745–1750.

[51] Ford, K. R., G. D. Myer, H. E. Toms, and T. E. Hewett (2005). Gender differences in the

kinematics of unanticipated cutting in young athletes. *Medicine and Science in Sports and Exercise 37*(1), 124–129.

[52] Ford, K. R., R. Shapiro, G. D. Myer, A. J. V. D. Bogert, and T. E. Hewett (2011). Longitudinal Sex Differences during Landing in Knee Abduction in Young Athletes. *Medicine & Science in Sports & Exercise 42*(10), 1923–1931.

[53] Gardner, J. K., S. Zhang, H. Liu, G. Klipple, C. Stewart, C. E. Milner, and I. M. Asif (2015). Effects of toe-in angles on knee biomechanics in cycling of patients with medial knee osteoarthritis. *Clinical Biomechanics 30*(3), 276–282.

[54] Gerber, D., E. Papa, and E. Kendall (2019). Biomechanical Differences in Knee Valgus Angles in Collegiate Female Athletes Participating in Different Sports. *International Journal of Kinesiology and Sports Science 7*(2), 8–14.

[55] Ghosh, K. M., W. A. Manning, A. P. Blain, S. P. Rushton, L. M. Longstaff, A. A. Amis, and D. J. Deehan (2016). Influence of increasing construct constraint in the presence of posterolateral deficiency at knee replacement: A biomechanical study. *Journal of Orthopaedic Research 34*(3), 427–434.

[56] Graci, V., L. R. Van Dillen, and G. B. Salsich (2012). Gender differences in trunk, pelvis and lower limb kinematics during a single leg squat. *Gait and Posture 36*(3), 461–466.

[57] Grood, E. S. and W. J. Suntay (1983). A Joint Coordinate System for the Clinical Description of Three-Dimensional Motions: Application to the Knee. *Journal of Biomechanical Engineering 105*(2), 136–144.

[58] Guo, J., Z. Wang, J. Fu, and K. M. Lee (2019). Articular Geometry Reconstruction for Knee Joint with a Wearable Compliant Device. *Robotica 37*(12), 2104–2118.

[59] Hall, M., R. S. Hinman, T. V. Wrigley, J. Kasza, B. W. Lim, and K. L. Bennell (2018). Knee extensor strength gains mediate symptom improvement in knee osteoarthritis: secondary analysis of a randomised controlled trial. *Osteoarthritis and Cartilage 26*(4), 495–500.

[60] Hardgrib, N., M. Gottliebsen, O. Rahbek, M. B. Hellfritzsch, and B. Møller-Madsen (2018). Correlation of radiological and clinical measurement of genu valgum in children. *Danish Medical Journal 65*(5), 3–6.

[61] Harris, M. D., S. P. Reese, C. L. Peters, J. A. Weiss, and A. E. Anderson (2013). Three-dimensional quantification of femoral head shape in controls and patients with cam-type femoroacetabular impingement. *Annals of Biomedical Engineering 41*(6), 1162–1171.

[62] Herrington, L. and A. Munro (2010). Drop jump landing knee valgus angle; normative data in a physically active population. *Physical Therapy in Sport 11*(2), 56–59.

[63] Hewett, T. E., K. R. Ford, B. J. Hoogenboom, and G. D. Myer (2010). Understanding and preventing acl injuries: current biomechanical and epidemiologic considerations - update 2010. *North American Journal of Sports Physical Therapy 5*(4), 234–251.

[64] Hewett, T. E., G. D. Myer, and K. R. Ford (2006). Anterior cruciate ligament injuries in female athletes: Part 1, mechanisms and risk factors. *American Journal of Sports Medicine 34*(2), 299–311.

[65] Hewett, T. E., G. D. Myer, K. R. Ford, R. S. Heidt, A. J. Colosimo, S. G. McLean, A. J. Van Den Bogert, M. V. Paterno, and P. Succop (2005). Biomechanical measures of neuromuscular control and valgus loading of the knee predict anterior cruciate ligament injury risk in female athletes: A prospective study. *American Journal of Sports Medicine 33*(4), 492–501.

[66] Hewett, T. E., G. D. Myer, K. R. Ford, M. V. Paterno, and C. E. Quatman (2016). Mechanisms, prediction, and prevention of ACL injuries: Cut risk with three sharpened and validated tools. *Journal of Orthopaedic Research 34*(11), 1843–1855.

[67] Hewett, T. E., G. D. Myer, A. W. Kiefer, and K. R. Ford (2015). Longitudinal Increases in Knee Abduction Moments in Females during Adolescent Growth. *Medicine and Science in Sports and Exercise 47*(12), 2579–2585.

[68] Hewett, T. E., G. D. Myer, and B. T. Zazulak (2008). Hamstrings to quadriceps peak torque ratios diverge between sexes with increasing isokinetic angular velocity. *Journal of Science and Medicine in Sport 11*(5), 452–459.

[69] Hewett, T. E., J. S. Torg, and B. P. Boden (2009, jun). Video analysis of trunk and knee motion during non-contact anterior cruciate ligament injury in female athletes: Lateral trunk and knee abduction motion are combined components of the injury mechanism. *British Journal of Sports Medicine 43*(6), 417–422.

[70] Hewett, Timothy E; Myer, G. (2014). The Mechanical Connection Between Trunk Knee and ACL Injury. *Exercise and Sport Sciences Reviews 39*(4), 161–166.

[71] Hewett, Timothy; Paterno, Mark; Myers, G. (2002). Strategies for Enhancing Proprioception and Neuromuscular Control of the Knee. *Clinical Orthopaedics and Related Research 402*, 76–94.

[72] Hicks, J. L. and J. G. Richards (2005). Clinical applicability of using spherical fitting to find hip joint centers. *Gait and Posture 22*(2), 138–145.

[73] Ho, K. C., S. K. Saevarsson, H. Ramm, R. Lieck, S. Zachow, G. B. Sharma, E. L. Rex, S. Amiri, B. C. Wu, A. Leumann, and C. Anglin (2012). Computed tomography analysis

of knee pose and geometry before and after total knee arthroplasty. *Journal of Biomechanics 45*(13), 2215–2221.

[74] Hoch, M. C. and J. T. Weinhandl (2017). Effect of valgus knee alignment on gait biomechanics in healthy women. *Journal of Electromyography and Kinesiology 35*, 17–23.

[75] Holden, S., C. Boreham, C. Doherty, and E. Delahunt (2017). Two-dimensional knee valgus displacement as a predictor of patellofemoral pain in adolescent females. *Scandinavian Journal of Medicine and Science in Sports 27*(2), 188–194.

[76] Hollman, J. H., B. E. Ginos, J. Kozuchowski, A. S. Vaughn, D. A. Krause, and J. W. Youdas (2009). Relationships between Knee Valgus, Hip-Muscle Strength, and Hip-Muscle Recruitment during a Single-Limb Step-Down. *Journal of Sport Rehabilitation 18*(1), 104–117.

[77] Hopper, A. J., E. E. Haff, C. Joyce, R. S. Lloyd, and G. G. Haff (2017). Neuromuscular Training Improves Lower Extremity Biomechanics Associated with Knee Injury during Landing in 11 – 13 Year Old Female Netball Athletes : A Randomized Control Study. *Frontiers in Physiology 8*(883), 1–13.

[78] Howard, J. S., M. A. Fazio, C. G. Mattacola, T. L. Uhl, and C. A. Jacobs (2011). Structure, sex, and strength and knee and hip kinematics during landing. *Journal of Athletic Training 46*(4), 376–385.

[79] Hull, M. L., G. S. Berns, H. Varma, and H. A. Patterson (1996). Strain in the medial collateral ligament of the human knee under single and combined loads. *Journal of Biomechanics 29*(2), 199–206.

[80] Imhoff, F. B., B. Scheiderer, P. Zakko, E. Obopilwe, F. Liska, A. B. Imhoff, A. D. Maz-

zocca, R. A. Arciero, and K. Beitzel (2017). How to avoid unintended valgus alignment in distal femoral derotational osteotomy for treatment of femoral torsional malalignment - A concept study. *BMC Musculoskeletal Disorders 18*(1), 1–8.

[81] Imwalle, Laruen; Myer, Gregory; Ford, Kevin; Hewett, T. (2009). Relationship Between Hip and Knee Kinematics In Athletic Women During Cutting Maneuvers: A Possible Link to Noncontact Anterior Cruciate Ligament Injury and Prevention. *Journal of Strength and Conditioning Research 23*(8), 2223–2230.

[82] Ishida, K., T. Matsumoto, N. Tsumura, S. Kubo, A. Kitagawa, T. Chin, T. Iguchi, M. Kurosaka, and R. Kuroda (2011). Mid-term outcomes of computer-assisted total knee arthroplasty. *Knee Surgery, Sports Traumatology, Arthroscopy 19*(7), 1107–1112.

[83] Ishida, T., M. Yamanaka, N. Takeda, and Y. Aoki (2014). Knee rotation associated with dynamic knee valgus and toe direction. *Knee 21*(2), 563–566.

[84] Issa, S. N., D. Dunlop, A. Chang, J. Song, P. V. Prasad, A. Guermazi, C. Peterfy, S. Cahue, M. Marshall, D. Kapoor, K. Hayes, and L. Sharma (2007). Full-limb and knee radiography assessments of varus-valgus alignment and their relationship to osteoarthritis disease features by magnetic resonance imaging. *Arthritis Care and Research 57*(3), 398–406.

[85] Jingjit, W., P. Poomcharoen, S. Limmahakhun, K. Klunklin, T. Leerapun, and S. Rojanasthien (2014). Femoral mechanical-anatomical angle of osteoarthritic knees. *Journal of the Medical Association of Thailand 97*(12), 1314–1318.

[86] Jones, P. A., L. C. Herrington, A. G. Munro, and P. Graham-Smith (2014). Is there a relationship between landing, cutting, and pivoting tasks in terms of the characteristics of dynamic valgus? *American Journal of Sports Medicine 42*(9).

[87] Kagaya, Y., Y. Fujii, and H. Nishizono (2015). Association between hip abductor function , rear-foot dynamic alignment , and dynamic knee valgus during single-leg squats and drop landings. *Journal of Sport and Health Science 4*(2), 182–187.

[88] Kane, J. W. O., A. Tencer, M. Neradilek, N. Polissar, L. Sabado, and M. A. Schiff (2016). Is Knee Separation During a Drop Jump Associated With Lower Extremity Injury in Adolescent Female Soccer Players? *AJSM 44*(2), 318–323.

[89] Kellis, E., N. Galanis, and N. Kofotolis (2019). Hamstring-to-Quadriceps Ratio in Female Athletes with a Previous Hamstring Injury, Anterior Cruciate Ligament Reconstruction, and Controls. *Sports 7*(10), 214.

[90] Kezunovic, M. (2013). Overuse Knee Injuries in Athletes. *Montenegrin Journal of Sports Science and Medicine 2*, 29–32.

[91] Khasawneh, R. R., M. Z. Allouh, and E. Abu-El-rub (2019). Measurement of the quadriceps(Q)angle with respect to various body parameters in young Arab population. *PLoS ONE 14*(6), 1–13.

[92] Kim, M. S., J. M. Son, I. J. Koh, J. H. Bahk, and Y. In (2017). Intraoperative adjustment of alignment under valgus stress reduces outliers in patients undergoing medial opening-wedge high tibial osteotomy. *Archives of Orthopaedic and Trauma Surgery 137*(8), 1035–1045.

[93] Kim, S. Y., C. E. Spritzer, G. M. Utturkar, A. P. Toth, W. E. Garrett, and L. E. Defrate (2015). Knee Kinematics during Noncontact Anterior Cruciate Ligament Injury as Determined from Bone Bruise Location. *American Journal of Sports Medicine 43*(10), 2515–2521.

[94] Kim, Y. C., J.-H. Yang, H. J. Kim, T. Tawonsawatruk, Y. S. Chang, J. S. Lee, N. N. Bhan-

dare, K. S. Kim, G. D. Delgado, and K. W. Nha (2018). Distal Femoral Varus Osteotomy for Valgus Arthritis of the Knees: Systematic Review of Open versus Closed Wedge Osteotomy. *Knee Surgery and Related Research 30*(1), 3–16.

[95] Kobayashi, H., T. Kanamura, S. Koshida, K. Miyashita, T. Okado, T. Shimizu, and K. Yokoe (2010). Mechanisms of the anterior cruciate ligament injury in sports activities: A twenty-year clinical research of 1,700 athletes. *Journal of Sports Science and Medicine 9*(4), 669–675.

[96] Kocabiyik, A., A. Misir, T. B. Kizkapan, K. I. Yildiz, M. A. Kaygusuz, Y. Alpay, and A. Ezici (2017). Changes in Hip, Knee, and Ankle Coronal Alignments After Total Hip Arthroplasty With Transverse Femoral Shortening Osteotomy for Unilateral Crowe Type IV Developmental Dysplasia of the Hip. *Journal of Arthroplasty 32*(11), 3449–3456.

[97] Krosshaug, T., A. Nakamae, B. P. Boden, L. Engebretsen, G. Smith, J. R. Slauterbeck, T. E. Hewett, and R. Bahr (2007). Mechanisms of anterior cruciate ligament injury in basketball: Video analysis of 39 cases. *American Journal of Sports Medicine 35*(3), 359–367.

[98] Krosshaug, T., K. Steffen, E. Kristianslund, A. Nilstad, K. M. Mok, G. Myklebust, T. E. Andersen, I. Holme, L. Engebretsen, and R. Bahr (2015). The Vertical Drop Jump Is a Poor Screening Test for ACL Injuries in Female Elite Soccer and Handball Players. *American Journal of Sports Medicine 44*(4).

[99] Kunugi, S., A. Masunari, T. Koumura, A. Fujimoto, N. Yoshida, and S. Miyakawa (2018). Altered lower limb kinematics and muscle activities in soccer players with chronic ankle instability. *Physical Therapy in Sport 34*, 28–35.

[100] Kuo, M. Y., T. Y. Tsai, C. C. Lin, T. W. Lu, H. C. Hsu, and W. C. Shen (2011). Influence

of soft tissue artifacts on the calculated kinematics and kinetics of total knee replacements during sit-to-stand. *Gait and Posture 33*(3), 379–384.

[101] Kushner, Adam; Brent, Jensen; Schoenfeld, Brad; Hugentobler, Jason; Lloyd, Rhodri; Vermeil, Al; Chu, Donald; Harbin, Jason; McGill, Stuart; Myer, G. (2015). The Back Squat Part 2: Targeted Training Techniques to Correct Functional Deficits and Technical Factors that Limit Performance. *Strength & Conditioning Journal 37*(2), 13–60.

[102] Kusiak, M. and A. Kawczyński (2018). Ultrasonographic evaluation and comparison of articular cartilage of the femur condyles between the limbs in patients with an elevated Q angle. *Physiotherapy Quarterly 26*(2), 19–22.

[103] Lam, L. O. and D. Shakespeare (2003). Varus/valgus alignment of the femoral component in total knee arthroplasty. *The Knee 10*(3), 237–41.

[104] LaPorta, G. A., E. M. Nasser, J. L. Mulhern, and D. S. Malay (2016). The Mechanical Axis of the First Ray: A Radiographic Assessment in Hallux Abducto Valgus Evaluation. *Journal of Foot and Ankle Surgery 55*(1), 28–34.

[105] Learndini, A., L. Chiari, U. D. Croce, and A. Cappozzo (2005). Human movement analysis using stereophotogrammetry Part 3. Soft tissue artifact assessment and compensation. *Gait & Posture 21*, 212–225.

[106] Lee, S. S., Y. I. Lee, D. U. Kim, D. H. Lee, and Y. W. Moon (2018). Factors affecting femoral rotational angle based on the posterior condylar axis in gap-based navigation-assisted total knee arthroplasty for valgus knee. *PLoS ONE 13*(5), 1–12.

[107] Legaye, J. (2009). Influence of the sagittal balance of the spine on the anterior pelvic plane and on the acetabular orientation. *International Orthopaedics 33*(6), 1695–1700.

[108] Leppänen, M., K. Pasanen, T. Krosshaug, P. Kannus, T. Vasankari, U. M. Kujala, R. Bahr, J. Perttunen, and J. Parkkari (2017). Sagittal Plane Hip, Knee, and Ankle Biomechanics and the Risk of Anterior Cruciate Ligament Injury: A Prospective Study. *Orthopaedic Journal of Sports Medicine 5*(12), 1–6.

[109] Leppänen, M., K. Pasanen, U. M. Kujala, T. Vasankari, P. Kannus, S. Äyrämö, T. Krosshaug, R. Bahr, J. Avela, J. Perttunen, and J. Parkkari (2017). Stiff Landings Are Associated With Increased ACL Injury Risk in Young Female Basketball and Floorball Players. *The American Journal of Sports Medicine 45*(2), 386–393.

[110] Liederbach, M., F. E. Dilgen, and D. J. Rose (2008). Incidence of anterior cruciate ligament injuries among elite ballet and modern dancers: A 5-year prospective study. *American Journal of Sports Medicine 36*(9), 1779–1788.

[111] Liederbach, M., I. J. Kremenic, K. F. Orishimo, E. Pappas, and M. Hagins (2014). Comparison of landing biomechanics between male and female dancers and athletes, part 2: Influence of fatigue and implications for anterior cruciate ligament injury. *American Journal of Sports Medicine 42*(5).

[112] Lopes, T. J. A., M. Simic, G. D. Myer, K. R. Ford, T. E. Hewett, and E. Pappas (2018). The Effects of Injury Prevention Programs on the Biomechanics of Landing Tasks: A Systematic Review With Meta-analysis. *American Journal of Sports Medicine 46*(6), 1492–1499.

[113] Lopomo, N., L. Sun, S. Zaffagnini, G. Giordano, and M. R. Safran (2010). Evaluation of formal methods in hip joint center assessment: An in vitro analysis. *Clinical Biomechanics 25*(3), 206–212.

[114] Lu, L., C. Dai, Z. Zhang, H. Du, S. Li, P. Ye, Q. Fu, L. Zhang, X. Wu, Y. Dong, Y. Song, D. Zhao, Y. Pang, and C. Bao (2019). Treatment of knee osteoarthritis with intra-articular injection of autologous adipose-derived mesenchymal progenitor cells: A prospective, randomized, double-blind, active-controlled, phase IIb clinical trial. *Stem Cell Research and Therapy 10*(1), 1–10.

[115] Malfait, B., B. Dingenen, A. Smeets, F. Staes, T. Pataky, M. A. Robinson, J. Vanrenterghem, and S. Verschueren (2016). Knee and hip joint kinematics predict quadriceps and hamstrings neuromuscular activation patterns in drop jump landings. *PLoS ONE 11*(4).

[116] Masouros, S. D., A. M. Bull, and A. A. Amis (2010). (i) Biomechanics of the knee joint. *Orthopaedics and Trauma 24*(2), 84–91.

[117] Mayr, E., O. Kessler, A. Prassl, F. Rachbauer, M. Krismer, and M. Nogler (2005). The frontal pelvic plane provides a valid reference system for implantation of the acetabular cup: Spatial orientation of the pelvis in different positions. *Acta Orthopaedica 76*(6), 848–853.

[118] McLean, S., K. Walker, K. Ford, G. Myer, T. Hewett, and A. Bogert (2005). Evaluation of a two dimensional analysis method as a screening and evaluation tool for anterior cruciate ligament injury. *British Journal of Sports Medicine 39*, 355–362.

[119] McLean, S. G., S. M. Lucey, S. Rohrer, and C. Brandon (2010). Knee joint anatomy predicts high-risk in vivo dynamic landing knee biomechanics. *Clinical Biomechanics 25*(8), 781–788.

[120] McLean, S. G., K. Walker, K. R. Ford, G. D. Myer, T. E. Hewett, and A. J. Van Den Bogert (2005). Evaluation of a two dimensional analysis method as a screening and evaluation tool for anterior cruciate ligament injury. *British Journal of Sports Medicine 39*(6), 355–362.

[121] Mendiguchia, Jurdan; Ford, Kevin; Quatman, Carmen; Alentorn-Geli, Eduard; Hewett, T. (2011). Sex Differences in Proximal Control of the Knee Joint Jurdan. *Sports Medicine 41*(7), 541–557.

[122] Mentiplay, B. F. and R. A. Clark (2018). Modified conventional gait model versus cluster tracking : Test-retest reliability , agreement and impact of inverse kinematics with joint constraints on kinematic and kinetic data. *Gait & Posture 64*(May), 75–83.

[123] Miranda, D. L., M. J. Rainbow, E. L. Leventhal, J. J. Crisco, and B. C. Fleming (2010). Automatic determination of anatomical coordinate systems for three-dimensional bone models of the isolated human knee. *Journal of Biomechanics 43*(8), 1623–1626.

[124] Mizuno, Y., M. Kumagai, S. M. Mattessich, J. J. Elias, N. Ramrattan, A. J. Cosgarea, and E. Y. Chao (2001). Q-angle influences tibiofemoral and patellofemoral kinematics. *Journal of Orthopaedic Research 19*(5), 834–840.

[125] Mokhtarzadeh, H., K. Ewing, I. Janssen, C. H. Yeow, N. Brown, and P. V. S. Lee (2017). The effect of leg dominance and landing height on ACL loading among female athletes. *Journal of Biomechanics 60*, 181–187.

[126] Myer, G., J. Brent, K. Ford, and T. Hewett (2011). Real-time assessment and neuromuscular training feedback techniques to prevent ACL injury in female athletes. *Strength & Conditioning Journal 33*(3), 21–35.

[127] Myer, G. D., K. R. Ford, J. L. Brent, and T. E. Hewett (2006). The effects of plyometric vs. dynamic stabilization and balance training on power, balance, and landing force in female athletes. *Journal of Strength and Conditioning Research 20*(2), 345–353.

[128] Myer, G. D., K. R. Ford, K. D. Foss, M. J. Rauh, M. V. Paterno, and T. E. Hewett (2014).

A predictive model to estimate knee-abduction moment: Implications for development of a clinically applicable patellofemoral pain screening tool in female athletes. *Journal of Athletic Training 49*(3), 389–398.

[129] Myer, G. D., K. R. Ford, and T. E. Hewett (2004). Rationale and clinical techniques for anterior cruciate ligament injury prevention among female athletes. *Journal of Athletic Training 39*(4), 352–364.

[130] Myer, G. D., K. R. Ford, and T. E. Hewett (2009). Tuck Jump Assessment for Reducing Anterior Cruciate Ligament Injury Risk. *Athletic Therapy Today 13*(5), 39–44.

[131] Myer, G. D., K. R. Ford, S. G. McLean, and T. E. Hewett (2006). The effects of plyometric versus dynamic stabilization and balance training on lower extremity biomechanics. *American Journal of Sports Medicine 34*(3), 445–455.

[132] Myer, Gregory; Ford, Kevin; Brent, Jensen; Hewett, T. (2012). An Integrated Approach to Change the Outcome Part II: Targeted Neuromuscular Training Techniques to Reduce Identified ACL Injury Risk Factors. *Journal of Strength Conditioning Research 26*(8), 2272–2292.

[133] Nagano, Y., H. Ida, M. Akai, and T. Fukubayashi (2007). Gender differences in knee kinematics and muscle activity during single limb drop landing. *The Knee 14*, 218–223.

[134] Nagano, Y., M. Sakagami, H. Ida, M. Akai, T. Fukubayashi, M. Sakagami, H. Ida, M. Akai, and T. F. Statistical (2008). Statistical modelling of knee valgus during a continuous jump test. *Sports Biomechanics 7*(3), 342–350.

[135] Naili, J. E., M. D. Iversen, A. C. Esbjörnsson, M. Hedström, M. H. Schwartz, C. K. Häger, and E. W. Broström (2017). Deficits in functional performance and gait one year

after total knee arthroplasty despite improved self-reported function. *Knee Surgery, Sports Traumatology, Arthroscopy 25*(11), 3378–3386.

[136] Negus, V., D. Hopper, S. B. Information, N. K. Briffa, and F. Email (2003). Associations Between Turnout and Lower extremity injuries in classical ballet dancers. *Journal of Orthopaedic & Sports Physical Therapy*, 307–318.

[137] Neil, M. J., J. B. Atupan, J. P. L. Panti, R. A. Massera, and S. Howard (2016). Evaluation of lower limb axial alignment using digital radiography stitched films in pre-operative planning for total knee replacement. *Journal of Orthopaedics 13*(4), 285–289.

[138] Ng, V. Y., J. H. DeClaire, K. R. Berend, B. C. Gulick, and A. V. Lombardi (2012). Improved accuracy of alignment with patient-specific positioning guides compared with manual instrumentation in TKA. *Clinical Orthopaedics and Related Research 470*(1), 99–107.

[139] Nguyen, A. D. and S. J. Shultz (2007). Sex differences in clinical measures of lower extremity alignment. *Journal of Orthopaedic and Sports Physical Therapy 37*(7), 389–398.

[140] Nguyen, A. D., S. J. Shultz, and R. J. Schmitz (2015). Landing biomechanics in participants with different static lower extremity alignment profiles. *Journal of Athletic Training 50*(5), 498–507.

[141] Nguyen, U. S. D., Y. Zhang, Y. Zhu, J. Niu, B. Zhang, and D. T. Felson (2011). Increasing prevalence of knee pain and symptomatic knee osteoarthritis: Survey and cohort data. *Annals of Internal Medicine 155*(11), 725–732.

[142] Nilstad, A., T. Krosshaug, K.-M. Mok, R. Bahr, and T. E. Andersen (2015). Association Between Anatomical Characteristics, Knee Laxity, Muscle Strength, and Peak Knee

Valgus During Vertical Drop-Jump Landings. *Journal of Orthopaedic & Sports Physical Therapy 45*(12), 998–1005.

[143] Noce, R., E. G. Culham, and P. Costigan (1999). Radiographic and non-invasive determination of the hip joint center location: effect on hip joint moments. *Clinical Biomechanics 14*, 227–235.

[144] Numata, H., J. Nakase, K. Kitaoka, and Y. Shima (2018). Two - dimensional motion analysis of dynamic knee valgus identifies female high school athletes at risk of non - contact anterior cruciate ligament injury. *Knee Surgery, Sports Traumatology, Arthroscopy 26*(2), 442–447.

[145] O'Kane, J. W., M. Neradilek, N. Polissar, L. Sabado, A. Tencer, and M. A. Schiff (2017). Risk factors for lower extremity overuse injuries in female youth soccer players. *Orthopaedic Journal of Sports Medicine 5*(10), 1–8.

[146] Olesen, M. L., B. B. Christensen, C. B. Foldager, K. C. Hede, N. L. Jørgensen, and M. Lind (2019). No Effect of Platelet-Rich Plasma Injections as an Adjuvant to Autologous Cartilage Chips Implantation for the Treatment of Chondral Defects. *Cartilage*.

[147] Olsen, O.-E., G. Myklebust, L. Engebretsen, and R. Bahr (2004). Injury Mechanisms for Anterior Cruciate Ligament Injuries in Team Handball. *The American Journal of Sports Medicine 32*(4), 1002–1012.

[148] Omi, Y., D. Sugimoto, S. Kuriyama, T. Kurihara, K. Miyamoto, S. Yun, T. Kawashima, and N. Hirose (2018). Effect of Hip-Focused Injury Prevention Training for Anterior Cruciate Ligament Injury Reduction in Female Basketball Players: A 12-Year Prospective Intervention Study. *American Journal of Sports Medicine 46*(4).

[149] Orishimo, K. F., M. Liederbach, I. J. Kremenic, M. Hagins, and E. Pappas (2014). Comparison of landing biomechanics between male and female dancers and athletes, part 1: Influence of sex on risk of anterior cruciate ligament injury. *American Journal of Sports Medicine 42*(5), 1082–1088.

[150] Padua, D. A., L. J. DiStefano, A. I. Beutler, S. J. De La Motte, M. J. DiStefano, and S. W. Marshall (2015). The landing error scoring system as a screening tool for an anterior cruciate ligament injury-prevention program in elite-youth soccer athletes. *Journal of Athletic Training 50*(6).

[151] Padua, D. A., S. W. Marshall, M. C. Boling, C. A. Thigpen, W. E. Garrett, and A. I. Beutler (2009). The Landing Error Scoring System (LESS) is a valid and reliable clinical assessment tool of jump-landing biomechanics: The jump-ACL Study. *American Journal of Sports Medicine 37*(10), 1996–2002.

[152] Palad, Y. Y., A. M. Leaver, M. J. McKay, J. N. Baldwin, F. R. Lunar, F. D. Caube, J. Burns, and M. Simic (2018). Knee thrust prevalence and normative hip-knee-ankle angle deviation values among healthy individuals across the lifespan. *Osteoarthritis and Cartilage 26*(10), 1326–1332.

[153] Palanisami, D., C. P. Jagdishbhai, M. Manohar, P. Ramesh, R. Natesan, and R. Shanmuganathan (2019). Improving the accuracy of tibial component placement during total knee replacement in varus knees with tibial bowing: A prospective randomised controlled study. *Knee 26*(5), 1088–1095.

[154] Palmer, T., J. Pineda, and D. Rachel (2018). Effects of Knee Position on the Reliability and Production of Maximal and Rapid Strength Characteristics During an Isometric Squat Test. *Journal of Applied Biomechanics 34*(2), 111–117.

[155] Palmieri-Smith, R. M., J. Kreinbrink, J. A. Ashton-Miller, and E. M. Wojtys (2007). Quadriceps inhibition induced by an experimental knee joint effusion affects knee joint mechanics during a single-legged drop landing. *American Journal of Sports Medicine 35*(8), 1269–1275.

[156] Patel, J. V., J. L. Masonis, J. Guerin, R. B. Bourne, and C. H. Rorabeck (2004). The fate of augments to treat-type-2 bone defects in revision knee arthroplasty. *Journal of Bone and Joint Surgery 86*(2), 195–199.

[157] Paterno, M. V., L. C. Schmitt, K. R. Ford, M. J. Rauh, G. D. Myer, B. Huang, and T. E. Hewett (2010). Biomechanical measures during landing and postural stability predict second anterior cruciate ligament injury after anterior cruciate ligament reconstruction and return to sport. *American Journal of Sports Medicine 38*(10), 1968–1978.

[158] Patrek, M. F., T. W. Kernozek, J. D. Willson, G. A. Wright, and S. T. Doberstein (2011). Hip-abductor fatigue and single-leg landing mechanics in women athletes. *Journal of Athletic Training 46*(1), 31–42.

[159] Petersen, W., I. Rembitzki, and C. Liebau (2017). Patellofemoral pain in athletes. *Open Access Journal of Sports Medicine Volume 8*, 143–154.

[160] Piazza, S. J., N. Okita, and P. R. Cavanagh (2001). Accuracy of the functional method of hip joint center location: Effects of limited motion and varied implementation. *Journal of Biomechanics 34*(7), 967–973.

[161] Pillet, H., M. Sangeux, J. Hausselle, R. El Rachkidi, and W. Skalli (2014). A reference method for the evaluation of femoral head joint center location technique based on external markers. *Gait and Posture 39*(1), 655–658.

[162] Pitcairn, S., B. Lesniak, and W. Anderst (2018). In vivo validation of patellofemoral kinematics during overground gait and stair ascent. *Gait and Posture 64*(March), 191–197.

[163] Pollard, C. D., S. M. Sigward, and C. M. Powers (2009). Injury Prevention Training Results in Biomechanical Changes. *Knee 4*.

[164] Popkov, D. (2017). Guided growth for valgus deformity correction of knees in a girl with osteopetrosis: A case report. *Strategies in Trauma and Limb Reconstruction 12*(3), 197–204.

[165] Rajasekar, S., A. Kumar, J. Patel, M. Ramprasad, and A. J. Samuel (2018). Does Kinesio taping correct exaggerated dynamic knee valgus? A randomized double blinded sham-controlled trial. *Journal of Bodywork and Movement Therapies 22*(3), 727–732.

[166] Resende, R. A., R. N. Kirkwood, K. J. Deluzio, E. A. Hassan, and S. T. Fonseca (2016). Ipsilateral and contralateral foot pronation affect lower limb and trunk biomechanics of individuals with knee osteoarthritis during gait. *Clinical Biomechanics 34*, 30–37.

[167] Ribeiro, C. H., N. R. Severino, and P. M. De Moraes Barros Fucs (2013). Preoperative surgical planning versus navigation system in valgus tibial osteotomy: A cross-sectional study. *International Orthopaedics 37*(8), 1483–1486.

[168] Saç, A. and M. Y. Taşmektepligil (2018). Correlation between the Q angle and the isokinetic knee strength and muscle activity. *Turkish Journal of Physical Medicine and Rehabilitation 64*(4), 308–313.

[169] Sailhan, F., L. Jacob, and M. Hamadouche (2017). Differences in limb alignment and femoral mechanical-anatomical angles using two dimension versus three dimension radiographic imaging. *International Orthopaedics 41*(10), 2009–2016.

[170] Sakurai, A., K. Harato, Y. Morishige, S. Kobayashi, Y. Niki, and T. Nagura (2019). The effects of toe direction on three-dimensional knee kinematics during closed kinetic chain exercise in patients with anterior cruciate ligament deficient knee. *Asia-Pacific Journal of Sports Medicine, Arthroscopy, Rehabilitation and Technology 18*, 1–5.

[171] Salsich, G. B. and W. H. Perman (2013). Tibiofemoral and patellofemoral mechanics are altered at small knee flexion angles in people with patellofemoral pain. *Journal of Science and Medicine in Sport 16*(1), 13–17.

[172] Sanfridsson, J., A. Arnbjörnsson, T. Fridén, L. Ryd, G. Svahn, and K. Jonsson (2001). Femorotibial rotation and the Q-angle related to the dislocating patella. *Acta Radiologica 42*(2), 218–224.

[173] Schellenberg, F., W. R. Taylor, I. Jonkers, and S. Lorenzetti (2017). Robustness of kinematic weighting and scaling concepts for musculoskeletal simulation. *Computer Methods in Biomechanics and Biomedical Engineering 20*(7), 720–729.

[174] Schmidt, E., M. Harris-hayes, and G. B. Salsich (2017). Dynamic knee valgus kinematics and their relationship to pain in women with patellofemoral pain compared to women with chronic hip joint pain. *Journal of Sport and Health Science* (October).

[175] Seidel, G. K., D. M. Marchinda, M. Dijkers, and R. W. Soutas-Little (1995). Hip joint center location from palpable bony landmarks-A cadaver study. *Journal of Biomechanics 28*(8), 995–998.

[176] Setuain, I., M. González-Izal, J. Alfaro, E. Gorostiaga, and M. Izquierdo (2015). Acceleration and Orientation Jumping Performance Differences Among Elite Professional Male Handball Players With or Without Previous ACL Reconstruction: An Inertial Sensor Unit-Based Study. *PM and R 7*(12).

[177] Sheehy, L., E. Culham, L. McLean, J. Niu, J. Lynch, N. A. Segal, J. A. Singh, M. Nevitt, and T. D. Cooke (2015). Validity and sensitivity to change of three scales for the radiographic assessment of knee osteoarthritis using images from the Multicenter Osteoarthritis Study (MOST). *Osteoarthritis and Cartilage 23*(9), 1491–1498.

[178] Sheehy, L., D. Felson, Y. Zhang, J. Niu, Y. M. Lam, N. Segal, J. Lynch, and T. D. Cooke (2011). Does measurement of the anatomic axis consistently predict hip-knee-ankle angle (HKA) for knee alignment studies in osteoarthritis? Analysis of long limb radiographs from the multicenter osteoarthritis (MOST) study. *Osteoarthritis and Cartilage 19*(1), 58–64.

[179] Shin, C. S., A. M. Chaudhari, and T. P. Andriacchi (2009). The effect of isolated valgus moments on ACL strain during single-leg landing: A simulation study. *Journal of Biomechanics 42*, 280–285.

[180] Shoji, H. (1973). High Tibial Osteotomy for Osteoarthritis of the Knee with Valgus Deformity. *The Hospital for Special Surgery 55*(5), 963–73.

[181] Shultz, S. J., W. N. Dudley, and Y. Kong (2012). Identifying multiplanar knee laxity profiles and associated physical characteristics. *Journal of Athletic Training 47*(2), 159–169.

[182] Siston, R. A. and S. L. Delp (2006). Evaluation of a new algorithm to determine the hip joint center. *Journal of Biomechanics 39*(1), 125–130.

[183] Smith, R., K. R. Ford, G. D. Myer, A. Holleran, E. Treadway, and T. E. Hewett (2007). Biomechanical and performance differences between female soccer athletes in National Collegiate Athletic Association Divisions I and III. *Journal of Athletic Training 42*(4), 470–476.

[184] Springer, B., U. Bechler, W. Waldstein, K. Rueckl, C. S. Boettner, and F. Boettner

(2019). The influence of femoral and tibial bony anatomy on valgus OA of the knee. *Knee Surgery, Sports Traumatology, Arthroscopy*.

[185] Stagni, R., S. Fantozzi, A. Cappello, and A. Leardini (2005). Quantification of soft tissue artefact in motion analysis by combining 3D fluoroscopy and stereophotogrammetry: A study on two subjects. *Clinical Biomechanics 20*(3), 320–329.

[186] Stagni, R., A. Leardini, A. Cappozzo, M. Grazia Benedetti, and A. Cappello (2000). Effects of hip joint centre mislocation on gait analysis results. *Journal of Biomechanics 33*(11), 1479–1487.

[187] Stearns, K. M. and C. M. Powers (2014). Improvements in hip muscle performance result in increased use of the hip extensors and abductors during a landing task. *American Journal of Sports Medicine 42*(3).

[188] Stickler, L., M. Finley, and H. Gulgin (2015). Relationship between hip and core strength and frontal plane alignment during a single leg squat. *Physical Therapy in Sport 16*(1), 66–71.

[189] Tamura, A., K. Akasaka, T. Otsudo, J. Shiozawa, Y. Toda, and K. Yamada (2017). Dynamic knee valgus alignment influences impact attenuation in the lower extremity during the deceleration phase of a single-leg landing. *PLoS ONE 12*(6).

[190] Taylor, J. B., K. R. Ford, A. D. Nguyen, and S. J. Shultz (2016). Biomechanical Comparison of Single- and Double-Leg Jump Landings in the Sagittal and Frontal Plane. *Orthopaedic Journal of Sports Medicine 4*(6).

[191] Teng, H. L. and C. M. Powers (2014). Sagittal plane trunk posture influences

patellofemoral joint stress during running. *Journal of Orthopaedic and Sports Physical Therapy 44*(10), 785–792.

[192] Teng, P., P. Kong, and K. Leong (2017). Effects of foot rotation positions on knee valgus during single-leg drop landing: Implications for acl injury risk reduction. *The Knee 24*(3), 547–554.

[193] Tokuhara, Y., Y. Kadoya, S. Nakagawa, A. Kobayashi, and K. Takaoka (2004). The flexion gap in normal knees. An MRI study. *Journal of Bone and Joint Surgery 86*(8), 1133–1136.

[194] Tran, A. A., C. Gatewood, A. H. S. Harris, J. A. Thompson, and J. L. Dragoo (2016). The effect of foot landing position on biomechanical risk factors associated with anterior cruciate ligament injury. *Journal of Experimental Orthopaedics 3*(1), 13.

[195] Tsai, L. C., Y. A. Ko, K. E. Hammond, J. W. Xerogeanes, G. L. Warren, and C. M. Powers (2017). Increasing hip and knee flexion during a drop-jump task reduces tibiofemoral shear and compressive forces: implications for ACL injury prevention training. *Journal of Sports Sciences 35*(24).

[196] Tsai, T. Y., T. W. Lu, M. Y. Kuo, and C. C. Lin (2011). Effects of soft tissue artifacts on the calculated kinematics and kinetics of the knee during stair-ascent. *Journal of Biomechanics 44*(6), 1182–1188.

[197] Turner, C., S. Crow, T. Crowther, B. Keating, T. Saupan, J. Pyfer, K. Vialpando, and S. P. Lee (2018). Preventing non-contact ACL injuries in female athletes: What can we learn from dancers? *Physical Therapy in Sport 31*, 1–8.

[198] Utturkar, G., L. Irribarra, K. Taylor, C. Spritzer, D. Taylor, W. Garrett, and L. DeFrate

(2013). The Effects of a Valgus Collapse Knee Position on In Vivo ACL Elongation. *Annals of Biomedical Engineering 41*(1), 123–130.

[199] Vanrenterghem, J., E. Venables, T. Pataky, and M. A. Robinson (2012). The effect of running speed on knee mechanical loading in females during side cutting. *Journal of Biomechanics 45*(14), 2444–2449.

[200] Vasta, S., M. Rosi, A. Tecame, R. Papalia, and P. Adravanti (2020). Aiming for anatomical femoral axis on the coronal plane leads to good-to-excellent short-term outcomes in isolated patellofemoral arthroplasty. *Knee 27*(3), 1–7.

[201] Watt, R. (1801). Mr. Watt, on Varus and Valgus. *Account of Diseases in Liverpool Dispensary*, 119–20.

[202] Weinhandl, J. T., B. S. Irmischer, and Z. A. Sievert (2015). Sex differences in unilateral landing mechanics from absolute and relative heights. *Knee 22*(4), 298–303.

[203] Welling, W., A. Benjaminse, A. Gokeler, and B. Otten (2016). Enhanced retention of drop vertical jump landing technique: A randomized controlled trial. *Human Movement Science 45*.

[204] Wu, G., S. Siegler, P. Allard, C. Kirtley, A. Leardini, D. Rosenbaum, M. Whittle, D. D. D'Lima, L. Cristofolini, H. Witte, O. Schmid, and I. Stokes (2002). ISB recommendation on definitions of joint coordinate system of various joints for the reporting of human joint motion—part I: ankle, hip, and spine. *Journal of Biomechanics 35*(4), 543–548.

[205] Wu, G., F. C. T. Van der Helm, H. E. J. Veeger, M. Makhsous, P. V. Roy, C. Anglin, J. Nagels, A. R. Karduna, K. McQuade, X. Wang, F. W. Werner, and B. Buchholz (2005). ISB recommendation on definitions of joint coordinate systems of various joints for the re-

porting of human joint motioN, Part II: shoulder, elbow, wrist and hand. *Journal of Biomechanics 38*(5), 981–992.

[206] Xie, W., Y. Zhang, X. Qin, L. Song, and Q. Chen (2018). Ground reaction vector readjustment–the secret of success in treatment of medial compartment knee osteoarthritis by novel high fibular osteotomy. *Journal of Orthopaedics 15*(1), 143–145.

[207] Yang, N. H., H. Nayeb-Hashemi, P. K. Canavan, and A. Vaziri (2010). Effect of frontal plane tibiofemoral angle on the stress and strain at the knee cartilage during the stance phase of gait. *Journal of Orthopaedic Research 28*(12), 1539–1547.

[208] Yoo, J. H., I. H. Choi, T.-J. Cho, C. Y. Chun, and W. J. Yoo (2008). Development of tibiofemoral angle in Korean children. *Journal of Korean Medical Science 23*(4), 714–717.

[209] Zazulak, B. T., S. J. Straub, M. J. Medvecky, L. Avedisian, and T. E. Hewett (2005). Gender Comparison of Hip Muscle Activity. *Journal of Orthopaedic and Sports Physical Therapy* (35), 292–299.

12 Appendix A: JCS and Euler Rotations

The dimensionality of biological joints, specifically synovial joints, make clinical defining and quantifying the orientation difficult as the reference plane change with time. Grood and Suntay mathematically describe the rotations of joint angles using anatomical terms in their joint coordinate system (JCS), and has been frequently used since their publication in 1983[57]. The following definitions are the clinical definitions used to describe joint rotations in each of the three planes:

- Flexion and Extension: Decreasing or increasing the angle between two segments in the sagittal plane.
- Adduction and Abduction: Decreasing or increasing the angle between a segment and the reference segment midline in the frontal plane.
- Internal and External Rotation: Decreasing or increasing the angle between the segment and the anterior-axis in the transverse plane about the superior-inferior-axis.

Since the development of their method, an equivalent measure of the rotations in each plane has been used. An X-Y-Z Euler Angle sequence measures equivalent angles and can be used to calculate the same angles proposed by Grood & Suntay[57]. The adaptation of Grood & Suntay's method to Euler Angles provide a more commonly understood method to calculate anatomically relevant angles. Therefore, the X-Y-Z Euler Angle sequence is indirectly related to anatomical meanings through the JCS. Therefore, the translation component will not be addressed in this paper. The following sections explain, in detail, how these two methods of measuring angles are equivalent.

Each segment (the thigh and shank) can be defined with two sets of coordinate axis, one for Grood & Suntay's analysis and the other for the Euler analysis. Grood & Suntay define the

proximal segment with e_1 and e_1^r, and the distal segment with e_3 and e_3^r, where the axes are unit vectors[57]. Anatomically, the e_1 and X axes are along the medial-lateral axis, where positive is in the lateral direction; the e_1^r, e_3^r, and Y axes are along the anterior-posterior axis, where positive is in the anterior direction; and the e_3 and Z axes are along the superior-inferior axes, where positive is in the superior direction. This nomenclature matches the work done in Grood & Suntay, 1983[57]. Additionally, these axes define the anatomical rotations where the flexion angle is α, the abduction angle is β, and the internal rotation angle is γ. The JCS axes and anatomical rotations can be seen in Figure 40 and the JCS axes along with each of the axes of the Euler rotation sequence can be seen in Figure 41.

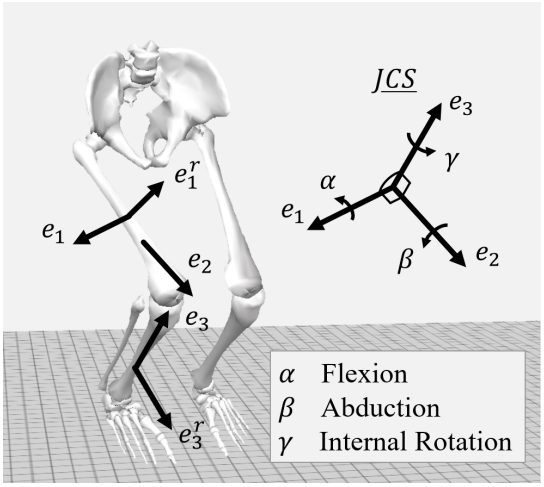

Figure 40: The JCS by Grood and Suntay using the local coordinates (e_1, e_1^r, e_3, and e_3^r) and floating vector (e_2) to calculate flexion (α), abduction (β), and internal rotation (γ)[57].

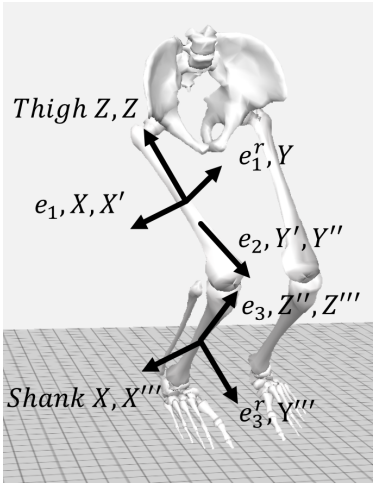

Figure 41: The axes of the JCS and axes of the Euler rotation sequence[57].

12.1 Flexion Angle

Grood & Suntay's evaluation flexion and extension angle, α, is shown in Equation 11[57]. The rotation occurs in the sagittal plane of the proximal segment defined by the e_1 or X axis. The angle can be defined by creating what Grood & Suntay define as a floating vector, e_2, shown in Equation 11[57]. When the floating vector is dotted with the reference axis for the proximal segment, e_1^r, the cosine can be used to calculate the flexion angle (α) shown in Equation 12[57].

$$e_2 = \frac{e_3 \times e_1}{\|e_3 \times e_1\|} \tag{11}$$

$$cos\alpha = e_1^r \cdot e_2 \tag{12}$$

The calculation for the flexion angle using the JCS is shown in Figure 42 where one configuration depicts the orientation of the axes in 0-degrees of flexion and the other depicts the orientation of the axes in 60-degrees of flexion.

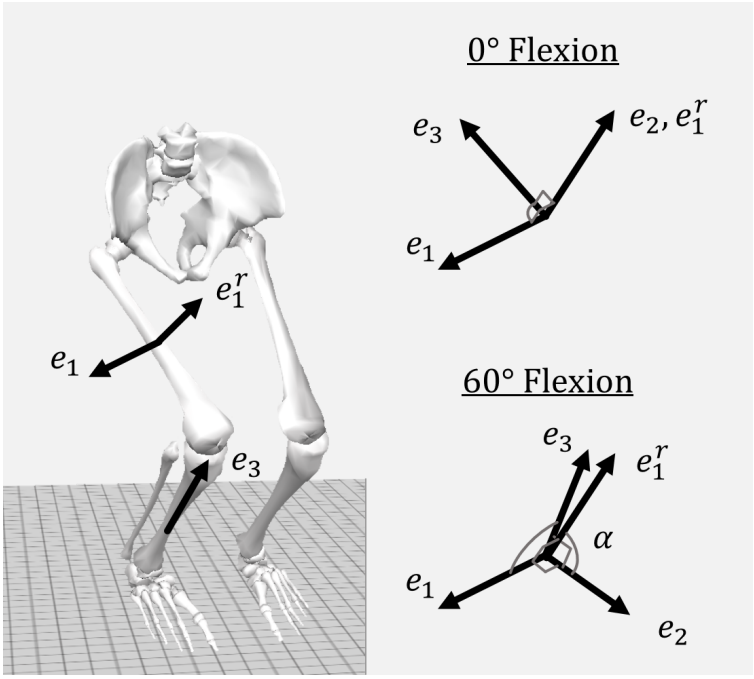

Figure 42: JCS axes orientation for flexion in 0-degrees of flexion and 60-degrees of flexion. Note that in the 60-degree of flexion condition, both e_1 and e_3 are orthogonal to e_2, but are not orthogonal to one another; both e_2 and e_1^r are orthogonal to e_1, but are not orthogonal to one another; and e_1^r and e_2 are orthogonal to e_1, but not to one another.

The vector e_3 can be projected onto the sagittal plane ($e_{3,sag}$) which is defined by e_1 and then normalized ($e'_{3,sag}$) shown in Equation 13 and 14.

$$e_{3,sag} = e_3 - \frac{e_3 \cdot e_1}{\|e_1\|} \cdot e_1 \tag{13}$$

$$e'_{3,sag} = \frac{e_{3,sag}}{\|e_{3,sag}\|} \tag{14}$$

The e_2 vector is on the sagittal plane as it is orthogonal to both e_1 and e_3 (Equation 11); therefore, e_2 can be calculated using either $e'_{3,sag}$ or e_3, as shown in Equation 15 For this reason, the orientation of e_2 on the sagittal plane is not influenced by abduction or internal and external

rotation.

$$e_2 = \frac{e_3 \times e_1}{\|e_3 \times e_1\|} = \frac{e'_{3,sag} \times e_1}{\|e'_{3,sag} \times e_1\|} \tag{15}$$

The flexion angle can also be found using the first rotation of an X-Y-Z Euler sequence when the Equations 16 and 17 are true.

$$X = e_1 \tag{16}$$

$$Y = e_1^r \tag{17}$$

The first rotation of θ_1 about the I-axis can be defined with the rotation matrix R_X shown in Equation 18.

$$R_X = \begin{bmatrix} 1 & 0 & 0 \\ 0 & \cos\theta_1 & -\sin\theta_1 \\ 0 & \sin\theta_1 & \cos\theta_1 \end{bmatrix} \tag{18}$$

Given Equations 14 and 15 and the rotation in Equation 18, the Z' axis can be defined as $e'_{3,sag}$ as shown in Equation 19.

$$Z' = e'_{3,sag} \tag{19}$$

Therefore, using the relationships defined in Equations 15, 17, and 19 the floating vector e_2 can also be found and is shown in Equation 20 where I' is the orientation proximal segment

after the first rotation.

$$X' = \frac{Z' \times X}{\|Z' \times X\|} = \frac{e'_{(3,sag)} \times e_1}{\|e'_{(3,sag)} \times e_1\|} = e_2 \tag{20}$$

The angle θ_1 is directly related to the orientation of Y' with respect to Y, where Y' is the orientation of the Y axis after the first rotation. The angle between the two axes can be found using the dot product, as shown in Equation 21.

$$cos\theta_1 = Y \cdot Y' \tag{21}$$

Given that $X = X'$ and that X', Y', and Z' are orthogonal, Y' can be found by either using Z' and X or Z' and X', as shown in Equation 22.

$$Y' = \frac{Z' \times X'}{\|Z' \times X'\|} = \frac{Z' \times I}{\|Z' \times X\|} \tag{22}$$

Substituting Equation 22 into 21 the following equation can be made (Equation 23).

$$cos\theta_1 = Y \cdot \frac{Z' \times X}{\|Z' \times X\|} \tag{23}$$

When Equations 16, 17, 19, and 23 are combined, the rotation from the Grood & Suntay method can be described using $e'_{(3,sag)}$ and e_1, as shown in Equation 24.

$$cos\theta_1 = e_1^r \cdot \frac{e'_{(3,sag)} \times e_1}{\|e'_{(3,sag)} \times e_1\|} \tag{24}$$

By substituting Equation 11 and 15 into Equation 24 the relationship can be further defined

Equation 23 can be further defined, as shown in Equation 25.

$$cos\theta_1 = e_1^r \cdot \frac{e_3 \times e_1}{\|e_3 \times e_1\|} = e_1^r \cdot e_2 \tag{25}$$

The angles α and θ_1 can be shown to be equivalent when Equation 12 and 25 are combined, shown in Equation 26.

$$cos\theta_1 = e_1^r \cdot e_2 = cos\alpha \tag{26}$$

Because the α and θ_1 angles are equivalent, Equation 26, the Grood & Suntay measure of flexion and extension can be calculated using the Euler rotation about the X axis.

The axes used in Equations 11-26 to determine the equivalency of the JCS and Euler rotation sequence for flexion are shown in Figure 43.

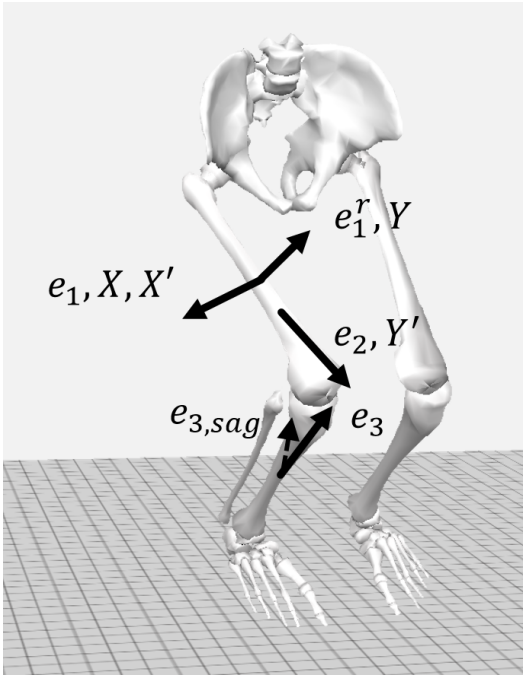

Figure 43: JCS axes used in Equations 11-26.

12.2 Abduction Angle

The abduction angle (β) of a joint can be found using e_3 and e_1 where β' is the angle between e_3 and e_1, as shown in Equation 27[57].

$$cos\beta' = e_3 \cdot e_1 \tag{27}$$

The abduction angle for the right knee (β_{Right}) is β' minus $\frac{\pi}{2}$ (Equation 28, and the abduction angle for the left knee (β_{Left}) is $\frac{\pi}{2}$ minus β' (Equation 29)[57].

$$\beta_{Right} = \beta' - \frac{\pi}{2} \tag{28}$$

$$\beta_{Left} = \frac{\pi}{2} - \beta' \tag{29}$$

Therefore, Equation 30 is the right knee abduction angle (Equation 28 substituted into Equation 27, and equation 31 is the left knee abduction angle (Equation 29 substituted into Equation 27).

$$cos\beta' = cos(\beta_{Right} + \frac{\pi}{2}) = e_3 \cdot e_1 \tag{30}$$

$$cos\beta' = cos(\frac{\pi}{2} - \beta_{Left}) = e_3 \cdot e_1 \tag{31}$$

The abduction angle can also be found using the second rotation of an S-Y-Z Euler sequence when Equations 32 and 33 are true.

$$X = X' = e_1 \tag{32}$$

$$Z'' = e_3 \tag{33}$$

The second rotation, θ_2, about the J' axis can be found using the rotation matrix shown in Equation 34 defined as $R_{Y'}$.

$$R_{Y'} = \begin{bmatrix} \cos\theta_2 & & \sin\theta_2 \\ 0 & 1 & 0 \\ -\sin\theta_2 & & \cos\theta_2 \end{bmatrix} \tag{34}$$

The angle θ_2 is directly related to the position of Z'' with respect to Z'. The angle can be found using the dot product between Z'' and Z', shown in Equation 35.

$$cos\theta_2 = Z' \cdot Z'' \tag{35}$$

The angle $\frac{\pi}{2}$ can be added to θ_2 to define θ_2', as shown in Equation 36.

$$\theta_2' = \theta_2 + \frac{\pi}{2} \tag{36}$$

Equation 35 can be modified by adding $\frac{\pi}{2}$ (which changes Z' to X') and substituting 36 into it, as shown in Equation 37.

$$cos\theta_2' = cos(\theta_2 + \frac{\pi}{2}) = X' \cdot Z'' \tag{37}$$

When Equations 27, 32, 33, and 35 are combined, the relationship between the Grood & Suntay rotation and the second rotation in the X-Y-Z Euler sequence can be made, as shown

in Equation 38.

$$cos\theta_2' = e_3 \cdot e_1 = cos\beta' \tag{38}$$

Because this relationship exists between β and θ_2, both methods can be used to calculate the abduction angle.

12.3 Internal Rotation Angle

Grood & Suntay's evaluation internal and external rotation angle, γ, is shown in Equation 39. Where the motion occurs in the distal transverse plane of the distal segment defined by e_3 and about the e_3 or Z''' axes. The distal frontal plane can be defined by creating the floating vector, e_2, as shown in Equation 11. When the floating vector is dotted with the reference axis, e_3^r, the resultant angle represents the degree of internal or external rotation of the distal segment on the distal transverse plane, as shown in Equation 39[57].

$$cos\gamma = e_3^r \cdot e_2 \tag{39}$$

The calculation for the internal rotation angle using the JCS is shown in Figure 44 where one configuration depicts the orientation of the axes in 0-degrees of internal rotation and the other depicts the orientation of the axes in 10-degrees of internal rotation.

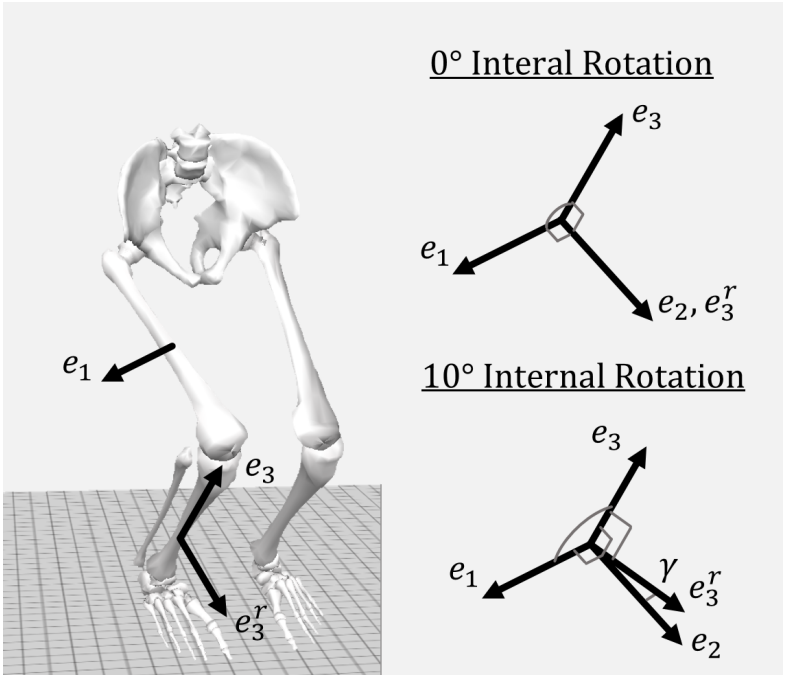

Figure 44: JCS axes orientation for internal rotation in 0-degrees of internal rotation and 10-degrees of internal rotation. Note that in the 10-degree of internal rotation condition, both e_1 and e_3 are orthogonal to e_2, but are not orthogonal to one another; both e_2 and e_3^r are orthogonal to e_3, but are not orthogonal to one another; and e_3^r and e_2 are orthogonal to e_3, but not to one another.

The vector e_1 can be projected onto the distal transverse plane ($e_{1,tran}$) which is defined by e_3 and then normalized ($e'_{1,tran}$) shown in Equation 40 and 41.

$$e_{1,tran} = e_1 - \frac{e_1 \cdot e_3}{\|e_3\|} \cdot e_3 \tag{40}$$

$$e'_{1,tran} = \frac{e_{1,tran}}{\|e_1, tran\|} \tag{41}$$

The e_2 vector is oriented on the transverse plane as it is orthogonal to e_3; therefore, e_2 can be calculated using either $e'_{1,tran}$ or e_1, as shown in Equation 42. Therefore, the orientation of

e_2 in the transverse plane is not affected by abduction or internal rotation.

$$e_2 = \frac{e_3 \times e_1}{\|e_3 \times e_1\|} = \frac{e_3 \times e'_{1,tran}}{\|e_3 \times e'_{1,tran}\|} \tag{42}$$

The rotation angle can also be found with the third rotation of the X-Y-Z Euler sequence when Equations 43 - 45 are true.

$$X'' = e'_{1,tran} \tag{43}$$

$$Z''' = Z'' = e_3 \tag{44}$$

$$Y''' = e_3^r \tag{45}$$

Therefore, the e_2 vector can also be found by combining Equation 42-44, as shown in Equation 46.

$$e_2 = \frac{Z''' \times X''}{\|Z''' \times X''\|} \tag{46}$$

The third rotation, θ_3, about the Z'' axis can be defined with the following rotation matrix ($R_{Z''}$) shown in Equation 47.

$$R_{Z''} \begin{bmatrix} cos\theta_3 & -sin\theta_3 & 0 \\ sin\theta_3 & cos\theta_3 & 0 \\ 0 & 0 & 1 \end{bmatrix} \tag{47}$$

The angle θ_3 is directly related to the position of Y''' with respect to Y'' (Equation 47). The

relationship between the two vectors can be found using the dot product between Y''' and Y'', shown in Equation 48.

$$cos\theta_3 = Y''' \cdot Y'' \tag{48}$$

Given that $Z'' = Z'''$ and X'''-Y'''-Z''' are orthogonal, Y''' can also be found using Z''' and X''' or Z''' and X'' as shown in Equation 49.

$$Y'' = \frac{Z''' \times X'''}{\|Z''' \times X'''\|} = \frac{Z''' \times X''}{\|Z''' \times X''\|} \tag{49}$$

Substituting Equation 49 into 48, the following relationship, Equation 50, can be made.

$$cos\theta_3 = Y''' \cdot \frac{Z''' \times X''}{\|Z''' \times X''\|} \tag{50}$$

When Equation 43, 45, and 50 are combined, the rotation from the Grood & Suntay method can be described, as shown in Equation 51.

$$cos\theta_3 = e_3^r \cdot \frac{e_3 \times e'_{1,tran}}{\|e_3 \times e'_{1,tran}\|} \tag{51}$$

Substituting Equation 42 into Equaiton 51 the Equation 51 can be further defined to use e_3^r and e_1, as shown in Equation 52.

$$cos\theta_3 = e_3^r \cdot \frac{e_3 \times e_1}{\|e_3 \times e_1\|} = e_3^r \cdot e_2 \tag{52}$$

The angles γ and θ_3 can be shown to be equivalent when Equation 39 and 52 are combined,

as shown in Equation 53.

$$cos\theta_3 = e_3^r \cdot e_2 = cos\gamma \tag{53}$$

Because the γ and θ_3 are equivalent (Equation 53) the Grood & Suntay measure of internal and external rotation can be calculated using the rotation about the Z''' axis in the X-Y-Z Euler Sequence.

The axes used in Equations 11 and Equations 39-53 to determine the equivalency of the JCS and Euler rotation sequence for internal rotation are shown in Figure 45.

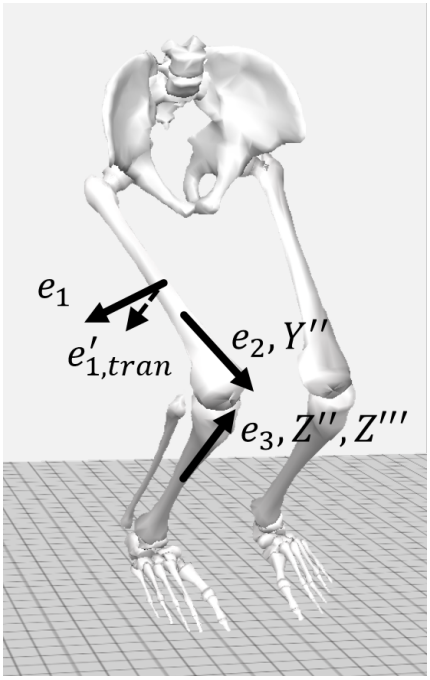

Figure 45: JCS axes used in Equations 11-26.

13 Appendix B: IRB Documentation

"Biomechanics, biomarkers, and MRI: A three-pronged approach to predicting anterior cruciate ligament (ACL) rupture"

Women's Basketball and Soccer

All Women Basketball and Soccer athletes are invited to participate in a research study intended to ultimately improve ACL injury prevention for at-risk athletes.

The purpose of this study is to accurately predict ACL injury risk. The goal is to develop a complete ACL injury risk profile, develop a useful screening protocol for at-risk athletes, and better characterize the success of ACL reconstructive surgeries.

Testing will consist of 5 parts:

1. **Biomechanical testing** – Motion capture of various athletic task (i.e. jogging, drop jumps, run-to-cut), in 3401 Wiggins Hall.
2. **Biodex** – Strength testing in the Auburn Athletic weight room.
3. **Knee MRI** – Knee MRI scans will be conducted (3 per knee) at the AU MRI Center to analyze ACL properties.
4. **Blood Draw** – Biomarkers in blood will be analyzed for evaluation of local knee joint biology and estrogen levels.
5. **Surveys** – Questions about joint pain and activities.

Total testing time will take approximately 3 hours and 50 minutes.

The Auburn University Institution Review Board has approved this Document for use from 05/10/2017 to 05/09/2018
Protocol # 17-096 MR 1705

If interested, please contact Taylor Wright at tkw0006@auburn.edu or Dr. Michael Zabala at (332) 844-4916 or zabalme@auburn.edu.

ACL Injury Prevention Study Contact: Taylor Wright tkw0006@auburn.edu

The Auburn University Institutional Review Board has approved this Document for use from 07/06/2017 to 05/09/2018 Protocol # 17-096 MR 1705

AUBURN UNIVERSITY
DEPARTMENT OF MECHANICAL ENGINEERING

(NOTE: DO NOT SIGN THIS DOCUMENT UNLESS AN IRB APPROVAL STAMP WITH CURRENT DATES HAS BEEN APPLIED TO THIS DOCUMENT.)

INFORMED CONSENT

for a research study entitled

"Biomechanics, biomarkers, and MRI: A three-pronged approach to predicting anterior cruciate ligament (ACL) rupture"

Auburn University Mechanical Engineering/Auburn University MRI Research Center

Investigators: Michael Zabala, Ph.D.,[1] Thomas S. Denney Jr., Ph.D.,[2] Auburn University Department of Mechanical Engineering,[1] Auburn University MRI Research Center.[2]

PURPOSE OF RESEARCH

You are invited to participate in a research study of individuals who are prone to anterior cruciate ligament (ACL) injuries. The ACL is one of the four major ligaments of the knee. We hope to discover if there is a combination of biomechanical, biochemistry, and MRI-detectible ACL biological composition which can predict ACL injury risk. You were selected as a possible participant in this study because you participate in a sport that reports a concentration of ACL injuries.

This research study is looking for individuals who are members of Auburn's women's soccer or women's basketball team.

Your participation in this study is entirely voluntary.

If you decide to participate, you are **free to withdraw** your consent, including your authorization regarding the use and disclosure of your health information, and to discontinue participation at any time without prejudice to you. If you decide to terminate your participation in this study, you should notify Dr. Michael Zabala at (334) 844-4916 (zabalme@auburn.edu).

DURATION OF STUDY INVOLVEMENT

This research study is ongoing with 4 hours max of active participation in one to seven days.

1418 Wiggins Hall, Auburn, AL 36849-5341; Telephone: 334-844-4820; Fax: 334-844-3307

www.auburn.edu

PROCEDURES

There will be four parts to this study. They are the following:

1) Biomechanical Analysis
2) Biodex Strength Test
3) Blood Analysis
4) Magnetic Resonance Imaging (MRI) analysis
5) Surveys

1) Biomechanical Analysis

We will ask you to wear a pair of your own tennis or gym shoes and a pair of shorts that we will provide. We will then measure different aspects of your legs with a tape measure. We will put little squares of double sided tape on your lower and upper body. To the other side of the double sided tape we will stick small balls with reflective material on the outside.

We will then take a number of still photographs of you from the chest down. We will ask you to perform a number of activities similar, but no harder, to those of a practice associated with your sport. These activities include walking, jogging, run-to-cut, squat, and drops from a box. We will ask you to perform each of these activities at least three times for each leg. We expect the entire test to take no more than an hour and a half. This testing will take place at Auburn University, Wiggins Hall, Room 3401.

Only testing personnel will observe you during the experiment.

The biomechanical analysis is expected to take approximately one hour and a half.

2) Biodex Strength Test

You will be asked to remove your shoes to minimize the effect of gravity on torque production. A technician will position straps over your chest, thighs and hips to stabilize you during the test. The lever of the machine will be placed according to the length of your leg. To warm up, you will complete 5 to 10 submaximal repetitions of straightening and bending your leg. To perform the test, you will begin with a straight leg then bend it to 90 degrees, pushing against the force of the Biodex. This will be repeated 5 times. This testing will take place in the Auburn University Football Training Room in the Athletic Complex.

3) Blood Analysis

The blood sample will be drawn at the Auburn University Medical Clinic immediately prior to or after the MRI scan. A phlebotomist will place a thin needle in a vein of your arm using sterile, disposable equipment and collect 3 tubes of whole blood. Each tube will contain 7.5 mL or 1 tablespoon of whole blood.

1418 Wiggins Hall, Auburn, AL 36849-5341; Telephone: 334-844-4820; Fax: 334-844-3307

www.auburn.edu

The blood draw is expected to take no longer than 20 minutes.

4) MRI Analysis

You will first be asked screening questions to make sure it is safe for you to undergo an MRI scan. The screening questions will be provided by the Auburn University MRI Research Center. You will not be excluded from MRI scanning if you have metal dental work (including a permanent retainer, braces, or other dental implants) or body piercings outside of the region being imaged, your knees. If you have any metal in your knee from previous surgery, you will be scanned on the 3 T MRI, as opposed to the 7 T MRI. You will then be asked to lie on a bed that slides into the long tube of the scanner. The scanner is a magnet with a small enclosed space. Radio waves and strong, changing magnetic fields are used to make images of your body. You will be given earplugs and earphones to protect your ears since these changing magnetic fields cause loud knocking, thumping, or pinging noises. You will be asked to remain very still at these times. To help you keep your knee perfectly still, we will put cushions around your leg. We will ask you to undergo an MRI of both knees.

Visual and verbal contact will be maintained during the scan to determine if you are having any negative feelings or sensations. If some unknown risk becomes a safety issue, the research team will immediately stop the scan and remove you from the scanner. You can stop the scan at any time and immediately be removed from the scanner.

The MRI analysis will take approximately one hour and a half.

5) Surveys

The surveys will be filled out prior to the biomechanical analysis. We will ask you to answer survey questions about your knees, your pain, your activities, and your quality of life.

Answering the survey questions should take approximately 20 minutes.

POSSIBLE RISKS, DISCOMFORTS, AND INCONVENIENCES

There are risks, discomforts, and inconveniences associated with any research study. These deserve careful thought. You should talk with the Protocol Director if you have any questions.

Possible risks include, but are not limited to, the inconvenience of travel from home to the laboratory and the following biomechanical, biochemical, and MRI analysis risks.

Biomechanical analysis risks, discomforts and/or inconveniences:

A discomfort that can reasonably be expected is the possibility that you will become tired from the activities. In addition, you may experience sprains, strains, and/or soreness.

Biodex strength test risks, discomforts, and/or inconveniences:

1418 Wiggins Hall, Auburn, AL 36849-5341; Telephone: 334-844-4820; Fax: 334-844-3307

www.auburn.edu

Because of the nature of this test, you may experience fatigue and/or sore from the test. In very rare cases you may experience sharp pain from exertion. In addition, you may experience sprains, strains, and/or soreness.

Blood draw risks, discomforts, and/or inconveniences:

The risks of drawing blood are that you may possibly get a bruise on your arm or soreness and/or redness at the site of the needle stick (venipuncture). There is minimal risk for getting an infection from where the needle stick blood sample is collected. During the time of the blood draw, every precaution will be taken to minimize discomforts or risk of infection. Pain/discomfort may be felt during the duration of the needle stick.

We will not be screening for drugs or disease (e.g., HIV or hepatitis C). Furthermore, we will not be looking for genes that predispose someone to a specific medical condition such as heart disease, Alzheimer's, and others. Please see below for additional blood banking information.

MRI (Magnetic Resonance Imagine) analysis risks, discomforts, and/or inconveniences

MRI machines use a strong magnet and radiofrequency magnetic fields to make images of the body interior. You will be asked to lie on a long narrow couch for approximately 1.5 hrs while the machine gathers data. During this time you will not be exposed to x-rays, but rather a strong magnetic field and radiofrequency magnetic fields, which you will not feel. You will, however, hear repetitive tapping noises that arise from the Magnetic Resonance scanner. We will provide earplugs or headphones that you will be required to wear. The space within the large magnet in which you lie is somewhat confined. The following steps have been taken in an attempt to relieve the claustrophobic feeling: allow you to view the scanner before consenting, you are given a ball to squeeze if you want to be removed from the scanner, we will have verbal communication with you throughout the duration of the scan, and you will be able to listen to music.

Magnetic fields do not cause harmful effects at the levels used in the MRI machine. However, the MR scanner uses a very strong magnet that will attract some metals and affect some electronic devices. If you have a cardiac pacemaker or any other biomedical device in or on your body, it is very important that you tell the operator/investigator immediately. As metallic objects may experience a strong attraction to the magnet, it is also very important that you notify the operator of any metal objects (especially surgical clips), devices, or implants that are in or on your body before entering the magnet room. All such objects must be removed (if possible) before entering the magnet room. In some cases, having those devices means you should not have an MRI scan performed. In addition, watches and credit cards should also be removed as these could be damaged. You will be provided a way to secure these items. If you have any history of head or eye injury involving metal fragments, if you have ever worked in a metal shop, or if you could be pregnant, you should notify the operator/investigator.

The MRI machine produces an intermittent loud noise, which some people find annoying. Some participants may feel uncomfortable being in an enclosed place (claustrophobia) and others may find

1418 Wiggins Hall, Auburn, AL 36849-5341; Telephone: 334-844-4820; Fax: 334-844-3307

www.auburn.edu

it difficult to remain still. Dizziness or nausea may occur if you move your head rapidly within the magnet. Some people experience brief nausea when being put into or taken out of the scanner.

Although long-term risk of exposure to the magnet is not known, the possibility of any long-term risk extremely low based on information accumulated over the past 30 years.

IF YOU FEEL DISCOMFORT AT ANY TIME, NOTIFY THE OPERATOR AND YOU CAN DISCONTINUE THE EXAM AT ANY TIME.

The scans performed in this study are for specific research purposes and are not optimized to find medical abnormalities. The investigators for this project may not be trained to perform medical diagnosis. The investigators and Auburn University are not responsible for failure to find existing abnormalities with these MRI scans. However, on occasion the investigator may notice a finding on an MRI scan that seems abnormal. **When this occurs, a physician will be consulted as to whether the findings merit further investigation, in which case the investigator will contactyou and your primary care physician and inform you of the finding.** The decision as to whether to proceed with further examination or treatment lies solely with you and your physician. The investigators, the consulting physician, and Auburn are not responsible for any examination or treatment that you undertake based on these findings. Because the images collected in this study may not comprise a proper clinical MRI scan, these images will not be made available for diagnostic purposes.

WOMEN OF CHILDBEARING POTENTIAL

If you are pregnant or currently breast feeding, you may not participate in this study. You understand that if you are pregnant, if you become pregnant, or if you are breast-feeding during this study, you or your child may be exposed to an unknown risk.

Participant's Initials _____

1418 Wiggins Hall, Auburn, AL 36849-5341; Telephone: 334-844-4820; Fax: 334-844-3307

www.auburn.edu

PARTICIPANT RESPONSIBILITIES

As a participant, your responsibilities include:

- Ask questions as you think of them.
- Tell the Protocol Director or research staff if you change your mind about staying in the study.
- Follow the instructions of the Protocol Director and study staff.

WITHDRAWAL FROM STUDY

You can withdraw at any time during the study. Your participation is completely voluntary. If you choose to withdraw, your data can be withdrawn as long as it is identifiable. Your decision about whether or not to participate or to stop participating will not jeopardize your future relations with Auburn University, the Department of Mechanical or Electrical Engineering.

There are no adverse consequences of discontinuing the study.

If you decide to withdraw from the study, please contact the Protocol Director, Dr. Michael Zabala, or his staff at (334) 844-4916 (zabalme@auburn.edu).

The Protocol Director may also withdraw you from the study without your consent for one or more of the following reasons:

- Failure to follow the instructions of the Protocol Director and/or study staff.
- The Protocol Director decides that continuing your participation could be harmful to you.
- The study is cancelled.
- Other administrative reasons.
- Unanticipated circumstances.

POTENTIAL BENEFITS

These procedures are carried out purely for experimental purposes. The MRI scans and biochemistry testing acquired in this study are not the same as those acquired during a clinical examination as requested by a medical doctor. Therefore, they are not useful to investigate any abnormalities or medical conditions you may have. The scans collected in the MRI testing will not be made available for diagnostic purposes. Furthermore, the investigators who analyze these images are not medical doctors.

WE CANNOT AND DO NOT GUARANTEE OR PROMISE THAT YOU WILL RECEIVE ANY BENEFITS FROM THIS STUDY.

1418 Wiggins Hall, Auburn, AL 36849-5341; Telephone: 334-844-4820; Fax: 334-844-3307

www.auburn.edu

PARTICIPANT'S RIGHTS

You should not feel obligated to agree to participate. Your questions should be answered clearly and to your satisfaction.

If you decide not to participate, tell the Protocol Director. I cannot promise you that you will receive any or all of the benefits described.

You will be told of any important new information that is learned during the course of this research study, which might affect your condition or your willingness to continue participation in this study.

CONFIDENTIALITY

Any information obtained in connection with this study will remain confidential. Information obtained through your participation may be presented at scientific or medical meetings or published in scientific journals.

Your privacy will be protected. Any information obtained for this study is strictly confidential and your name will not be identified on any data. The data collected will be stored on a password-protected computer and a locked file cabinet. The principal investigator and Ms. Wright will be the only people to have access to the data. Your information may be shared with representatives of Auburn University and government authorities if required by law.

Except as required by law, you will not be identified by name, social security number, address, telephone number, or any other direct personal identifier. Your research records may be disclosed outside of Auburn University, but in this case, you will be identified only by a unique code number. Information about the code will be kept in a secure location and access limited to research study personnel.

The code list will be stored in a password protected spreadsheet stored on a password-protected College of Engineering server in a location that is only accessible by Dr. Zabala and Julie Rodiek (MRI Academic Programs Administrator). The screening forms and consent forms will be stored in a locked filing cabinet in room 266A of the MRI Research Center building. Anonymized image data will be stored on a password-protected College of Engineering server.

FINANCIAL CONSIDERATIONS

Sponsor: ***Auburn University*** is providing financial support and/or material for this study.

There is no cost to you for participating in this study.

1418 Wiggins Hall, Auburn, AL 36849-5341; Telephone: 334-844-4820; Fax: 334-844-3307

www.auburn.edu

COMPENSATION FOR RESEARCH-RELATED INJURY

In the unlikely event that you sustain an injury from participation in this study, the investigators have no current plans to provide funds for any medical expenses or other costs you may incur.

In the unlikely event that your child may sustain an injury from participation in the study, the investigators have no current plans to provide funds for any medical expenses or other costs you may incur.

FOLLOW-UP STUDY

We may have future studies related to this topic.

May we contact you for related future studies?
(Please circle) YES / NO _____
Initials

We would like to keep your data and use it in other research projects not specifically related to the current study.

May we use your data for other research studies?
(Please circle) YES / NO _____
Initials

CONTACT INFORMATION

- **Appointment Contact**: If you need to change your appointment, please contact Taylor Wright at tkw0006@tigermail.auburn.edu
- **Questions, Concerns, or Complaints**: If you have any questions, concerns or complaints about this research study, its procedures, risks and benefits, or alternative courses of treatment, you should ask the Protocol Director, Dr. Michael Zabala at (334) 844-4916 (zabalme@auburn.edu).
- **Injury Contact**: If you feel you have been hurt by being a part of this study, or need immediate assistance please contact the Protocol Director, Dr. Michael Zabala at (334) 844-4916 (zabalme@auburn.edu).
- **Alternate Contact**: If you cannot reach the Protocol Director, please contact Taylor Wright at tkw0006@tigermail.auburn.edu.
- **Independent of the Research Team Contact**: If you are not satisfied with how this study is being conducted, or if you have any concerns, complaints, or general questions about the research or your rights as a research study subject, please contact the Auburn Office of Human Research (IRB) to speak to someone independent of the research team at (334)-844-5966. Or write the Auburn IRB, Office of Human Research, Auburn University, 115 Ramsay Hall, Auburn, AL, 36849.

1418 Wiggins Hall, Auburn, AL 36849-5341; Telephone: 334-844-4820; Fax: 334-844-3307

www.auburn.edu

- **If you have any questions about your rights as a research participant,** you may contact the Auburn University Office of Research Compliance or the Institutional Review Board by phone (334)-844-5966 or e-mail at IRBadmin@auburn.edu or IRBChair@auburn.edu.

Participant's Initials _____

1418 Wiggins Hall, Auburn, AL 36849-5341; Telephone: 334-844-4820; Fax: 334-844-3307

www.auburn.edu

SIGNATURE REQUIRED

HAVING READ THE INFORMATION PROVIDED, YOU MUST DECIDE WHETHER OR NOT YOU WISH TO PARTICIPATE IN THIS RESEARCH STUDY. YOUR SIGNATURE INDICATES YOUR WILLINGNESS TO PARTICIPATE.

_____ _____

Signature of Participant Date

_____

Printed name of Participant

_____ _____

Signature of Person Obtaining Consent Date

_____

Printed name of Person Obtaining Consent

1418 Wiggins Hall, Auburn, AL 36849-5341; Telephone: 334-844-4820; Fax: 334-844-3307

www.auburn.edu

AUBURN UNIVERSITY
DEPARTMENT OF MECHANICAL ENGINEERING

(NOTE: DO NOT SIGN THIS DOCUMENT UNLESS AN IRB APPROVAL STAMP WITH CURRENT DATES HAS BEEN APPLIED TO THIS DOCUMENT.)

INFORMED CONSENT

for a research study entitled

"Biomechanics, biomarkers, and MRI: A three-pronged approach to predicting anterior cruciate ligament (ACL) rupture"

Auburn University Mechanical Engineering/Auburn University MRI Research Center

Investigators: Michael Zabala, Ph.D.,[1] Thomas S. Denney Jr., Ph.D.,[2] Auburn University Department of Mechanical Engineering,[1] Auburn University MRI Research Center.[2]

PURPOSE OF RESEARCH

Your son or daughter is invited to participate in a research study of individuals who are prone to anterior cruciate ligament (ACL) injuries. The ACL is one of the four major ligaments of the knee. We hope to discover if there is a combination of biomechanical, biochemistry, and MRI-detectible ACL biological composition which can predict ACL injury risk. Your daughter was selected as a possible participant in this study because she participates in a sport that reports a concentration of ACL injuries.

Since your daughter is age 18 or younger we must have your permission to include her in the study.

This research study is looking for individuals who are members of Auburn's women's soccer or women's basketball team.

Your daughter's participation in this study is entirely voluntary.

If you choose to let your daughter participate, she is **free to withdraw** her consent, including her authorization regarding the use and disclosure of her health information, and to discontinue participation at any time without prejudice to her. If she decides to terminate her participation in this study, you or your daughter should notify Dr. Michael Zabala at (334) 844-4916 (zabalme@auburn.edu).

Guardian's Initials _____

1418 Wiggins Hall, Auburn, AL 36849-5341; Telephone: 334-844-4820; Fax: 334-844-3307

www.auburn.edu

DURATION OF STUDY INVOLVEMENT

This research study is ongoing with 4 hours max of active participation in one to seven days.

PROCEDURES

There will be four parts to this study. They are the following:

1) Biomechanical Analysis
2) Biodex Strength Test
3) Blood Analysis
4) Magnetic Resonance Imaging (MRI) analysis
5) Surveys

1) Biomechanical Analysis

We will ask her to wear a pair of her own tennis or gym shoes and a pair of shorts that we will provide. We will then measure different aspects of her legs with a tape measure. We will put little squares of double sided tape on her lower and upper body. To the other side of the double sided tape we will stick small balls with reflective material on the outside.

We will then take a number of still photographs of her from the chest down. We will ask her to perform a number of activities similar, but no harder, to those of a practice associated with her sport. These activities include walking, jogging, run-to-cut, squat, and drops from a box. We will ask her to perform each of these activities at least three times for each leg. We expect the entire test to take no more than an hour and a half. This testing will take place at Auburn University, Wiggins Hall, Room 3401.

Only testing personnel will observe her during the experiment.

The biomechanical analysis is expected to take approximately one hour and a half.

2) Biodex Strength Test

Your daughter will be asked to remove her shoes to minimize the effect of gravity on torque production. A technician will position straps over her chest, thighs and hips to stabilize her during the test. The lever of the machine will be placed according to the length of her leg. To warm up, she will complete 5 to 10 submaximal repetitions of straightening and bending her leg. To perform the test, she will begin with a straight leg then bend it to 90 degrees, pushing against the force of the Biodex. This will be repeated 5 times. This testing will take place in the Auburn University Football Training Room in the Athletic Complex.

3) Blood Analysis

Guardian's Initials _____

1418 Wiggins Hall, Auburn, AL 36849-5341; Telephone: 334-844-4820; Fax: 334-844-3307

www.auburn.edu

The blood sample will be drawn at the Auburn University Medical Clinic immediately prior to or after the MRI scan. A phlebotomist will place a thin needle in a vein of your arm using sterile, disposable equipment and collect 3 tubes of whole blood. Each tube will contain 7.5 mL or 1 tablespoon of whole blood.

The blood draw is expected to take no longer than 20 minutes.

4) MRI Analysis

She will first be asked screening questions to make sure it is safe for her to undergo an MRI scan. The screening questions will be provided by the Auburn University MRI Research Center. Your daughter will not be excluded from MRI scanning if she has metal dental work (including a permanent retainer, braces, or other dental implants) or body piercings outside of the region being imaged, her knees. If she has any metal in her knee from previous surgery, she will be scanned on the 3 T MRI, as opposed to the 7 T MRI. She will then be asked to lie on a bed that slides into the long tube of the scanner. The scanner is a magnet with a small enclosed space. Radio waves and strong, changing magnetic fields are used to make images of her body. She will be given earplugs and earphones to protect your ears since these changing magnetic fields cause loud knocking, thumping, or pinging noises. She will be asked to remain very still at these times. To help her keep her knee perfectly still, we will put cushions around her leg. We will ask you to undergo an MRI of both knees.

Visual and verbal contact will be maintained during the scan to determine if she is having any negative feelings or sensations. If some unknown risk becomes a safety issue, the research team will immediately stop the scan and remove her from the scanner. She can stop the scan at any time and immediately be removed from the scanner.

The MRI analysis will take approximately one hour and a half.

5) Surveys

The surveys will be filled out prior to the biomechanical analysis. We will ask her to answer survey questions about her knees, her pain, her activities, and her quality of life.

Answering the survey questions should take approximately 20 minutes.

POSSIBLE RISKS, DISCOMFORTS, AND INCONVENIENCES

There are risks, discomforts, and inconveniences associated with any research study. These deserve careful thought. You or your daughter should talk with the Protocol Director if either of you have any questions.

Possible risks include, but are not limited to, the inconvenience of travel from home to the laboratory and the following biomechanical, biochemical, and MRI analysis risks.

Biomechanical analysis risks, discomforts and/or inconveniences:

A discomfort that can reasonably be expected is the possibility that she will become tired from the activities. In addition, she may experience sprains, strains, and/or soreness.

1418 Wiggins Hall, Auburn, AL 36849-5341; Telephone: 334-844-4820; Fax: 334-844-3307

www.auburn.edu

Biodex strength test risks, discomforts, and/or inconveniences:

Because of the nature of this test, she may experience fatigue and/or sore from the test. In very rare cases she may experience sharp pain from exertion. In addition, she may experience sprains, strains, and/or soreness.

Blood draw risks, discomforts, and/or inconveniences:

The risks of drawing blood are that she may possibly get a bruise on her arm or soreness and/or redness at the site of the needle stick (venipuncture). There is minimal risk for getting an infection from where the needle stick blood sample is collected. During the time of the blood draw, every precaution will be taken to minimize discomforts or risk of infection. Pain/discomfort may be felt during the duration of the needle stick.

We will not be screening for drugs or disease (e.g., HIV or hepatitis C). Furthermore, we will not be looking for genes that predispose someone to a specific medical condition such as heart disease, Alzheimer's, and others. Please see below for additional blood banking information.

MRI (Magnetic Resonance Imagine) analysis risks, discomforts, and/or inconveniences

MRI machines use a strong magnet and radiofrequency magnetic fields to make images of the body interior. She will be asked to lie on a long narrow couch for approximately 1.5 hours while the machine gathers data. During this time she will not be exposed to x-rays, but rather a strong magnetic field and radiofrequency magnetic fields, which she will not feel. She will, however, hear repetitive tapping noises that arise from the Magnetic Resonance scanner. We will provide earplugs or headphones that she will be required to wear. The space within the large magnet in which she is to lie is somewhat confine. The following steps have been taken in an attempt to relieve the claustrophobic feeling: allow you to view the scanner before consenting, you are given a ball to squeeze if you want to be removed from the scanner, we will have verbal communication with you throughout the duration of the scan, and you will be able to listen to music.

Magnetic fields do not cause harmful effects at the levels used in the MRI machine. However, the MR scanner uses a very strong magnet that will attract some metals and affect some electronic devices. If she has a cardiac pacemaker or any other biomedical device in or on her body, it is very important that you or your daughter tell the operator/investigator immediately. As metallic objects may experience a strong attraction to the magnet, it is also very important that you or your daughter notify the operator of any metal objects (especially surgical clips), devices, or implants that are in or on her body before entering the magnet room. All such objects must be removed (if possible) before entering the magnet room. In some cases, having those devices means she should not have an MRI scan performed. In addition, watches and credit cards should also be removed as these could be damaged. She will be provided a way to secure these items. If she have any history of head or eye injury involving metal fragments, if she have ever worked in a metal shop, or if she could be pregnant, you or your daughter should notify the operator/investigator.

The MRI machine produces an intermittent loud noise, which some people find annoying. Some participants may feel uncomfortable being in an enclosed place (claustrophobia) and others may find

1418 Wiggins Hall, Auburn, AL 36849-5341; Telephone: 334-844-4820; Fax: 334-844-3307

www.auburn.edu

it difficult to remain still. Dizziness or nausea may occur if you move your head rapidly within the magnet. Some people experience brief nausea when being put into or taken out of the scanner.

Although long-term risk of exposure to the magnet is not known, the possibility of any long-term risk extremely low based on information accumulated over the past 30 years.

IF SHE FEELS DISCOMFORT AT ANY TIME, SHE SHOULD NOTIFY THE OPERATOR AND SHE CAN DISCONTINUE THE EXAM AT ANY TIME.

The scans performed in this study are for specific research purposes and are not optimized to find medical abnormalities. The investigators for this project may not be trained to perform medical diagnosis. The investigators and Auburn University are not responsible for failure to find existing abnormalities with these MRI scans. However, on occasion the investigator may notice a finding on an MRI scan that seems abnormal. **When this occurs, a physician will be consulted as to whether the findings merit further investigation, in which case the investigator will contactyou or your daughter and your primary care physician and inform you or your daughter of the finding.** The decision as to whether to proceed with further examination or treatment lies solely with you and your physician. The investigators, the consulting physician, and Auburn are not responsible for any examination or treatment that you undertake based on these findings. Because the images collected in this study may not comprise a proper clinical MRI scan, these images will not be made available for diagnostic purposes.

WOMEN OF CHILDBEARING POTENTIAL

If your daughter is pregnant or currently breast feeding, she may not participate in this study. You and your daughter understand that if she is pregnant, if she becomes pregnant, or if she is breast-feeding during this study, your daughter or her child may be exposed to an unknown risk.

PARTICIPANT RESPONSIBILITIES

As a participant, your daughter's responsibilities include:

- Ask questions as she thinks of them.
- Tell the Protocol Director or research staff if she changes her mind about staying in the study.
- Follow the instructions of the Protocol Director and study staff.

WITHDRAWAL FROM STUDY

Your daughter can withdraw at any time during the study. Her participation is completely voluntary. If she chooses to withdraw, her data can be withdrawn as long as it is identifiable. Her decision about whether or not to participate or to stop participating will not jeopardize her future relations with Auburn University, the Department of Mechanical or Electrical Engineering.

There are no adverse consequences of discontinuing the study.

1418 Wiggins Hall, Auburn, AL 36849-5341; Telephone: 334-844-4820; Fax: 334-844-3307

www.auburn.edu

If she decides to withdraw from the study, please contact the Protocol Director, Dr. Michael Zabala, or his staff at (334) 844-4916 (zabalme@auburn.edu).

The Protocol Director may also withdraw her from the study without her consent for one or more of the following reasons:

- Failure to follow the instructions of the Protocol Director and/or study staff.
- The Protocol Director decides that continuing her participation could be harmful to her.
- The study is cancelled.
- Other administrative reasons.
- Unanticipated circumstances.

POTENTIAL BENEFITS

These procedures are carried out purely for experimental purposes. The MRI scans and biochemistry testing acquired in this study are not the same as those acquired during a clinical examination as requested by a medical doctor. Therefore, they are not useful to investigate any abnormalities or medical conditions you may have. The scans collected in the MRI testing will not be made available for diagnostic purposes. Furthermore, the investigators who analyze these images are not medical doctors.

WE CANNOT AND DO NOT GUARANTEE OR PROMISE THAT YOU WILL RECEIVE ANY BENEFITS FROM THIS STUDY.

PARTICIPANT'S RIGHTS

Your daughter should not feel obligated to agree to participate. You and your daughter's questions should be answered clearly and to both of your satisfaction.

If she decides not to participate, tell the Protocol Director. We/I cannot promise you that you will receive any or all of the benefits described.

She will be told of any important new information that is learned during the course of this research study, which might affect her condition or her willingness to continue participation in this study.

CONFIDENTIALITY

Any information obtained in connection with this study will remain confidential. Information obtained through your participation may be presented at scientific or medical meetings or published in scientific journals.

Except as required by law, she will not be identified by name, social security number, address, telephone number, or any other direct personal identifier. Her research records may be disclosed outside of Auburn University, but in this case, she will be identified only by a unique code number.

Information about the code will be kept in a secure location and access limited to research study personnel.

The code list will be stored in a password protected spreadsheet stored on a password-protected College of Engineering server in a location that is only accessible by Dr. Zabala and Julie Rodiek (MRI Academic Programs Administrator). The screening forms and consent forms will be stored in a locked filing cabinet in room 266A of the MRI Research Center building. Anonymized image data will be stored on a password-protected College of Engineering server.

FINANCIAL CONSIDERATIONS

Sponsor: ***Auburn University*** is providing financial support and/or material for this study.

There is no cost to you or your daughter for participating in this study.

COMPENSATION FOR RESEARCH-RELATED INJURY

In the unlikely event that you sustain an injury from participation in this study, the investigators have no current plans to provide funds for any medical expenses or other costs you may incur.

FOLLOW-UP STUDY

We may have future studies related to this topic.

May we contact your daughter for related future studies?

(Please circle) YES / NO _____
Initials

We would like to keep your daughter's data and use it in other research projects not specifically related to the current study.

May we use your daughter's data for other research studies?
(Please circle) YES / NO _____
Initials

CONTACT INFORMATION

- **Appointment Contact**: If your daughter needs to change her appointment, please contact Taylor Wright at tkw0006@tigermail.auburn.edu
- **Questions, Concerns, or Complaints**: If you or your daughter have any questions, concerns or complaints about this research study, its procedures, risks and benefits, or alternative courses of treatment, you or your daughter should ask the Protocol Director, Dr. Michael Zabala at (334) 844-4916 (zabalme@auburn.edu).

- **Injury Contact**: If your daughter feels she has been hurt by being a part of this study, or need immediate assistance please contact the Protocol Director, Dr. Michael Zabala at (334) 844-4916 (zabalme@auburn.edu).
- **Alternate Contact**: If you or your daughter cannot reach the Protocol Director, please contact Taylor Wright at tkw0006@tigermail.auburn.edu.
- **Independent of the Research Team Contact**: If you or your daughter are not satisfied with how this study is being conducted, or if you or your daughter have any concerns, complaints, or general questions about the research or your daughter's rights as a research study subject, please contact the Auburn Office of Human Research (IRB) to speak to someone independent of the research team at (334)-844-5966. Or write the Auburn IRB, Office of Human Research, Auburn University, 115 Ramsay Hall, Auburn, AL, 36849.
- **If you have questions about your child's rights as a research participant,** you may contact the Auburn University Office of Research Compliance or the Institutional Review Board by phone (334)-844-5966 or e-mail at IRBadmin@auburn.edu or IRBChair@auburn.edu.

SIGNATURE REQUIRED

HAVING READ THE INFORMATION PROVIDED, YOU MUST DECIDE WHETHER OR NOT YOU WISH FOR YOUR SON OR DAUGHTER TO PARTICIPATE IN THIS RESEARCH STUDY. YOUR SIGNATURE INDICATES YOUR WILLINGNESS TO ALLOW HIM OR HER TO PARTICIPATE.

_____ _____
Signature of Participant Date

_____
Printed name of Participant

_____ _____
Signature of Parent/Guardian Date

_____
Printed name of Parent/Guardian

_____ _____
Signature of Person Obtaining Consent Date

_____
Printed name of Person Obtaining Consent

Guardian's Initials _____

1418 Wiggins Hall, Auburn, AL 36849-5341; Telephone: 334-844-4820; Fax: 334-844-3307

www.auburn.edu

Office of Research Compliance
115 Ramsay Hall, basement
Auburn University, AL 36849

Telephone: 334-844-5966
Fax: 334-844-4391
IRBadmin@auburn.edu
IRBsubmit@auburn.edu

September 14, 2017

MEMORANDUM TO: Dr. Michael Zabala
College of Engineering

PROTOCOL TITLE: "Biomechanics, Biomarkers, and MRI: A three-prongued approach to predicting anterior cruciate ligament (ACL) rupture"

IRB AUTHORIZATION NO.: 17-096 MR 1705
AUBURN UNIVERISTY FWA NO.: FWA00001104

APPROVAL DATE: May 10, 2017
EXPIRATION DATE: May 09, 2018

The referenced protocol was approved as "Minimum Risk" after having been reviewed by the full IRB #1 Institutional Review Board.

Note the following:

1. CONSENTS AND/OR INFORMATION LETTERS: Only use documents that have been approved by the IRB with an approval stamp or approval information added.
2. RECORDS: Keep this and all protocol approval documents in your files. Please reference the complete protocol number in any correspondence.
3. MODIFICATIONS: You must request approval of any changes to your protocol before implementation. Some changes may affect the assigned review category.
4. RENEWAL: Your protocol will expire on May 09, 2018. Submit a renewal a month before expiration. If your protocol expires and is administratively closed, you will have to submit a new protocol.
5. FINAL REPORT: When your study is complete, please submit a final report to the Office of Research Compliance, Human Subjects.

If you have any questions concerning this Board action, please contact the Office of Research Compliance.

Sincerely,

Dr. Kathy Jo Ellison, RN, DSN, CIP
Chair, Institutional Review Board #1 for the Use of Human Subjects in Research

cc: file

14 Appendix C: Study 1 Additional Results

Tables 32 and 33 are the results from Study 1. †r is the Pearson correlation coefficient and P is the significance; * Significance less than 0.05; and ** Significance less than 0.01.

Table 32: The KVA 2G, 3GC, 3GA, 2P, and knee abduction angle compared to the same angle across all tasks.

			LESS	**Squat**	**DS**	**LR**	**Walk**	**Jog**	**Pivot**
	Angle	†				KVA 2G			
Respective Task	**KVA 3GC**	r	**0.857**	**0.627**	0.399	**0.680**	0.050	0.108	N/A
		P	**≪0.001**	**0.001**	0.073	**≪0.001**	0.820	0.642	
	KVA 3GA	r	**0.857**	0.184	-0.048	**0.680**	**0.762**	0.108	
		P	**≪0.001**	0.400	0.836	**≪0.001**	**≪0.001**	0.642	
	KVA 2P	r	**0.782**	**0.731**	**0.722**	**0.708**	**0.773**	**0.689**	
		P	**≪0.001**	**≪0.001**	**≪0.001**	**≪0.001**	**≪0.001**	**0.001**	
	Knee Abduction	r	0.324	**0.427**	**0.587**	0.159	**0.800**	0.192	
		P	0.141	0.042	**0.005**	0.468	**≪0.001**	0.416	
						KVA 3GC			
Respective Task	KVA 2G	r	**0.857**	**0.627**	0.399	**0.680**	0.050	0.108	N/A
		P	**≪0.001**	**0.001**	0.073	**≪0.001**	0.820	0.642	
	KVA 3GA	r	**1.000**	0.353	0.373	**1.000**	0.025	**1.000**	
		P	**≪0.001**	0.099	0.096	**≪0.001**	0.910	**≪0.001**	
	KVA 2P	r	**0.689**	**0.821**	0.363	0.267	-0.200	0.031	
		P	**≪0.001**	**≪0.001**	0.106	0.218	0.359	0.895	
	Knee Abduction	r	0.382	0.099	0.259	0.249	0.073	**-0.568**	
		P	0.079	0.653	0.257	0.252	0.741	**0.009**	

Continued from Table 32.

			KVA 2P						
Respective Task	KVA 2G	r	**0.782**	**0.731**	**0.722**	**0.708**	**0.773**	**0.689**	
		P	**≪0.001**	**≪0.001**	**≪0.001**	**≪0.001**	**≪0.001**	**0.001**	
	KVA 3GC	r	**0.689**	**0.821**	0.363	0.267	-0.200	0.031	N/A
		P	**≪0.001**	**≪0.001**	0.106	0.218	0.359	0.895	
	KVA 3GA	r	**0.689**	0.150	-0.105	0.267	**0.424**	0.031	
		P	**≪0.001**	0.496	0.651	0.218	0.044	0.895	
	Knee Abduction	r	0.192	0.121	0.359	0.128	**0.527**	0.041	-0.021
		P	0.391	0.581	0.110	0.562	**0.010**	0.863	0.927

			Knee Abduction Angle						
Respective Task	KVA 2G	r	0.324	**0.427**	**0.587**	0.159	**0.800**	0.192	
		P	0.141	**0.042**	**0.005**	0.468	**≪0.001**	0.416	
	KVA 3GC	r	0.382	0.099	0.259	0.249	0.073	**-0.568**	N/A
		P	0.079	0.653	0.257	0.252	0.741	**0.009**	
	KVA 3GA	r	0.382	0.087	-0.313	0.249	**0.576**	**-0.568**	
		P	0.079	0.695	0.167	0.252	**0.004**	**0.009**	
	KVA 2P	r	0.192	0.121	0.359	0.128	**0.527**	0.041	-0.021
		P	0.391	0.581	0.110	0.562	**0.010**	0.863	0.927

Table 33: Each angle measured during the LESS tasks compared to the KVA 2G, 3GC, 3GA, 2P, and abduction angle of the other six tasks.

			LESS				
Angle	Task	†	KVA 2G	KVA 3GC	KVA 2GP	KVA 2P	Knee Abduction
KVA 2G	Squat	r	0.402	0.282	0.282	**0.481**	0.137
		P	0.064	0.203	0.203	**0.023**	0.544
	DS	r	0.077	0.042	0.042	0.294	-0.111
		P	0.747	0.862	0.862	0.208	0.641
	LR	r	-0.114	-0.174	-0.174	0.173	0.149
		P	0.612	0.440	0.440	0.442	0.508
	Walk	r	0.179	0.211	0.211	0.332	-0.176
		P	0.426	0.347	0.347	0.131	0.433
	Jog	r	-0.062	0.071	0.071	0.124	-0.200
		P	0.796	0.765	0.765	0.602	0.398
	Pivot	r	N/A				
		P					
KVA 3GC	Squatting	r	0.178	0.101	0.101	0.249	-0.127
		P	0.429	0.656	0.656	0.265	0.572
	DS	r	-0.164	-0.395	-0.395	-0.058	-0.198
		P	0.490	0.085	0.085	0.807	0.402
	LR	r	-0.201	-0.215	-0.215	-0.121	0.056
		P	0.371	0.336	0.336	0.590	0.806
	Walk	r	-0.041	0.002	0.002	-0.252	0.146
		P	0.857	0.994	0.994	0.257	0.517
	Jog	r	0.273	0.324	0.324	0.299	-0.251
		P	0.244	0.163	0.163	0.201	0.287
	Pivot	r	N/A				
		P					

Table 7: Continued.

KVA 2P	Squatting	r	0.267	0.228	0.228	0.337	-0.059
		P	0.230	0.308	0.308	0.125	0.793
	DS	r	0.004	-0.030	-0.030	0.383	-0.398
		P	0.987	0.900	0.900	0.096	0.082
	LR	r	0.176	0.078	0.078	0.500*	-0.019
		P	0.433	0.729	0.729	0.018	0.934
	Walk	r	0.202	0.131	0.131	**0.525**	-0.192
		P	0.368	0.562	0.562	**0.012**	0.393
	Jog	r	-0.027	-0.063	-0.063	0.357	-0.326
		P	0.910	0.792	0.792	0.122	0.161
	Pivot	r	-0.003	-0.013	-0.013	0.003	-0.083
		P	0.989	0.954	0.954	0.989	0.715

			LESS				
		†	KVA 2G	KVA 3GC	KVA 2GP	KVA 2P	Knee Abduction
Knee Abduction	Squatting	r	-0.337	-0.366	-0.366	-0.246	0.301
		P	0.125	0.094	0.094	0.269	0.173
	DS	r	-0.108	-0.064	-0.064	-0.176	0.121
		P	0.652	0.789	0.789	0.458	0.610
	LR	r	-0.275	-0.270	-0.270	-0.280	0.378
		P	0.215	0.225	0.225	0.207	0.083
	Walk	r	-0.093	-0.066	-0.066	-0.061	-0.131
		P	0.682	0.769	0.769	0.789	0.562
	Jog	r	-0.142	-0.133	-0.133	-0.321	0.177
		P	0.551	0.575	0.575	0.167	0.456
	Pivot	r	0.079	0.101	0.101	-0.091	**0.479**
		P	0.727	0.656	0.656	0.687	**0.024**